

**HOT ALKALINE TREATMENT TO STIMULATE AND
CONSOLIDATE THE HEAVY OIL BACHAQUERO-01 SAND**

A Thesis

by

CÉSAR AMABILIS VALERA VILLARROEL

Submitted to the Office of Graduate Studies of
Texas A&M University
in partial fulfillment of the requirements for the degree of

MASTER OF SCIENCE

December 2003

Major Subject: Petroleum Engineering

**HOT ALKALINE TREATMENT TO STIMULATE AND
CONSOLIDATE THE HEAVY OIL BACHAQUERO-01 SAND**

A Thesis

by

CÉSAR AMABILIS VALERA-VILLARROEL

Submitted to Texas A&M University
in partial fulfillment of the requirements
for the degree of

MASTER OF SCIENCE

Approved as to style and content by:

Daulat D. Mamora
(Chair of Committee)

Renald Guillemette
(Member)

James E. Russell
(Member)

Hans Juvkam-Wold
(Head of Department)

December 2003

Major Subject: Petroleum Engineering

ABSTRACT

Hot Alkaline Treatment to Stimulate and Consolidate the Heavy Oil

Bachaquero-01 Sand. (December 2003)

Cesar Amabilis Valera Villarroel, B.S., Universidad Experimental de las Fuerzas

Armadas, Venezuela

Chair of Advisory Committee: Dr. Daulat Mamora

An experimental study was conducted to verify experimentally whether sand consolidation by high-temperature alkaline treatment was possible in the heavy oil Bachaquero-01 reservoir. The experiments were conducted using sand samples from a core taken from well LL-231 from Bachaquero-01 reservoir. The sample was placed in a vertical 18 in. long aluminum cylindrical cell with an ID of 1.5 in. The top half of the cell was thermally insulated and the bottom half was cooled. The alkaline treatment (pH 11 -12) at 230°C - 250°C and 900 – 1000 psig was injected at 20 ml/min for 3 to 6 hours at the top of the cell and liquid produced at the bottom of the cell. After each experiment, the cell contents were removed and analyzed to determine if consolidation occurred. An electron microprobe was used to analyze both loose and polished epoxy-mounted sand grains to determine any change in texture and composition of the sand pack and precipitation and growth of secondary phases.

Results showed that under the experimental conditions reached in the laboratory; the consolidation of Bachaquero-01 sand did not occur. However some secondary materials were produced in the runs where sand samples were cleaned of oil. It was noticed that the amount of these secondary phases was not sufficient to bridge the sand grains. These results indicate that further research is needed to better understand and optimize the parameters affecting the consolidation of Bachaquero-01 sands.

DEDICATION

To María Cecilia and César Augusto who are my inspiration and a motivation.

To my wife María Lourdes with all my love.

To my family for their love and continuous support.

ACKNOWLEDGEMENTS

First of all, I want to thank God and the Virgin Mary for giving me a life full of love and happiness.

My gratitude goes to my family and my wife's family for their love and support.

A special thanks to Dr. Daulat Mamora for receiving me in his research group and share his experience and good advice with me.

My appreciation to Dr. Renald Guillemette for his cooperation and support. This research would not have been possible without his contribution.

I also want to express my gratitude to Dr. James Russell for being part of my committee and sharing his knowledge through his classes.

It is also necessary to acknowledge those people from the Venezuelan Student Association who have been like a family during our stay in College Station. I also want to thank my classmates who have shared their experiences and cultures with me.

I also would like to thank PDVSA for their cooperation and for sponsoring my study at Texas A&M University.

Last but not least, I wish to thank my wife, Maria Lourdes, for her untiring support and seemingly unlimited belief in me.

TABLE OF CONTENTS

	Page
DEDICATION	v
ACKNOWLEDGEMENTS	vi
TABLE OF CONTENTS	vii
LIST OF TABLES	ix
LIST OF FIGURES	x
 CHAPTER	
I INTRODUCTION.....	1
1.1 Problem Description	5
1.2 Research Objectives	9
II LITERATURE REVIEW	11
2.1 Steam Injection	11
2.2 Dissolution and Cementation in Sandstones	13
2.3 Reservoir Damage Due to Steam Injection.....	20
2.4 The Wilmington Field Case	25
2.4.1 Analyses of Consolidated Sand	29
III EXPERIMENTAL APPARATUS AND PROCEDURE.....	31
3.1 Experimental Apparatus	31
3.2 Preparation of Experiments.....	37
3.3 Experimental Procedure	39
IV EXPERIMENTAL RESULTS	41
4.1 Cell Configuration and Variables	41
4.2 Run No. 1	44
4.3 Run No. 1a	52
4.4 Run No. 1b	58
4.5 Run No. 2	63

CHAPTER	Page
4.6 Run No. 2d.....	69
4.7 Run No. 2f.....	74
4.8 Run No. 3.....	80
4.9 Run No. 3a.....	85
4.10 Run No. 3b.....	93
4.11 Run No. 4.....	101
4.12 Discussion of Experimental Results	109
V SUMMARY, CONCLUSIONS AND RECOMMENDATIONS	113
5.1 Summary.....	113
5.2 Conclusions	115
5.3 Recommendations	116
NOMENCLATURE.....	117
REFERENCES	121
VITA.....	125

LIST OF TABLES

	Page
Table 1.1 Typical Mineralogy of Wilmington Sand.	8
Table 1.2 Typical Mineralogy of Bachaquero-01 Sands.	9
Table 2.1 Quartz Sand Dissolution During Flow of Water at Different Flow Rates, Temperatures, and pH's Adjusted with NaOH.	17
Table 2.2 Quartz Sand Dissolution During Flow of Water at Different Flow Rates, Temperatures, and pH's Adjusted with Na ₂ CO ₃	18
Table 3.1 Equipment and Materials Used.	36
Table 4.1 WDS Analysis of Atypical Zeolites in Run No. 3a.	92
Table 4.2 WDS Analysis of Atypical Zeolites in Run No. 3b.	100
Table 4.3 WDS Analysis of Atypical Zeolites in Run No. 4.	108
Table 4.4 WDS Analysis for Secondary Products in Run Nos. 3a, 3b and 4.	111
Table 4.5 Summary of Experimental Runs.	112

LIST OF FIGURES

	Page
Fig. 1.1 Location of Bachaquero-01 reservoir.....	1
Fig. 1.2 Type log for Bachaquero-01.	2
Fig. 1.3 Effect of pH on dissolution of gravel.	7
Fig. 2.1 Analcime crystals, (a) trapezohedron, (b) cube with trapezohedral truncations.	24
Fig. 2.2 SEM photograph of an analcime from Ischia, Italy.	24
Fig. 2.3 SEM photograph of an natrolite from Altavilla, Vicenza, Italy.....	25
Fig. 2.4 Schematic representation of an ideal perforation showing distribution of synthetic cements and dissolution wormholes.	28
Fig. 3.1 Photograph of cell and its parts.	32
Fig. 3.2 Schematic diagram of cell.	33
Fig. 3.3 Schematic diagram of experimental apparatus.	35
Fig. 4.1 Log from Well LL-231 and four intervals from which cores used in experiments were cut.	42
Fig. 4.2 Temperature profiles for run no. 1.	44
Fig. 4.3 Pressure profiles for run no. 1.	45
Fig. 4.4 Effluent liquid pH for run no. 1.	46
Fig. 4.5 Photograph of the effluent liquid after run no. 1.....	47
Fig. 4.6 Sand sample after run no. 1.....	48

	Page
Fig. 4.7 Photomicrographs of the Bachaquero-01 sand before run no.1, (a) BSE image of the sectioned and polished epoxy-mounted sand grains at 63x, (b) SE image of the loose sand grains at 63x.	49
Fig. 4.8 BSE image of Bachaquero-01 sand at 300x.	50
Fig. 4.9 Photomicrographs of the Bachaquero-01 sand at top of the cell after run no. 1 (a) BSE image of the sectioned and polished epoxy-mounted sand grains at 63x, (b) SE image of the sand grains at 250x.	50
Fig. 4.10 BSE image of Bachaquero-01 sand after run no. 1 at 300x.	51
Fig. 4.11 Temperature profiles for run no. 1a.	52
Fig. 4.12 Pressure profiles for run no. 1a.	53
Fig. 4.13 Effluent liquid pH for run no. 1a.	54
Fig. 4.14 Photograph of the effluent liquid samples after run no. 1a.	55
Fig. 4.15 Sand sample after run no. 1a.	56
Fig. 4.16 Photomicrographs of the Bachaquero-01 sand after run no.1a, (a) BSE image of the sectioned and polished epoxy-mounted sand grains at 63x, (b) SE image of the loose sand grains at 63x.	57
Fig. 4.17 Temperature profiles for run no. 1b.	52
Fig. 4.18 Pressure profiles for run no. 1b.	59
Fig. 4.19 Effluent liquid pH for run no. 1b.	60
Fig. 4.20 Photograph of the effluent liquid samples after run no. 1b.	60
Fig. 4.21 Sand sample after run no. 1b.	61
Fig. 4.22 Photomicrographs of the Bachaquero-01 sand after run no.1b, (a) BSE image of sectioned and polished epoxy-mounted sand grains at 63x, (b) SE image of the loose sand grains at 63x.	62
Fig. 4.23 Differential pressure profiles for run no.2.	64

	Page
Fig. 4.24 Temperature profiles for run no. 2.	64
Fig. 4.25 Pressure profiles for run no. 2.	65
Fig. 4.26 Effluent liquid pH for run no. 2.	66
Fig. 4.27 Photograph of the effluent liquid after run no. 2.	66
Fig. 4.28 Sand sample after run no. 2.	67
Fig. 4.29 Photomicrographs of the Bachaquero-01 sand after run no.2, (a) BSE image at 63x. (b) BSE image at 500x.	68
Fig. 4.30 Temperature profiles for run no. 2d.	69
Fig. 4.31 Pressure profiles for run no. 2d.	70
Fig. 4.32 Effluent liquid pH for run no. 2d.	71
Fig. 4.33 Photograph of the effluent liquid samples for run no. 2d.	71
Fig. 4.34 Sand sample after run no. 2d.	72
Fig. 4.35 Photomicrographs of the Bachaquero-01 sand after run no.2d, (a) BSE image of the sectioned and polished epoxy-mounted sand grains at 63x, (b) BSE image at 500x, (c) SE image of the loose sand grains at 500x (d) SE image at 2000x.	73
Fig. 4.36 Temperature profiles for run no. 2f.	74
Fig. 4.37 Pressure profiles for run no. 2f.	75
Fig. 4.38 Differential pressure profile for run no. 2f.	76
Fig. 4.39 Effluent liquid pH for run no. 2f.	77
Fig. 4.40 Photograph of the effluent liquid after run no. 2f.	77
Fig. 4.41 Sand sample after run no. 2f.	78

	Page
Fig. 4.42 Photomicrographs of the Bachaquero-01 sand after run no.2f, (a) BSE image of the sectioned and polished epoxy-mounted sand grains at 63x, (b) BSE image at 500x, (c) SE image of the loose sand grains at 500x (d) SE image at 1500x.	79
Fig. 4.43 Temperature profiles for run no. 3.	80
Fig. 4.44 Pressure profiles for run no. 3.	81
Fig. 4.45 Effluent liquid pH for run no. 3.	82
Fig. 4.46 Photograph of the effluent liquid after run no. 3.	83
Fig. 4.47 Photomicrographs of the Bachaquero-01 sand after run no.3, (a) BSE image at 63x, (b) BSE image at 100x.	84
Fig. 4.48 Temperature profiles for run no. 3a.	85
Fig. 4.49 Pressure profiles for run no. 3a.	86
Fig. 4.50 Effluent liquid pH for run no. 3a.	87
Fig. 4.51 Photograph of the effluent liquid after run no. 3a.	88
Fig. 4.52 Sand sample after run no. 3a.	89
Fig. 4.53 Photomicrographs of the Bachaquero-01 sand after run no.3a, (a) BSE image of the sectioned and polished epoxy-mounted sand grains at 63x, (b) BSE image at 1200x, (c) SE image of the loose sand grains at 500x (d) SE image at 7000x.	90
Fig. 4.54 EDS spectra of the fine-grained intergrain material after run no. 3a.	92
Fig. 4.55 Temperature profiles for run no. 3b.	94
Fig. 4.56 Pressure profiles for run no. 3b.	94
Fig. 4.57 Effluent liquid pH for run no. 3b.	95
Fig. 4.58 Photograph of the effluent liquid after run no. 3b.	96
Fig. 4.59 Sand sample after run no. 3b.	97

	Page
Fig. 4.60 Photomicrographs of the Bachaquero-01 sand before run no.3b, (a) BSE image of the sectioned and polished epoxy-mounted sand grains at 63x, (b) BSE image at 1200x, (c) SE image of the loose sand grains at 500x (d) SE image at 3000x.	98
Fig. 4.61 Photomicrographs of the Bachaquero-01 sand after run no.3b, (a) BSE image of the sectioned and polished epoxy-mounted sand grains at 63x, (b) BSE image at 500x, (c) SE image of the loose sand grains at 500x (d) SE image at 2000x.	99
Fig. 4.62 Temperature profiles for run no. 4.	101
Fig. 4.63 Pressure profiles for run no. 4.	102
Fig. 4.64 Effluent liquid pH for run no. 4.	103
Fig. 4.65 Photograph of the effluent liquid after run no. 4.	103
Fig. 4.66 Sand sample after run no. 4.	104
Fig. 4.67 Photomicrographs of the Bachaquero-01 sand before run no. 4, (a) BSE image of the sectioned and polished epoxy-mounted sand grains at 63x, (b) BSE image at 500x.	105
Fig. 4.68 Photomicrographs of the Bachaquero-01 sand after run no.4, (a) BSE image of the sectioned and polished epoxy-mounted sand grains at 500x, (b) BSE image at 2000x, (c) SE image of the loose sand grains at 500x (d) SE image at 2000x.	106
Fig. 4.69 EDS spectra of the needle-like material after run no. 4.	107
Fig. 4.70 EDS spectra of the round secondary mineral after run no. 4.	108

CHAPTER I

INTRODUCTION

The Bachaquero-01 reservoir in the Lagunillas field is located in the eastern part of Maracaibo Lake, approximately 75 miles southeast of the city of Maracaibo, Venezuela (**Fig. 1.1**). The national oil company of Venezuela, PDVSA (Petroleos de Venezuela, S.A.), operates the Lagunillas field. It represents one of the most important heavy oil accumulations in the Bolivar Coast group of fields. Bachaquero-01 reservoir covers 19,540 acres of unconsolidated sand and contains an OOIP of 7.037 BSTB. The

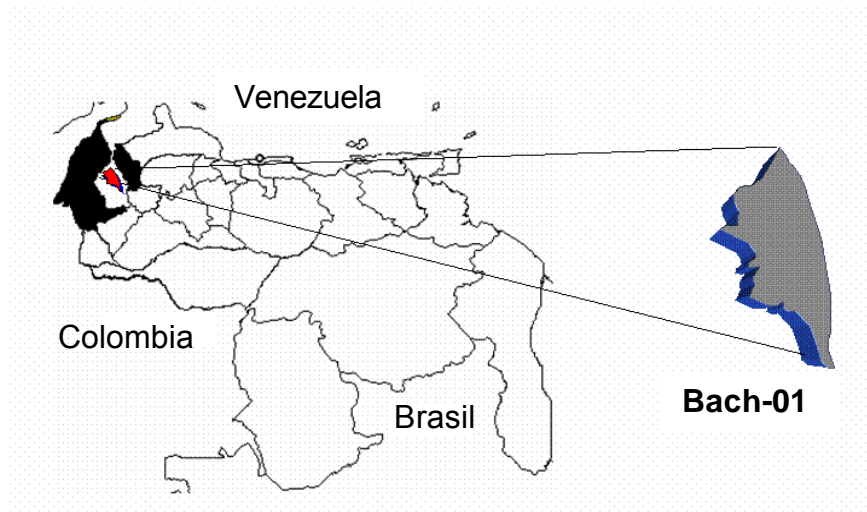


Fig. 1.1-Location of Bachaquero-01 reservoir.

This thesis follows the style of the *SPE Reservoir Evaluation & Engineering*.

oil has an oil gravity of 11.7°API with a viscosity of 635 cp at initial reservoir conditions of 1,360 psia and 128°F.¹ Currently the reservoir produces 36 MSTB/D oil.

Structurally, the reservoir is a simple monocline, dipping from 2° to 3° to the southwest. It is bounded on the south, west and northwest by a moderate aquifer. It is comprised of nine producing intervals of unconsolidated Miocene sands of the Lagunillas formation. **Fig. 1.2** presents a type log for Bachaquero-01. The sands, of fluvio-deltaic origin, are found at an average subsurface depth of 3,000 ft.¹

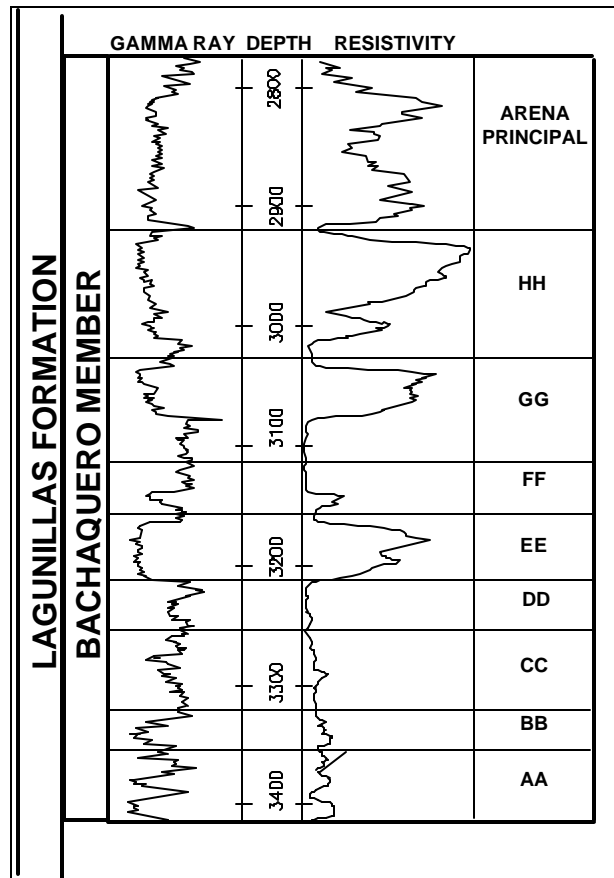


Fig. 1.2-Type log for Bachaquero-01.¹

The Bachaquero-01 reservoir was discovered in 1934. However, during the first 20 years, the reservoir was not extensively developed due to low well productivity and high sand production. In the 1960's new sand control techniques were developed resulting in increased development of the reservoir. In 1971 an extensive drilling program was initiated to complete the development at an average well-spacing of 19.3 acres/well. In 1982 infill drilling was conducted, reducing the well-spacing to about 6 acres/well. The resulting primary recovery factor was estimated to be about 14% OOIP.¹

Cyclic steam injection in the reservoir began in 1971.¹ As of January 2003, a total of 380 wells have been cyclic-steamed with a total of 1,200 cycles.

In the last 10 years the number of wells with sand problems has increased greatly, due in great part to the age of the completions which in most of the cases are more than 20 years old.

A typical cost of a workover for recovery and setting of a new gravel pack in perforated casing in a sanded vertical well in Bachaquero-01 reservoir is \$650,000. The cost of a side track is even higher, which in addition to the low selling price for a 12°API gravity oil, makes this kind of activity currently not feasible economically. For this reason the reservoir has about 30% inactive wells because of sand problems, waiting for an economically feasible technique to put them back into production.

Davies *et al.*^{2, 3} reported on a competitively priced completion technique for controlling sand production in Wilmington field unconsolidated sands, California by injecting high pressure and temperature steam. This completion technique was applied in 12 horizontal and 22 vertical wells with more than 90% of wells producing for as long as

two years after the treatment. They reported a geochemical bond between sand grains in the perforations.

In 1998-1999, under the sponsorship of Arco, Nilsen⁴ carried out an experimental study at Texas A & M University to better understand and optimize the process. The apparatus consisted of a vertical 18 in. long aluminum cylindrical cell with an ID of 1.5 in. into which loose Wilmington Tar Zone sand was tamped. The top half of the cell was thermally insulated while the bottom half was cooled by means of a cooling jacket. Steam was injected at the top of the cell and fluids produced at the bottom of the cell. Temperatures along the cell axis, and inlet and outlet pressures were measured. The cell contents were removed after each experiment and analyzed to determine if sand consolidation occurred. Thin slices of samples before and after the steam treatment were analyzed using an electron microprobe to determine any change in shape, size, and composition of the sand grains. Steam at 250-260°C and 700-800 psig was injected at rates of 5 cc/min and 20 cc/min. Steam with pH of 7 and 12 were used, the latter obtained by addition of sodium carbonate.

Results showed sand consolidation did not occur for steam with pH of 7. However, for steam of pH 11.4, the sand was consolidated, particularly at the top part of the cell in only 3-4 hours. Photomicrographs showed both needle-like and equant crystals of sodium-aluminum-silicate being formed between the consolidated sand grains. Contrary to the previous postulate that precipitation of dissolved quartz or feldspar "cements" the sand grains, the results indicate that the mechanism of sand consolidation is probably more complex.⁴

Moreno (2001) subsequently conducted experiments, to better understand the process, using samples of (a) pure quartz, (b) pure feldspar, and (c) a 50:50 (by weight) mixture of quartz and feldspar.⁵⁻⁸ In each case, the grain size was 20-40 mesh. For these cases, zeolites and amorphous silica were deposited on grain surfaces but were insufficient to cause overall sand consolidation. However, when a finer, poorly sorted (50-250 mesh) 50:50 mixture of feldspar and quartz was used, sand consolidation was obtained in 2.5 hours. At the top, hotter part of the cell, equant and acicular zeolite crystals (sodium aluminum silicates) weakly bound the sand grains. At the bottom and cooler part of the cell, the sand grains were strongly bound by amorphous silica. Results indicate that both zeolite and silica may be cementing agents, the grain-bonding strength depending on the grain surface area. Further, the temperature, injection rate, and pH of the alkaline solution, and "curing time" were important process parameters that need to be further investigated.

1.1 Problem Description

Most of the wells with unconsolidated sands are completed with the use of slotted liners, screens, and gravel packs.^{9,10} Formation damage in heavy-oil reservoirs during steam flooding has been reported by several authors. This is expensive and it can create substantial skins reducing the permeability, and thus reducing productivity.¹¹⁻¹⁶ Other sand control techniques used consist of in-situ sand consolidation methods but these have met with only limited success. Permeability reductions due to the amount of chemical needed to bond the sand grains together have been a major problem. In addition, chemically produced consolidations have not been able to withstand the high

temperatures generated by thermal operations. The cost of chemical injection equipment has been high, and long downtimes to cure the resins have been required.¹⁷⁻²²

A typical cost of a workover for recovery and setting of a new gravel pack in perforated casing in a sanded vertical well in Bachaquero-01 reservoir is \$650,000, the cost of a side track is even higher, which in addition to the low selling price for a 12° API gravity oil, makes this kind of activity currently not economically feasible. For this reason the reservoir has about 30% inactive wells because of sand problems, waiting for an economically feasible technique to put them back into production.

Solubility of quartz and other siliceous minerals increases significantly at high temperature and high pH, and often causes silicate scale problems in the producers.²³⁻²⁴ There are many published studies on formation dissolution and cementation and on formation damage during steamflooding.^{23,24} **Figure 1.3** shows the results of the study done by Rodriguez²⁴ on dissolution of quartz with pH.

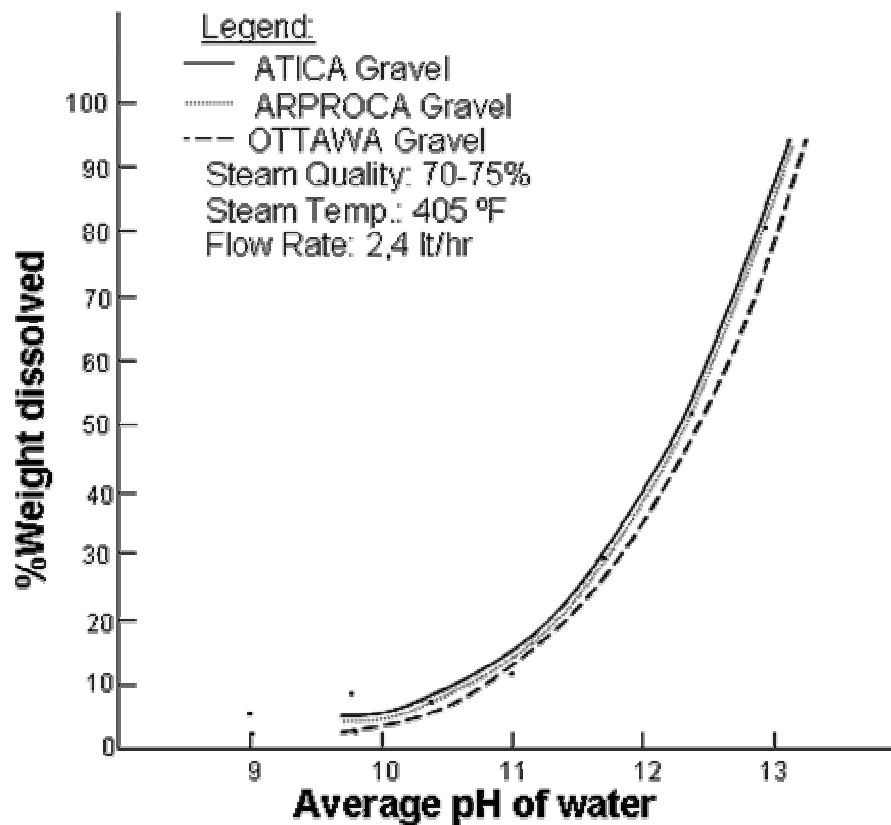


Fig. 1.3-Effect of pH on dissolution of gravel.²⁴

As mentioned before, Davies *et al.*^{2,3} described a novel sand consolidation procedure that uses steam to consolidate sands in the Tar Zone of the Wilmington field, California. This technique was successfully applied in 22 vertical and 12 horizontal producers and injectors in this field.^{2,3} After the steam treatment, the wells produced with no sand production, no reduction in productivity or injectivity, and resulted in significant cost savings.

The mineralogical composition of Wilmington sand^{2,3} is shown in **Table 1.1**. We see that this reservoir is mostly composed of quartz (50 wt%) and feldspars (47 wt%).

Table 1.1-Typical Mineralogy of Wilmington Sand.^{2,3}

Mineral	Composition	wt. %
Quartz	Quartz – SiO ₂	28 -50
	Calceony – SiO ₂	
Feldspars	Orthoclase – KAlSi ₃ O ₈	11-12
	Plagioclase – NaAlSi ₃ O ₈ to CaAl ₂ Si ₂ O ₈	32- 35
	Igneous rock fragments	
Mica	Biotite – K ₂ (Mg,Fe) ₂ (OH) ₂ (AlSi ₃ O ₁₀)	4 -6
Clays	Smectites, Illites, Chlorites	1 -2

Table 1.2 shows the mineralogy of Bachaquero-01 reservoir which also indicates quartz and feldspars as its main components although in different percentage.²⁵

Table 1.2-Typical Mineralogy of Bachaquero-01 Sands.²⁵

Mineral	wt%
Quartz	70 – 85
Feldspars	10 – 15
Siderite	0.5 – 3
Amorphous	1 – 5
Fines (<5 μ) Illite, Kaolinite, Chloride, Quartz, Siderite, Feldspars	5 – 9

Although the process is not fully understood, the field test results, laboratory analysis and comparison of composition of Bachaquero-01 and Wilmington sands, initially indicate that this new technique of sand consolidation using steam might be feasible in Bachaquero-01 reservoir.²⁻⁸

1.2 Research Objectives

The main objectives of this study are:

- (i) To verify experimentally whether sand consolidation by high-temperature alkaline treatment is possible for the Bachaquero-01 reservoir.
- (ii) To determine the main parameters responsible for sand consolidation, in case that it is possible, such as temperature, soak period and injection rate.

The benefits of applying this technique to Bachaquero-01's heavy oil unconsolidated sands will be cost reductions in new well completions and workovers, and a positive impact on well productivity index resulting from the absence of gravel pack.

CHAPTER II

LITERATURE REVIEW

The technique of sand consolidation using high-temperature alkaline solution is a novel technology and the works related with the Wilmington field were the earlier published literature.^{2,3} However, there are many published studies on several sand consolidation techniques, studies on formation dissolution and cementation, and on formation damage during steamflooding.^{11-16,22,23} These studies can help us better understand the sand consolidation process.

We also present a brief study of minerals commonly found during the dissolution/precipitation process of oil sands.

2.1 Steam Injection

Steam injection is the most widely used thermal EOR process. This process reduces the oil viscosity and increases its mobility.²⁶ Steamflooding has become an established enhanced oil recovery technique within the last 40 years.

The two principal methods of steam injection are steam flooding (or steam drive) and cyclic-steam injection (or steam soaking or huff-and-puff). During the steamflooding process, steam is injected into specific injection wells, called injectors, and oil is driven to separate production wells called producers. Typical steam injection projects utilize 5-spot, 7-spot and 9-spot vertical well patterns of injectors and producers. The recovery from steamflooding can reach 50% OOIP or even more.¹⁰

In cyclic steam injection, steam is injected via a well into the reservoir for a period ranging from one to several weeks. In Bachaquero-01 reservoir, it is common to have injection periods of two weeks. Then the well is closed in to allow steam to soak the reservoir. After the soaking period that lasts several days (usually five days in Bachaquero-01 reservoir), the well is opened up to production. When the pressure at the bottom of the well drops, the well is typically put under artificial lift. During this period, the well temperature continues to fall. When oil production falls to a low level, steam is injected again into the well. This cycle of injection, soaking and production is continued until the quantity of oil produced is no longer economic. At this time the oil recovery is typically of the order of 15% OOIP; the oil recovery depends on economics, the nature of the reservoir, well spacing, and other variables.

Cyclic-steam injection was discovered in 1959 by accident in the Mene Grande field (Venezuela), when steam broke out behind the casing in a steam injection well, as reported by Green and Willhite.²⁷ While attempting to relieve the formation pressure by opening the steam injector to production, oil was produced at a rate of 100 to 200 bbl/D. This caused surprise because the reservoir was unproductive by primary recovery methods.

In cyclic steam injection, the primary objective is to lower the oil viscosity. Besides some thermal expansion of oil, the reservoir drive energy is mainly supplied by gravity, compaction, and solution gas drive. In steamflooding, the injected steam not only serves to lower the oil viscosity, but also supplies the drive energy. Unlike cyclic steam injection, in this case the wellbore and formation heat losses may become

prohibitive at some stage in the life of the project, and it may be desirable to drive the steam slug and the oil bank by water. Steam injection is a misleading name. The fluid actually injected in most field operations is a two-phase mixture of hot water and steam vapor, typically about 80% by weight steam vapor.

2.2 Dissolution and Cementation in Sandstones

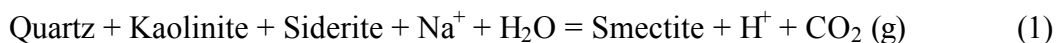
Determining the effect of water-rock interactions when hot fluids are injected into reservoirs is necessary to evaluate whether a field is a suitable candidate for steamflooding. The reactions between reservoir minerals and injected fluids in steamflooding are immediate and pervasive and can affect the permeability and oil recovery from a reservoir.

Minerals that are either near equilibrium or react very slowly with relatively low temperature reservoir fluids are subjected to fluids of low salinity (condensed steam) and temperatures as high as 300°C during steamflood operations. In response to these imposed conditions, a reaction path is initiated to bring reservoir minerals and fluid toward a new chemical equilibrium condition. This reaction path involves dissolution of existing minerals and precipitation of authigenic minerals. Physical migration of clay size particles may produce an additional prejudicial influence. Authigenic mineral precipitation often results in permeability reduction as pore spaces that were once fluid pathways become gradually more restricted with precipitated and mobilized mineral products as reactions progress. The after-effect of this permeability reduction can be reduced productivity, injection profile modification, and by-passed oil in damaged zones.

The chemistry of feedwater at a steam generator facility is field dependent, since it is generated using water from either local ground or surface sources. The process of steam generation usually produces two distinct fluids: a vapor phase and a residual liquid phase (RLP).

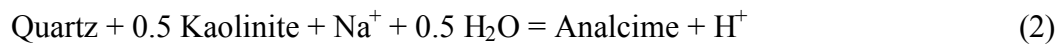
Keith *et al.* performed laboratory steamflood experiments using a high pressure/high temperature permeameter to simulate fluid/rock interactions involving vapor phase condensate (VPC) and RLP fluids.²³ After loading quartz, siderite, and kaolinite mixtures into Teflon tubes, influent solutions were prepared using deionized water, and reagent grade NaCl, NaOH, NaHCO₃, and KCl. The packed cores were placed in the permeameter and pressurized to approximately 1200 psi overburden and 800 psi backpressure for all experiments. Results showed that permeability decline is a function of the amount of authigenic minerals that were produced. Also, XRD analyses of the middle and effluent portions show that analcime, chlorite and smectite occur as authigenic products throughout these parts of the core. Analcime varies from well formed individual and intergrown crystals in the influent end to intergrown and bladed forms in the middle, and finally to rosettes in the effluent end of the core. These different morphologies are likely the result of different crystal growth rates at different saturation states of analcime and are discussed later.

The most severe reaction in Keith *et al.* experiments is as follows:



This general reaction was observed in all of the experiments that were conducted.

The exact stoichiometry of the reaction depends on the compositions of the clays and carbonates. Huang and Longo²⁸ proposed that smectite forms from silicate-carbonate reactions in dilute Na-bearing fluids and that analcime forms instead of smectite when pore fluids have a high Na^+/H^+ ratio. This hypothesis is supported by the VPC and RLP experimental results.²³ The following reaction can be written for the formation of analcime in the high Na^+/H^+ ratio RLP experiment:



Keith *et al.* concluded that the amount of dissolved silicon in the effluent of the experiments and the change in pH also provide some insight into the rate and extent of reaction that is occurring during an experiment. In general, reaction rates (and permeability declines) appear to increase with an increase in either pH or temperature.²³

Reed reported that quartz and other siliceous minerals have very low solubilities at room temperatures, but at elevated temperatures solubilities increase quite intensively.¹² When HCO_3^- ions in steam generator feedwater decompose to CO_2 and OH^- ions, the CO_2 splits into the vapor phase and the OH^- ions split up to the liquid phase. This causes the pH of the generator liquid effluent to increase markedly, the

extent of which is dependent on the HCO_3^- content of the feedwater. Measurements on samples of liquid effluent collected from field generators show that about one-third to one-half of the alkalinity is from CO_3^{2-} ions and the rest is from OH^- ions.

In the steam treatment of wells, the injected liquid phase is hot (some 260°C or 500°F) and quite alkaline; thus, it is expected that quartz and other siliceous minerals will be dissolved. During these experiments the sand grains were predominantly subrounded and about 98 wt% quartz as determined by X-ray diffraction. Either NaOH or Na_2CO_3 was added to the aqueous solution until the desired pH was reached.

Results of the experiments with NaOH are summarized in **Table 2.1**. At room temperature (23°C) Si concentration even at the highest pH levels are below the detection limit of 1 mg/l, which represents an insignificant dissolution rate. As shown in the table, quartz dissolution rates increase with both temperature and solution pH, especially at 177°C and higher. Dissolution rates increase sharply above pH 11; for example, at pH 12 the effluent contains about 10 times as much Si as at pH 11. At pH values of 10 and lower, dissolved Si concentrations are about one-third of those for pH 11 and are not very sensitive to changes in pH.

Table 2.1-Quartz Sand Dissolution During Flow of Water at Different Flow Rates, Temperatures, and pH's Adjusted with NaOH (Reed¹²).

Temperature		Flow rate (ml/min)	Si concentration in effluent (mg Si/l)		
°C	°F		pH 7	pH 11	pH 12
23	73	1	<1.0	<1.0	2.0
		3	<1.0	<1.0	<1.0
		5	<1.0	<1.0	<1.0
		9	<1.0	<1.0	<1.0
93	200	1	2.7	4.9	13.4
		3	<1.0	4.3	19.7
		5	<0.5	2.5	8.6
		9	<0.5	<1.0	3.2
177	350	1	11.0	40.3	1082
		3	6.0	42.7	1120
		5	3.0	36.6	805
		9	1.4	28.0	485
260	500	1	81.0	178	2000
		3	53.0	189	1920
		5	39.0	192	1948
		9	23.0	175	1930

A quantitative comparison of the results suggests that quartz dissolution may be greater with Na₂CO₃ solutions than with NaOH, even with the same initial pH. It is logical that the Na₂CO₃ solutions would dissolve more Si than NaOH solutions because for a given pH solution the Na₂CO₃ solutions would have more total alkalinity and, hence, more resistance to pH decline. The effect of flow rate on quartz dissolution by Na₂CO₃ solutions is similar to that for NaOH solutions as shown in **Table 2.2**. Again, at

Table 2.2-Quartz Sand Dissolution During Flow of Water at Different Flow Rates, Temperatures, and pH's Adjusted with Na₂CO₃ (Reed^{ll}).

Temperature		Flow rate (ml/min)	Si concentration in effluent (mg Si/l)		
°C	°F		pH 7	pH 11	pH 11.3
23	73	1	<0.1	<0.1	3.3
		3	<0.1	<0.1	2.5
		5	<0.1	<0.1	1.9
		9	<0.1	<0.1	1.1
93	200	1	2.7	1.3	12.2
		3	0.9	1.6	15.0
		5	0.5	<0.1	7.2
		9	<0.5	<0.1	5.8
177	350	1	11.0	56.2	780
		3	6.0	46.5	650
		5	3.0	39.5	530
		9	1.4	27.7	360
260	500	1	81.0	195	1800
		3	53.0	207	1700
		5	39.0	187	1700
		9	23.0	172	1700

the highest temperature (260°C) and at pH values of 11 and 11.3 there is little, if any, change in effluent Si concentration with change in flow rate.

Other important parameters to be considered in sand cementation would be the grain size and angularity. Heald *et al.* undertook an experimental research to evaluate the effects of physical properties of sands on rates of cementation and porosity reduction¹⁴. Sands of different physical characteristics were cemented with quartz in hydrothermal reactors at temperatures from 255°C to 360°C and pressures from 2,000 psig to 11,000

psig. Relatively high thermal gradients were used to develop the circulation of solution through the sands. Weak solutions of NaOH, Na₂CO₃ or K₂CO₃ were used. Some of the conclusions of this work may be of importance to the present research.

Heald reported that grain size have an important effect on rates of cementation. Well-sorted coarse sands became cemented faster than fine-grained sands due to the greater permeability. However, when the influx of cementing solutions was the same in both cases, finer grained sand samples were cemented more rapidly. These results suggest that porosity will be more reduced in coarse beds before significant porosity reduction occurred in the fine-grained beds.¹⁴

Heald also found that rates of cementation vary with the angularity of the grains. Cementation occurs faster in highly angular sands than in rounded sands of the same grain size. This could be caused by the greater specific surface areas of the angular sand. Also, the initial compaction is normally greater in angular sands. The combined effect of cementation and compaction results in a rapid reduction of porosity in highly angular sands. Heald concluded that quartz growth is independent of whether Na₂CO₃ or NaOH is used as a solute. In addition, the growth rate increases with time and quartz growth rate is reduced with lower temperatures. Finally, the rate of cementation is faster in pure quartz than in quartz/feldspars mixtures, implying a larger porosity reduction in pure quartz than in quartz/feldspars mixtures.¹⁴

2.3 Reservoir Damage Due to Steam Injection

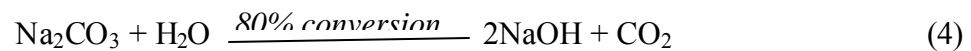
It is common practice in steam stimulation to inject 8,000 m³ or more, of 80% quality steam in each of several cycles per well. In the case of steam flood, or steam drive processes, the volume of injected steam can be many tens of thousands of cubic meters.

McCorrison *et al.* reported that the solubility of quartz sand and other silicate minerals rises rapidly with increasing temperature and pH, and therefore the present practice of steam injection can cause substantial dissolution and mobilization of the reservoir minerals.¹⁶ The most severe dissolution will be in the vicinity of the wellbore where temperatures and pH are highest. The creation of cavities with subsequent formation collapse and failure of liners and casings are also possibilities. In addition to these problems, areas of the reservoir more remote from the wellbore could be subject to a substantial reduction in permeability. As the hot injected fluids containing dissolved reservoir minerals migrate away from the wellbore, temperature and pH will fall causing the dissolved minerals to reprecipitate in the pore spaces. In the case of silica, the reprecipitated material will tend to be the more voluminous amorphous form, which will have the potential for significantly reducing the pore size and subsequently the permeability. Studies have also shown that silica is also capable of reacting with other minerals in the reservoir such as kaolinite and calcite to form, for example, the expandable clay montmorillonite.

A reservoir damage effect that can be developed by the injection of the total boiler effluent is caused by the incompatibility of the formation water and the injected

water. Mixing of the waters causes reactions between the dissolved salts, which produce precipitates. These insoluble compounds can reduce permeability, plug production wells, cause scale formation in production facilities and produce more stable water/oil emulsions.

At most field pilots, steam is raised in once-through steam generators, which are usually controlled to produce approximately 80% quality steam. The normal practice is then to inject the entire boiler effluent into the reservoir. Because of the following reactions (**Eqs. 3 and 4**), the pH of the water in the steam generator can increase by over 4 units. The large increase in pH is due to the formation of sodium hydroxide.



Okoye *et al.* undertook an experimental study to examine formation damage due to plugging caused by precipitates and scales generated from the dissolution of silicate compounds and associated minerals.¹³ The experimental tests include: roller oven tests, petrographic, SEM and EDS studies. The tests were carried out at various temperatures (200°F to 500°F) and steam alkalinity in order to ascertain the factors and conditions that lead to formation damage and wellbore erosion during steam injection. The results from this investigation indicate that elevated temperatures (above 200°F) can cause irreversible formation damage because of hydrothermal effects. Also high pH causes irreversible formation damage mostly due to hardness precipitation from divalent ion exchange processes. The combined effect of temperature and alkalinity increases the degree of formation damage at low temperatures (below 200°F). However, at high

temperatures, thermal effects can reduce the more severe formation damage caused by increased alkalinity.

Okoye *et al.* concluded that severe formation damage, in the form of pore plugging which causes drastic reduction in permeability, occurs when high pH steam interacts with the formation.¹³ This permeability reduction increases with increasing steam pH and temperature. The reduction in permeability and weight loss increases with the duration of the high pH steam injection. On the other hand, low temperature brine injection into Berea sandstone can cause virtually reversible formation damage because the damage is mostly due to fine migration. However, at temperature above 200°F the damage becomes more severe (up to 40%) and irreversible since hydrothermal effects dominate mechanical effects such as fine migration. Their experimental results show that high pH steam can convert feldspars into kaolinite, which becomes dissolved and precipitated as aluminum/silicates such as zeolite and amorphous silica. The precipitates fill up pore spaces, plug pore throats and hence diminish permeability. While elevated temperatures (above 300°F) tend to increase the rock dissolution process when high steam interacts with Berea sandstone, it also inhibits and degrades the crystallization of stable precipitates and this leads to improvement of permeability with increasing temperature. Finally, for a given temperature, the higher the pH of the steam the greater the dissolution and precipitation of Berea sandstone and consequently the degree of permeability damage.

Formation crystals and precipitates seem to be hindered at temperatures above 300°F. SEM, X-ray, EDS and petrographic analyses showed pseudo-hexagonal stacks of

mineral overgrowth, which blocked pore throats. They reported the dissolution of certain minerals such as kaolinite and the precipitation of aluminum/silicate compounds such as zeolites.

The zeolites form a large group of hydrous silicates that show close similarities in composition, association, and mode of occurrence. They are framework aluminosilicates with Na^+ , K^+ and Ca^{2+} , and highly variable amounts of H_2O in the voids of the framework.²⁹

The zeolites can be divided into those with fibrous habit and an underlying chain structure; those with a platy habit and an underlying sheet structure; and those with an equant habit and an underlying framework structure.²⁹

There are two zeolites that will be used in the discussion of results of the present work: analcime and natrolite. Analcime ($\text{NaAlSi}_2\text{O}_6\cdot\text{H}_2\text{O}$) is isometric, usually crystallizing as trapezohedrons (**Fig. 2.1 (a)**). Cubes with trapezohedral truncations are also known (**Fig. 2.1 (b)**). The chemical composition of most natural analcimes is fairly constant with minor amounts of K or Ca substituting for Na; some Al substitution for Si also occurs. Ideal $\text{NaAlSi}_2\text{O}_6\cdot\text{H}_2\text{O}$ contains Na_2O 14.1%, Al_2O_3 23.2%, SiO_2 54.5%, and H_2O 8.2% but synthetic analcime can vary quite widely in composition giving metastable solid phases. Analcime, also called analcite, occurs as a primary mineral in some igneous rocks and is also the product of hydrothermal action in the filling of basaltic cavities.²⁹ **Fig. 2.2** shows an Scanning Electron Microscope (SEM) photograph of an analcime from Ischia, Italy.²⁹

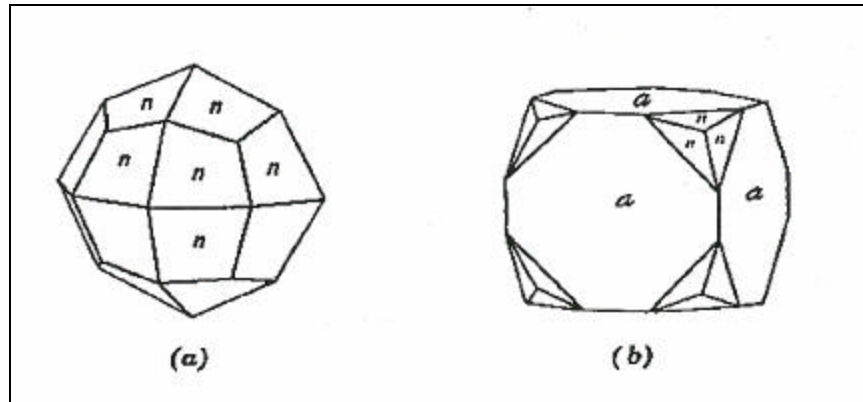


Fig. 2.1-Analcime crystals, (a) trapezohedron, (b) cube with trapezohedral truncations (Klein and Hurlbut¹⁹).

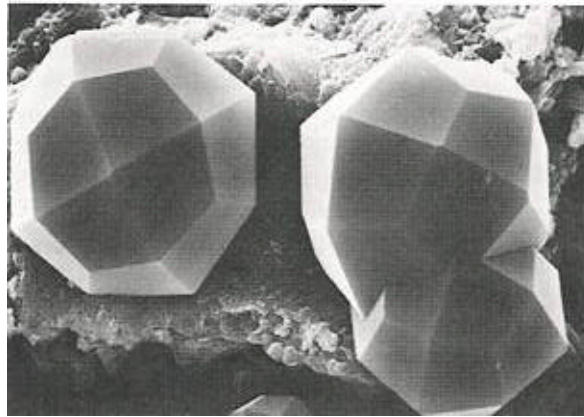


Fig. 2.2-SEM photograph of an analcime from Ischia, Italy.²⁹

Natrolite ($\text{Na}_2\text{Al}_2\text{Si}_3\text{O}_{10}\cdot 2\text{H}_2\text{O}$) is one of the groups of fibrous zeolites, and ideally contains Na20 16.3%, Al_2O_3 26.8%, SiO_2 47.4%, and H_2O 9.5%. Some K and Ca may replace Na. Its crystallography is orthorhombic, prismatic, and often acicular with prism zone vertically striated. It is usually in radiating crystal groups, also fibrous,

massive, granular, or compact. Natrolite is characteristically found lining cavities in basalt associated with other zeolites and calcites.²⁹ **Fig.2.3** shows a SEM photograph of a natrolite from Altavilla, Vicenza, Italy.

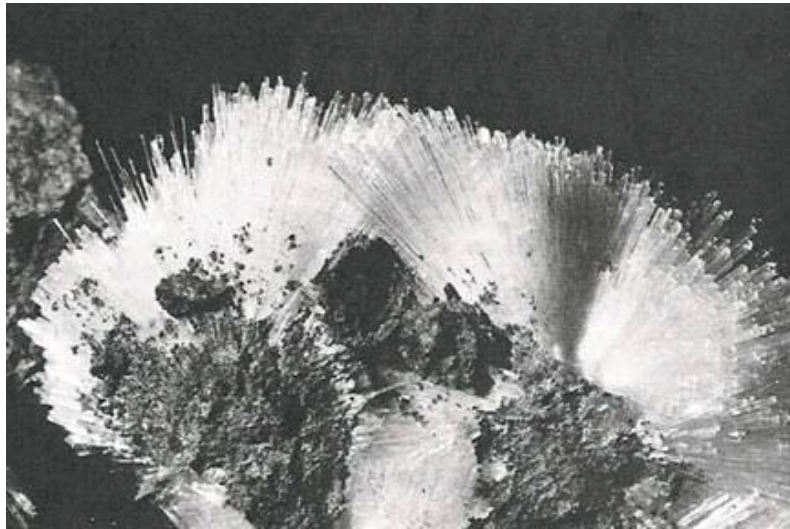


Fig. 2.3-SEM photograph of a natrolite from Altavilla, Vicenza, Italy.²⁹

2.4 The Wilmington Field Case

Many operational difficulties associated with its geology have been found in the thermal recovery operations in the Wilmington field.^{2,3} Early steam breakthrough and sanding have produced many premature well and downhole equipment failures during thermal operations. These problems are commonplace in other Slope and Basin clastic reservoirs with heterogeneous and unconsolidated sands. In addition, the high reservoir

pressure and associated high steam temperatures in the Wilmington field aggravate the wellbore completion and equipment problems associated with early steam breakthrough.^{2,3}

In order to reduce capital costs and to improve vertical injection profile control, two pilot vertical steam injection wells in the Fault Block II-A, Tar Zone (Tar II-A) were selected in 1990 to test a new well completion technique applying limited-entry perforation with the wells cased and cemented to total depth. After the treatment it was observed that the five steam injection wells had only minor to no sand inflow problems and it was suspected that a form of sand consolidation was occurring in the perforation tunnels, most likely bonding with silica cements. Between 1992 and 1994 the new sand consolidation technique was further tested in eight new vertical wells and two vertical well recompletions in the Tar II-A and two new horizontal wells in the Tar I using various numbers of perforations, perforation sizes, steam volumes and steam rates. A new empirical well completion process was developed, but it was only after its application in the four DOE project horizontal wells in the Tar II-A in 1996 when the actual detailed geochemistry of the sand consolidation process began to be understood. Consolidated sand samples were found attached to the steam injection tubing tail following a cyclic steam stimulation job in well UP-955 in October 1996. Those samples showed bonding of the sand grains with high temperature cements not found in the original formation rocks. They were geochemically created through the dissolution of formation minerals by the hot alkaline condensate phase of the steam. The success of the

sand consolidation technique led to its subsequent application in six new horizontal wells and in four vertical well recompletions.^{2,3}

The new sand consolidation technique has also been applied for purposes other than new well completions and has proven to have other beneficial qualities. In October 1994 the technique was used successfully to repair enlarged slots in the slotted liner of well UP-932. Its production was restored to its previous rates without sand production. In other attempts to repair damaged slotted liners, several wells with sand consolidation completions were given hydrochloric acid jobs to successfully remove scale damage without affecting the consolidated sands.^{2, 3}

Hara *et al.* reported on the alkaline hot water/steam sand consolidation procedure tested in the Wilmington field.³ The liquid phase and steam temperatures should be high enough ($>300^{\circ}\text{C}$), and the steam quality should range from 60-80%, in order to provide a highly alkaline (pH = 10-12) environment to create the cements for bonding the sand grains. They also reported that the steam rate should be high enough to achieve the critical velocities required by the limited-entry perforating theory. This ensures distribution of the steam into all of the perforations. The empirically calculated minimum steam volume necessary to achieve sand consolidation is 750 barrels of cold-water equivalent steam per 1/4 in. perforation.

The dissolution of the sandstone grains occurs preferentially in those with high specific surface area such as clays, rock fragments, and micas and is caused by the hot alkaline liquid phase in the 80% quality steam. As the fluid that was injected travels through the formation and cools, various precipitates drop out at different temperatures.

The high temperature precipitates or cements bond the sand grains around the perforation tunnels and control sand movement into the wellbore.

The fluid production of wells completed with this new technique appears to be equal to or better than that of wells completed with gravel-packed liners over a similar interval. It is believed that the sand consolidation treatment creates secondary porosity, or wormholes, through the selective dissolution of formation fines and thus increases permeability. Many wells also experience higher oil cuts after the sand consolidation treatment than offset wells. This could be attributable to the wormholes having less formation fines and therefore higher oil relative permeability. A schematic representation of the sand consolidation process is shown in **Fig. 2.4**.

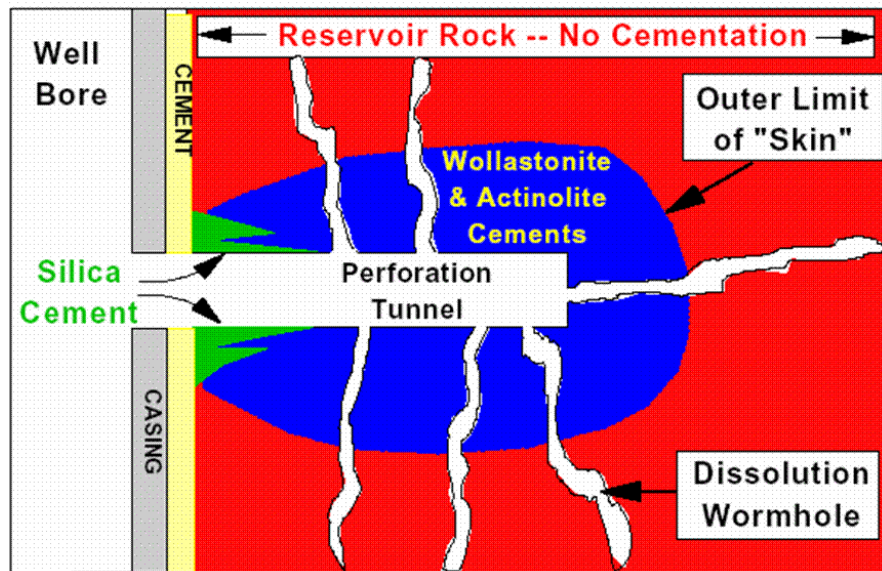


Fig. 2.4-Schematic representation of an ideal perforation showing distribution of synthetic cements and dissolution wormholes (Hara *et al.*³).

2.4.1 Analyses of Consolidated Sand

The thin section, X-ray diffraction and SEM analyses revealed that the grain composition and grain size of the artificially cemented sands were the same as the formation sands and that they entered into the wellbore by means of the open perforations. The analysis of the cemented sand samples points out the presence of three concentrically arranged layers. The first layer was the closest to the tubing wall and consisted of sand grains bonded with silica cement. With a thickness of 1 to 3 mm and a low porosity of <1 %, it was considered to be essentially impermeable. Silica cement precipitates at low temperatures around 150°C.³

Layer 1 is believed to have been initially bonded with high temperature Layer 2 cements and subsequently covered with Layer 1 cements when cyclic steam injection ceased and the tubing filled with cool kill fluids. The silica cement occurs as grain coating chalcedony and as quartz overgrowths.³

The second layer formed within and above Layer 1 with 1 to 3 mm of thickness consisting of artificially cemented sand grains, primarily by a complex calcium silicate (CaSiO₃) mineral. The crystals formed a plate structure, which extended from one grain to the next. This layer had a high porosity of > 25%, but, some reduction of permeability resulted from cemented pore throats. This layer is loosely referred to as the wollastonite layer, as wollastonite is the closest known mineral to this artificially made cement. Wollastonite is a cement that precipitates at high temperature about 300°C.³

Finally, the third layer (the outermost layer) was 1 to 3 mm thick. It was composed of synthetic acicular (needle-like) crystals of another complex calcium silicate

loosely cementing the sand grains. This layer has a high porosity of > 25%. Permeability is higher than layer 2 (by visual analysis), but like layer 2, cannot be accurately determined as the layers are too thin. This layer is loosely referred to as the actinolite layer, as actinolite is the closest known mineral phase of this artificially made cement. Actinolite is a cement that precipitates also at high temperatures around 250°C.³

Hara *et al.* concluded that the new sand consolidation technique was successfully applied in 13 vertical wells, 12 horizontal wells, 7 recompletions, and two repaired liners in three heavy oil zones in Fault Blocks I, II-A and V in the Wilmington field.³ They also reported that after 2 years of production and injection, over 90% of the wells experienced minor or no sand inflow problems. This method has significantly reduced the risk of wellbore completion failures, especially in horizontal wells.

Hara *et al.* also concluded that this sand consolidation technique can provide substantial cost savings in well drilling and completion operations by eliminating the need for "conventional" open-hole, gravel-packed, slotted-liner completions and replacing it with a simple cased-through and cemented completion with a limited number of selected small perforations.³ Moreover, the wells completed with this technique have equivalent to higher production or injection rates than wells with the "conventional" completions due to increased permeability from sandstone dissolution. Finally, the new sand consolidation technique allows both production and injection wells to be completed the same way, thereby making it possible to convert wells easily to either type.³

CHAPTER III

EXPERIMENTAL APPARATUS AND PROCEDURE

3.1 Experimental Apparatus

The main component of the apparatus is an 18-in. long by 1.6 in. ID aluminum cell in which the sample to be consolidated is placed. The specifications of the cell are as follows:

- (i) High-grade, high-yield (9000 psi), high-tensile strength (11000 psi), tempered aluminum 7075-T651.
- (ii) Cell dimensions are 18 in. long by 1.58 in. ID with WT of 0.46 in.
- (iii) To retain the high yield and tensile strengths of the metal, the whole cell (except for the end-caps and cover of the cooling jacket) was machined from one solid cylindrical aluminum block.
- (iv) A 12 in. long Teflon tubing (TFE, WT 0.040 in., maximum operating temp. 500° F) is inserted at the injection end of the cell and line the inner wall to minimize any possible interaction between the sample and aluminum wall at the hot end of the cell.
- (v) A 0.25 in thick Teflon disc is placed below the top end-cap to minimize corrosion of the end-cap.
- (vi) The cell was also anodized to prevent reactions with hot alkaline water.

The cell was completely fabricated at Texas A&M's physics workshop. **Fig. 3.1** shows a photograph of the cell and its parts.

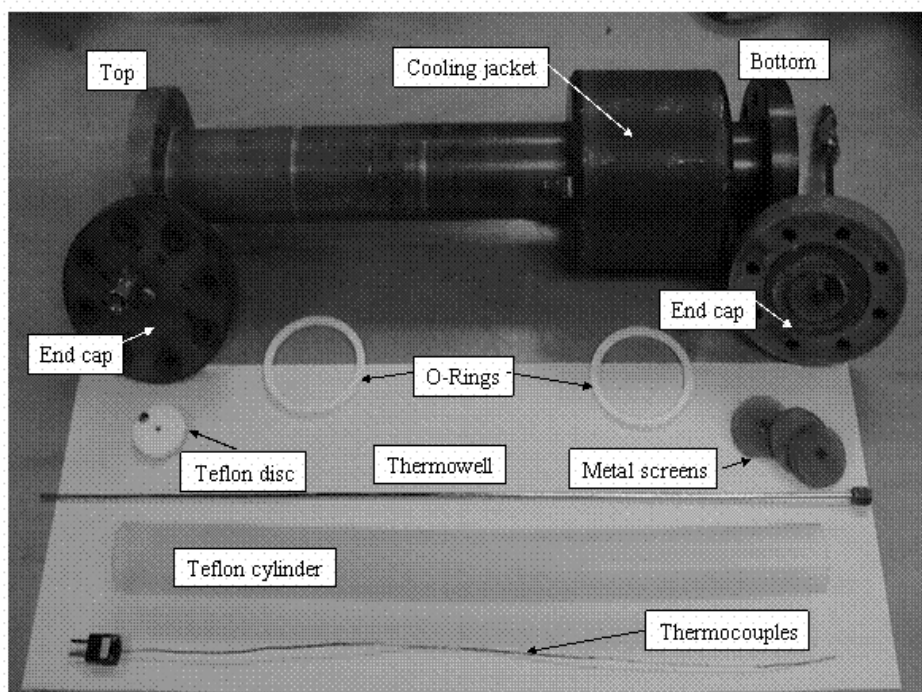


Fig. 3.1-Photograph of cell and its parts.

The cell was mounted on a metal support and the top part was insulated to help reduce the heat losses during the experiments. A schematic diagram of the cell is presented in **Fig. 3.2.**

The experimental apparatus includes two plastic containers; one containing distilled water and the other sodium carbonate solution. The water container is connected to a very accurate HPLC pump and the sodium carbonate is connected to a high velocity pump.

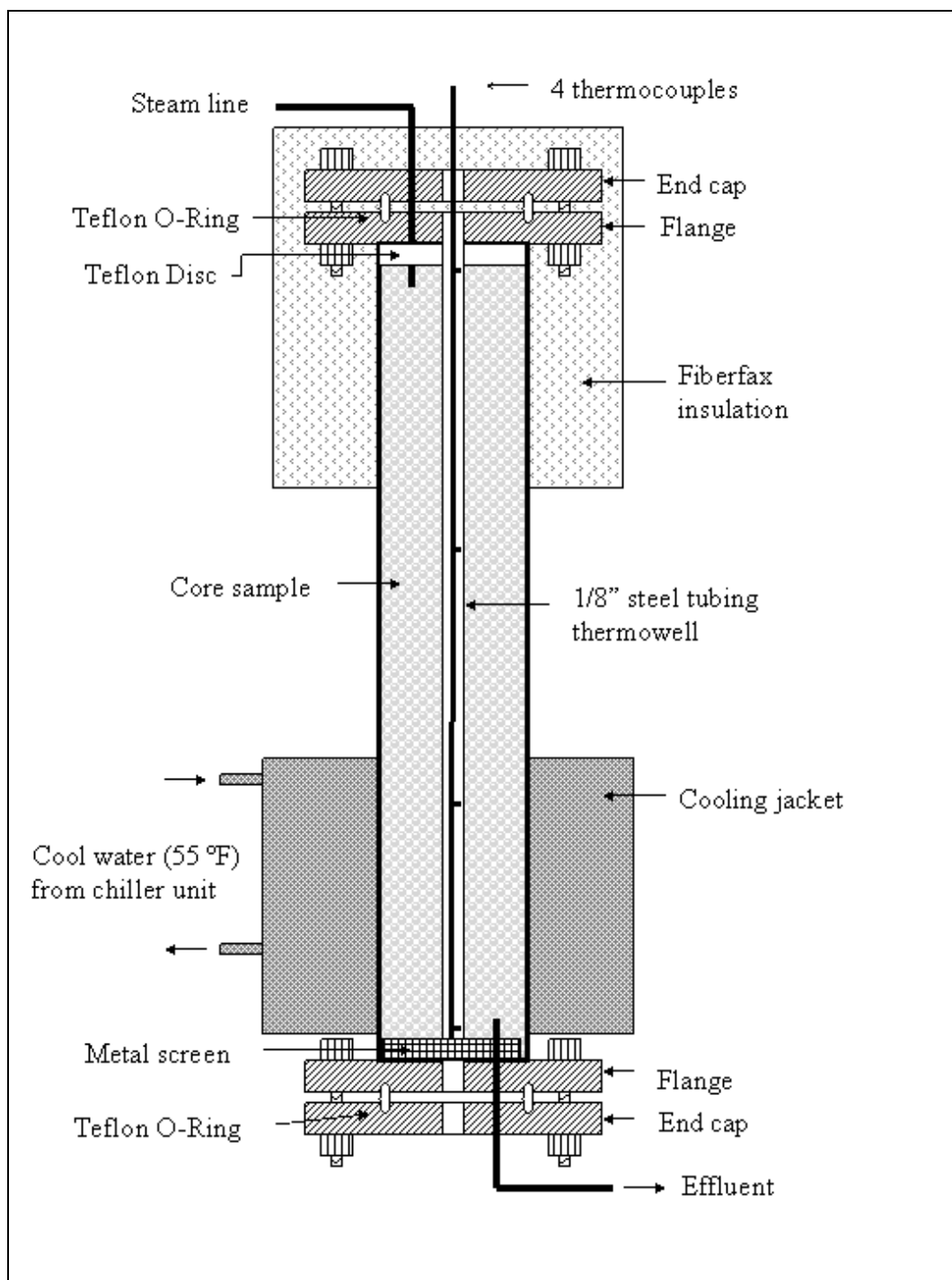


Fig. 3.2-Schematic diagram of cell.

These two pumps are connected to a pair of accumulators; water enters the bottom and sodium carbonate ingress the top, to allow the injection of the sodium carbonate solution into the steam-generator to produce hot fluid that is then injected into the cell. This modification of the injection scheme was done to avoid contact of the HPLC pump with the sodium carbonate solution in order to prevent damage to the pump heads.

A 1/8" stainless steel thermowell is placed along the longitudinal axis of the cell. At the bottom of the cell, the thermowell is connected to a stainless steel screen, which consists of two layers of 250-mesh sieves to prevent sand to be produced into the production lines and the backpressure regulator. The thermowell contains four thermocouples, which measure the temperature at four different locations inside the well. These, beginning from the top, are at 1 in. into the cell, 6 in. into the cell, 12 in. into the cell, and at the outlet end (18 in. into the cell). Pressure is measured at the inlet and outlet end using two Validyne pressure transducers to yield both absolute and differential pressures during the runs. The two pressure transducers are connected to a Validyne demodulator, which is connected to a HP 3497A data logger and PC that records pressure and temperature during the runs at 30-second intervals. A high-capacity chiller unit is used to cool the lower part of the cell and to create a thermal gradient through the cell. A high-pressure extra-fine metal filter is connected in-line after the outlet of the cell. Four by-pass lines were added to ensure the safety and continuity of an experiment, two at the top and bottom of the steam generator, one line with a pressurized vessel to by-pass the cell and one line to by-pass the final filter in order to clean the filter in case of a plugging of it without stopping the experiment. There is also a connection

between the two control valves to allow continuous control and cleaning in case one valve gets plugged. The effluent is collected during the experiment so its pH could be measured with a pH-meter. A schematic diagram of the experimental apparatus is shown in **Fig. 3.3**. A list of the equipment and materials used is shown in **Table 3.1**.

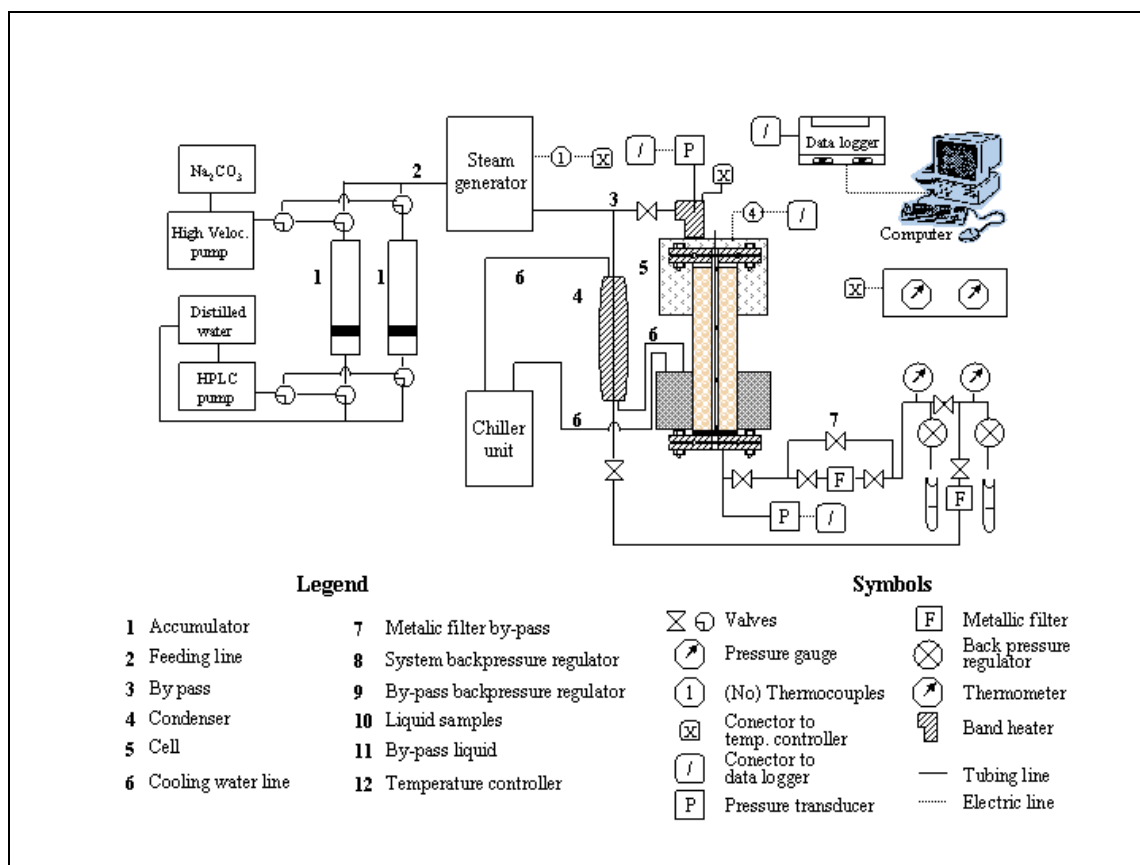


Fig. 3.3-Schematic diagram of experimental apparatus.

Table 3.1-Equipment and Materials Used.

Material/Equipment	Description
Water and solution	Two 8 liter and one 12 liter plastic containers
Sodium carbonate	SX 0400-3 2.5 kg EM Science
Distilled water	Culligan distilled water
HPLC pump	Beckman HPLC pump Model 100A
High velocity pump	Jabsco self priming pump, 1/6 HP, 1175 R.P.M.
Steam generator	Fabricated in Ramey Lab
Temperature controller	Fenwal model 550, type J thermocouple, max. temperature 1200 °F
Heater tape controller	Eurotherm, model 847
Pressure transducer	Validyne, model DP15-TL
Heater tape	Omegalux, model STH051-040, size 0.5 x 4 ft
Cell	Aluminum tube measuring 18 in. long by 1.58 in. ID with WT of 0.46 in.
Chiller unit	Haskriss Co. chiller unit, model R100, cooling temperature range 53°F - 64°F, max rate 18 liter/min
Condenser	Steel type condenser
Data logger/recording system	Hewlett-Packard data acquisition/control unit, model 3497 A with type 44422A T-couple acquisition assembly
Back-pressure regulators	Tescom corporation, max. pressure 6000 psig
Thermocouples	Omega JMQSS-040, type sheath, diameter 0.040 in.
Check valves	Whitney ¼ in. and 3/8 in.
Stainless steel tubing	¼ in. and 3/8 in. stainless steel tubing with swagelock connections
Electronic balance	Mettler PM 4600 Delta range, cap. 10.45 kg.
Stirrer	Thermolyne, model Nuova II
Graduate cylinders	Pyrex 10, 25 and 500 cc
Beakers	Kimax graduate beakers, 80, 200, 1000 ml
Quartz sand	Ottawa sand 20-40 mesh
Gauges	Heise, CM-105626 and Omega Test gauge, max. pressure 5000 and 3000 psig respectively
Sample bottles	10cc glass bottles with cap.
Mortar and pestle	Ceramic mortar and pestle

3.2 Preparation of Experiments

The sand material used during the experiments was obtained from a core of well LL-231 from Bachaquero-01 reservoir, and it was disaggregated using a ceramic mortar and pestle. In initial experiments, the samples used were straight from the cores (untreated). However when these did not consolidate during the runs, samples were subsequently cleaned of the oil using a soxhlet extraction apparatus.

The solution of sodium carbonate was also prepared in advance. In our experiments sodium carbonate (Na_2CO_3) was mixed with distilled water to a pH of 11.5-12 (100g of Na_2CO_3 per liter of water).

All the experiments have to be planned ahead, with at least two days to prepare each run. The preparation would usually include the following steps:

- (i) Clean all the lines with distilled water.
- (ii) Clean the backpressure regulators with distilled water and acetone.
- (iii) Clean the metal filter and its container with weak acid to get rid of any sodium carbonate from previous runs, then with water and finally acetone. Compress air was used to dry the filter and the container.
- (iv) Before installing the cell, all lines are flushed with distilled water, and dried with compressed air.
- (v) The pressure transducers and the demodulator are calibrated using a dead-weight tester.
- (vi) The cell and its parts are carefully cleaned with clean water, WD-40, and acetone.

- (vii) The metal screen is connected to the thermowell and is inserted into the cell.
- (viii) Place TFE O-ring in the groove at the outlet end of the cell and flange up.
- (ix) Close the bottom of the cell using the bottom blind flange, 8 bolts, washers and nuts.
- (x) Place the sample in a separate container.
- (xi) Place the cell in a vertical position with the injection end up and start introducing the sample into the cell in portions of approximately 50 grams. Use a tamping device, carefully tamp the sand between each portion. Add some distilled water. Continue this procedure until the cell is packed. In case when the sample is not enough to fill the cell, Ottawa sand 20-40 is used at the bottom of the cell to complete the volume required.
- (xii) Place TFE O-ring in the groove at the inlet end of the cell and flange up.
- (xiii) Close the top part of the cell using the top blind flange, 8 bolts, washers and nuts.
- (xiv) Secure the cell to the metal support and connect the injection lines to the steam-generator, pressure transducers, and the outlet flow lines. Connect the inlet and outlet water lines of the chiller unit to the cooling jacket.
- (xv) Introduce the thermocouples in the thermowell and connect them to their corresponding leads.
- (xvi) Start the data logger and PC and check that pressures and temperatures are recorded and confirm agreement with values at their respective display units.
- (xvii) Start injecting cold water and slowly increase the pressure while checking for leaks in the cell or in any of the lines. Test up to 1200 psig and make sure there

are no leaks. Also start the chiller unit and let it circulate for a while and check for leaks.

- (xviii) After making sure all components of apparatus are working, install band heater around the line from the steam generator and insulate the top part of the cell using fiberfrax to minimize heat-loss during the experiment.
- (xix) Prepare the Na_2CO_3 solution and place it in the plastic container.

All these preparations are completed the night before the experiment so that we could have a complete day to run an experiment if necessary.

3.3 Experimental Procedure

A typical experiment would be carried out in the following manner:

- (i) Turn on all the necessary devices/instruments.
- (ii) Start the data logger, PC, and the chiller unit.
- (iii) Set the rate on the HPLC pump at 20 cc/min and start pumping distilled water.
- (iv) Increase the temperature on the steam-generator slowly up to 270°C
- (v) Use the backpressure regulator to control the pressure in the system and keep it above saturation pressure corresponding to the temperature. This is to ensure that only a liquid-phase water exists throughout the experimental apparatus.
- (vi) Once the desired experimental conditions are reached, switch injection from water to sodium carbonate solution.
- (vii) During the experiment, control differential pressure and temperature in the cell. Take effluent liquid samples every 20-30 minutes and check pH.

- (viii) In case that the filter or the backpressure regulator get plugged (sudden increase in pressure in the steam generator and decrease in pressure at the outlet), bypass the filter or backpressure regulator, clean it, reinstall it and switch to the original set up.
- (ix) After completing a run, bypass the cell keeping the pressure in the system and turn off the steam-generator. Keep pumping until the system is below 100°C. This is made to ensure that liquid-phase water exists at all points in the flow system and to avoid the precipitation of sodium carbonate crystals that could plug the lines or the steam generator.
- (x) Slowly bleed off the pressure inside the cell using the backpressure regulator.
- (xi) Let the system cool down before shutting down devices/instruments.
- (xii) Disassemble the cell after 36 hours. Observe if sand consolidation occurs. Remove the sand carefully from the cell without disturbing it too much. Collect and photograph samples.
- (xiii) Dry samples in an oven. Polished epoxy-impregnated mounts of the sand are made and analyzed to determine mineral composition and type of mineral cement from electron microprobe analysis.
- (xiv) The techniques used in the microprobe lab include energy dispersive spectrometry (EDS), scanning electron microscopy (SEM), backscatter electron imaging (BSE) and wavelength dispersive spectrometry (WDS). The electron microprobe used is a CAMECA SX50 located at the Geology and Geophysics Department.

CHAPTER IV

EXPERIMENTAL RESULTS

The main objective of these experiments is to verify experimentally whether hot alkaline treatment is a viable technique for consolidating Bachaquero-01 sands and to determine the main parameters responsible for sand consolidation. The samples to use correspond to the core of well LL-231 (**Fig. 4.1**). Temperature and pressure will be held approximately constant at 250°C and 900 psi. The degree of success will be determined by disassembling the cell after the run and observing whether the sand has been consolidated or not. Samples from different locations in the cell will be analyzed using the electron microprobe and XRD analysis to determine differences in mineral composition and type of cement throughout the sample. Analysis of the original material will also be compared to the reacted material to observe any changes in composition and grain shapes.

4.1 Cell Configuration and Variables

The experimental apparatus was set up as described in Chapter IV. Before we started the run, the steam-generator, HPLC pump, steam injection cell, backpressure regulator, pressure transducers, thermo-couples, demodulator, data logger, and PC were function tested.

The cell used during all the experiments has a hot zone at the top where the hot alkaline solution is injected and a cool zone at the bottom where the cooling jacket is

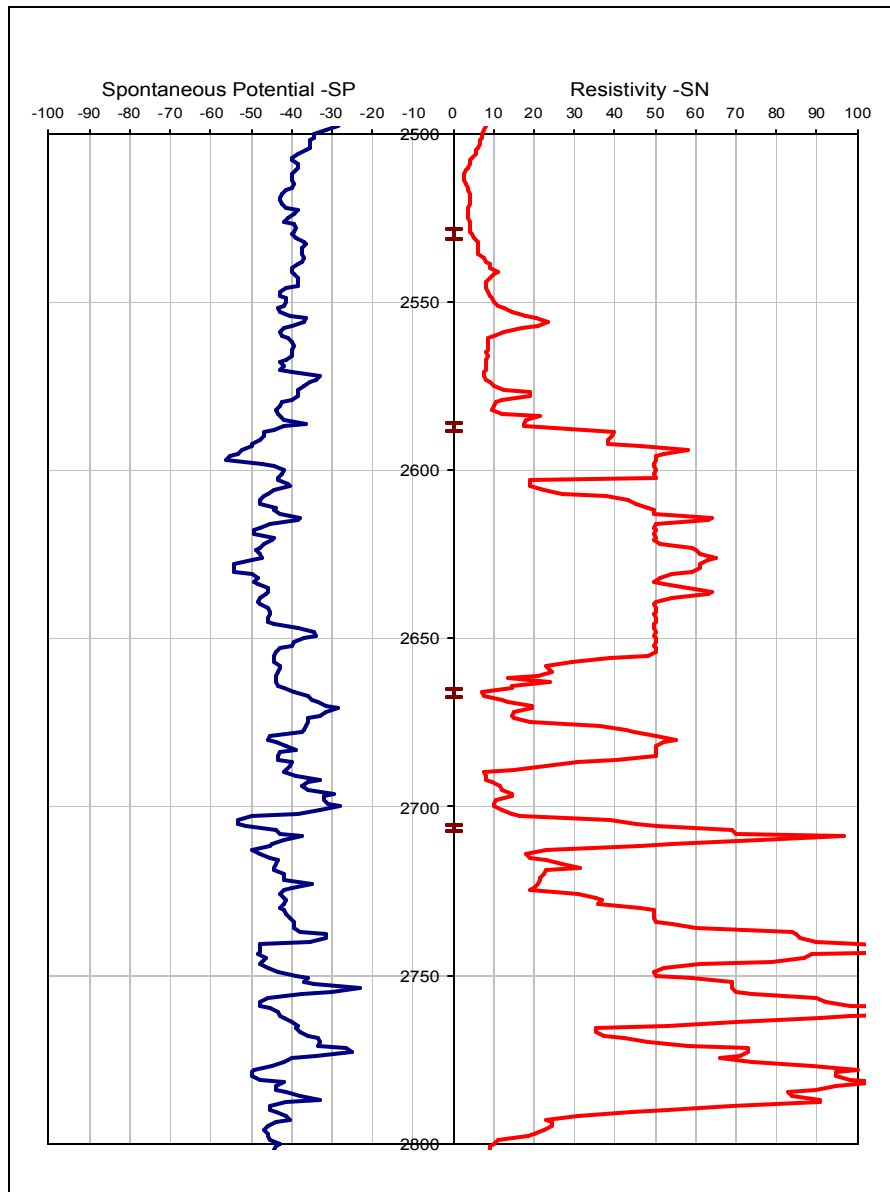


Fig. 4.1-Log from Well LL-231 and four intervals from which cores used in experiments were cut.

located. The configuration of the cell is meant to simulate the field conditions of a vertical well with the hotter zone being the one close to the wellbore and the cooler part

being furthest from the wellbore. However, the cell was placed in the vertical position to ensure a complete displacement of all the solution in the cell.

The main parameters related to the sand consolidation method most likely are as follows:

(i) Temperature and temperature gradient

The temperature and temperature gradient were controlled and measured during the experiments. Temperatures measured are at four different locations inside the cell (as explained in the previous chapter) and one right at the top of the cell to control the temperature of the solution entering the cell. Temperature data are recorded in 30-second intervals.

(ii) Treatment time

The treatment time is the period of time in which the sand pack is actually under the desired conditions of high temperature and pH. 6-hour treatment was attempted, based on the recommendation of Moreno⁴⁻⁷ to use more than 3 hours. However in some runs it was not possible to do so due to experimental conditions and for safety reasons.

(iii) Flow rate

The flow rate was kept constant at 20 cc/min in all the runs based on the procedure used by Nilsen³ and Moreno.⁴⁻⁷

(iv) *Solution composition (pH)*

The Na_2CO_3 concentration of 100 g/l was also kept constant to obtain a solution pH of 11.5 to 12. The same pH value was used in the experiments of Nilsen³ and Moreno⁴⁻⁷.

(v) *Soaking time after the experiment*

The soak time used was 2 to 3 days, following recommendations of Moreno.⁴⁻⁷

4.2 Run No. 1

This run was made with original sand (not cleaned of oil) from core taken from Bachaquero-01 reservoir, well LL-231 at depth 2528'-2531' (**Fig. 4.1**).

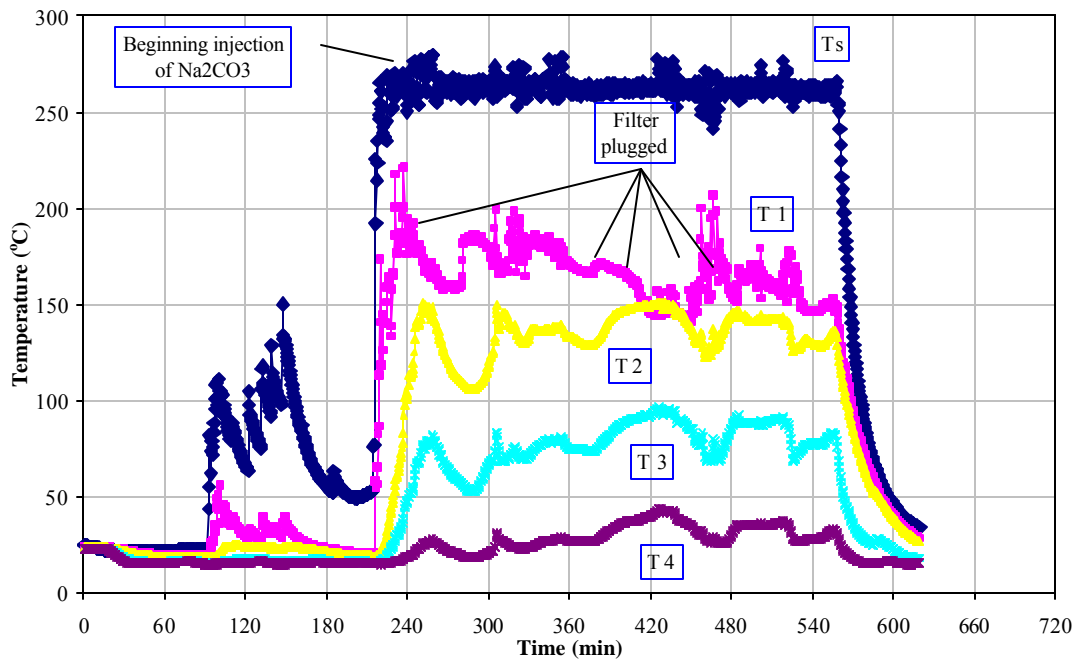


Fig. 4.2-Temperature profiles for run no. 1.

We start this run injecting distilled water until experimental conditions were reached, and then injection of sodium carbonate was initiated. Several times during the experiment the filter was plugged producing a sudden increase in injection pressure. We bypassed the filter, cleaned and installed it each time.

Temperature and pressure profiles for run no. 1 are shown in **Figs. 4.2** and **4.3**.

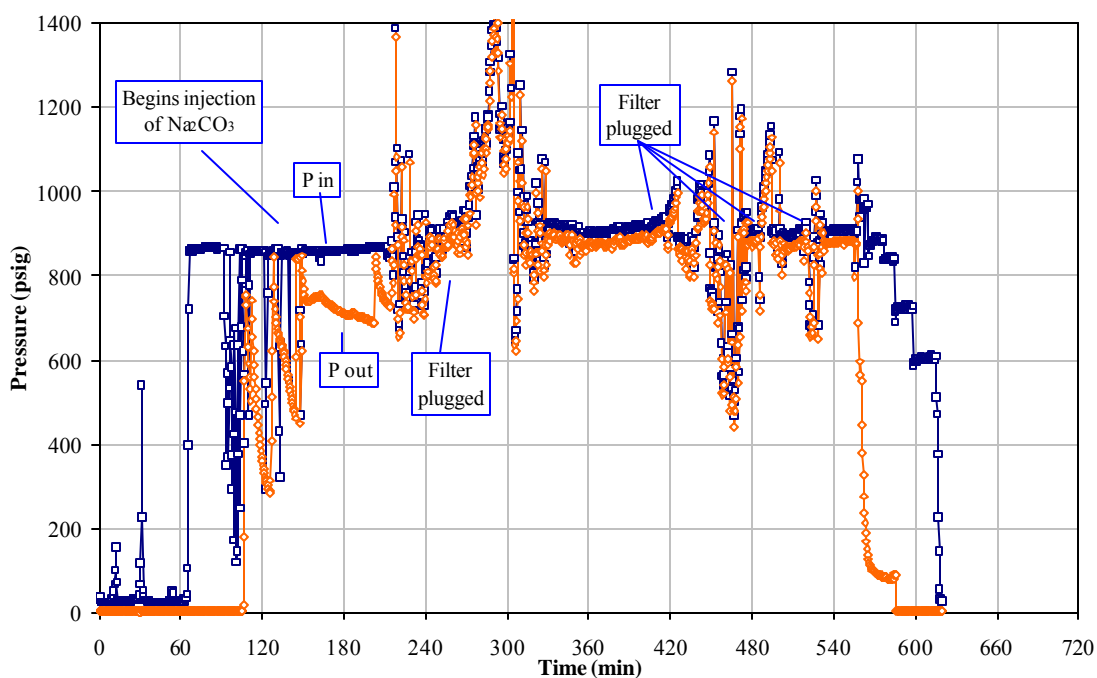


Fig. 4.3-Pressure profiles for run no. 1.

The temperature of the injected alkaline solution was kept around 260°C giving as a result 180°C at the top of the cell. The pressure profiles show that the pressure differential across the cell never exceeded 50 psig.

The pH of the effluent liquid was taken every 30 minutes. It stabilized around 11.3, almost the same as the original pH of 11.5, indicating little solution/sand-pack reaction. The curve showing the pH during this experiment is shown in **Fig. 4.4**.

The bottles of liquid samples after 60 until 240 minutes were dark because of the presence of oil. Little silica gel was observed the liquid samples. A picture of these is shown in **Fig. 4.5**.

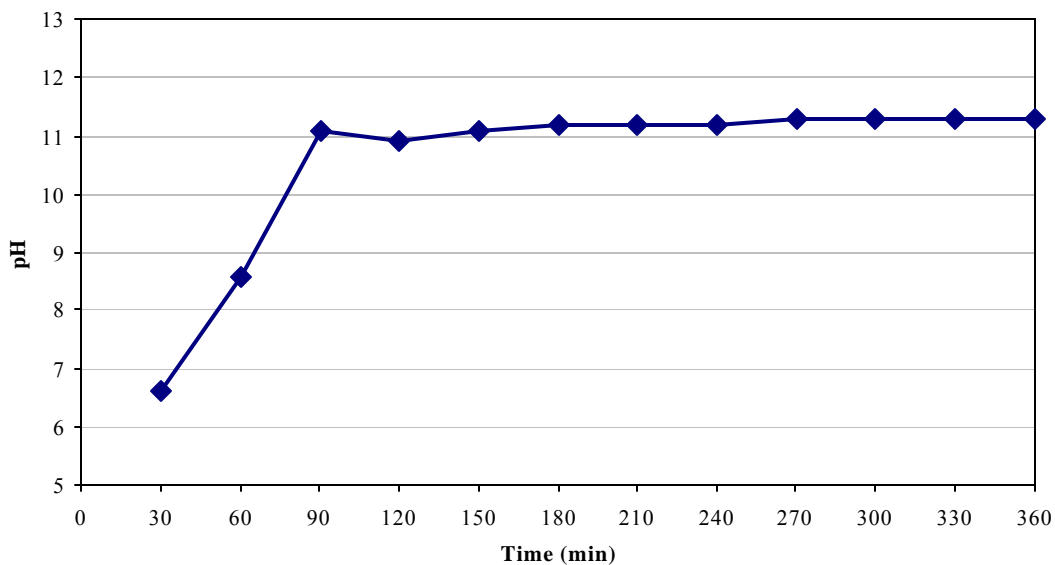


Fig. 4.4-Effluent liquid pH for run no. 1.



Fig. 4.5-Photograph of the effluent liquid after run no. 1.

After 60 hours, when the sand was removed we could see some packing and possible dissolution but no sign of consolidation was observed. Also the sample exhibited a very dark color indicating still high oil content. Photograph of the sample and the two zones are shown in **Fig. 4.6**.

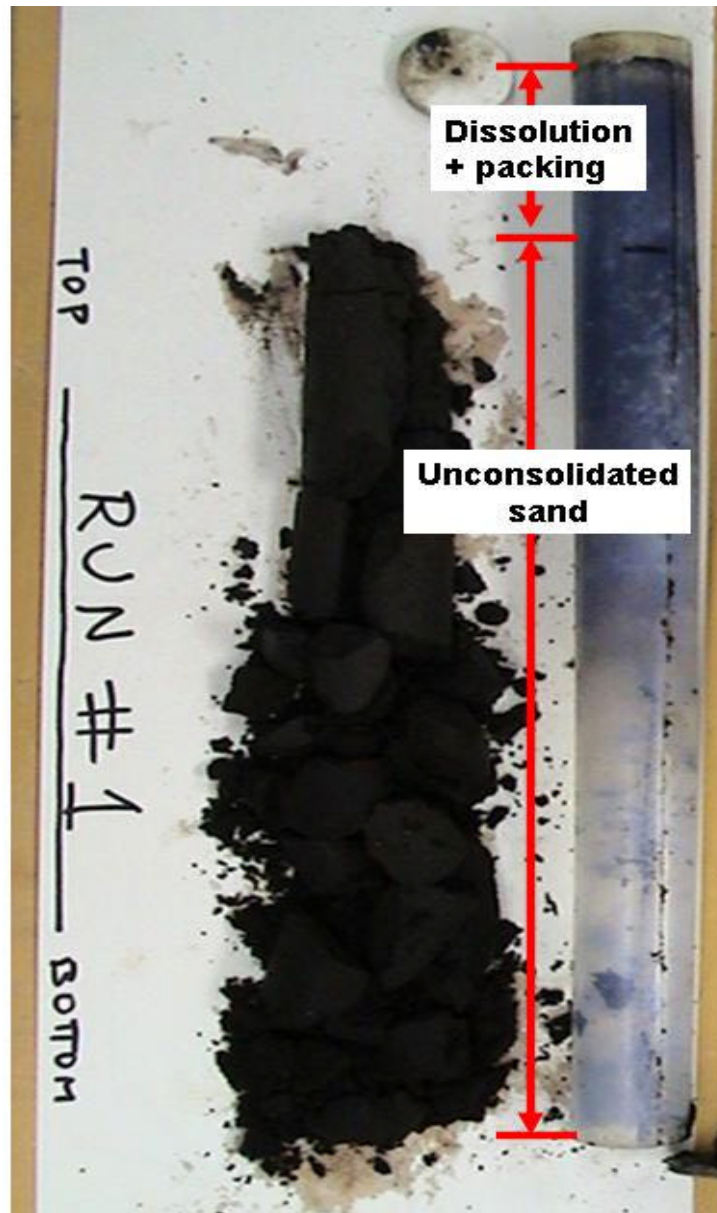


Fig. 4.6-Sand sample after run no. 1.

Sand samples were prepared and analyzed in the CAMECA SX50 Electron Microprobe at the Department of Geology and Geophysics. Photomicrographs of the sand before the experiment are presented in **Fig. 4.7**. These images show that poorly

sorted sand constitute the Bachaquero-01 reservoir. The composition of this sand was presented in **Table 1.2**. The BSE pictures show different tones of gray for different atomic weights, with the brighter being the heavier. The grains with two tones of gray in the BSE are feldspar grains with zones that have different compositions. Also, quartz grains, with only one tone of gray and rounded shape are common. Some grains of clays and mica (elongated and flakes) are also observed. At higher magnifications (**Fig. 4.8**), it is easier to observe also a fine grain aggregate mixture and hydrocarbon attached to the bigger grains.

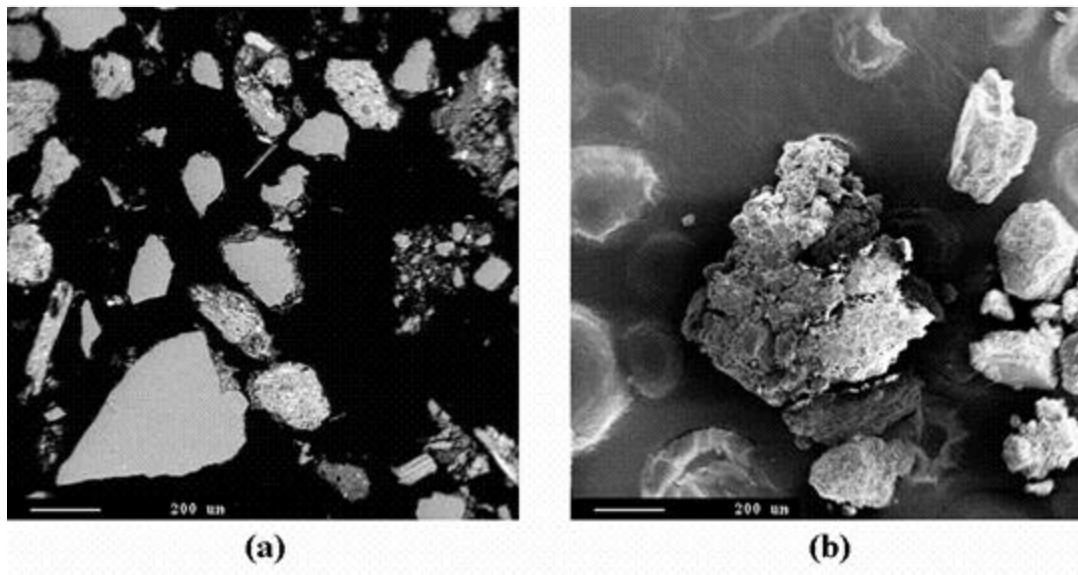


Fig. 4.7-Photomicrographs of the Bachaquero-01 sand before run no.1, (a) BSE image of the sectioned and polished epoxy-mounted sand grains at 63x, (b) SE image of the loose sand grains at 63x.

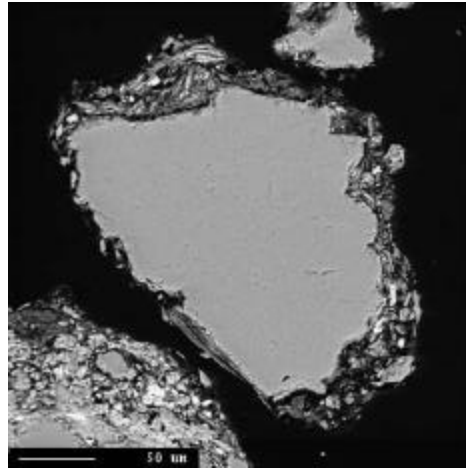


Fig. 4.8-BSE image of Bachaquero-01 sand at 300x.

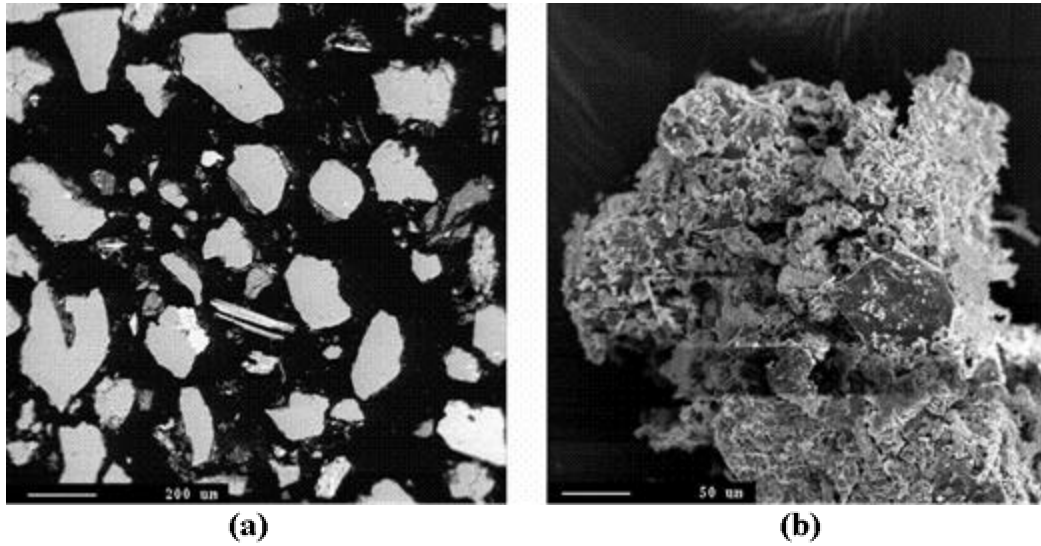


Fig. 4.9-Photomicrographs of the Bachaquero-01 sand at top of the cell after run no. 1 (a) BSE image of the sectioned and polished epoxy-mounted sands grains at 63x, (b) SE image of the sand grains at 250x.

Samples of the sand at the top of the cell after the experiments were also prepared and analyzed. Pictures of the sand sample are shown in **Fig. 4.9**.

At higher magnifications, we did not observe any signs of dissolution or evidence of formation of new minerals. Photograph of sand sample after run no. 1 at 300x is presented in **Fig. 4.10**.

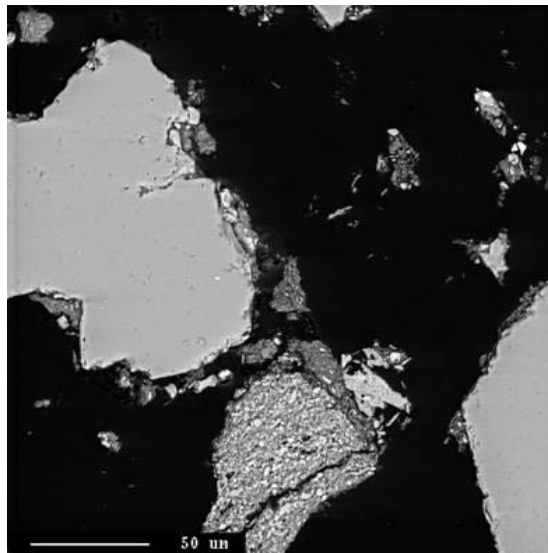


Fig. 4.10-BSE image of Bachaquero-01 sand after run no. 1 at 300x.

It is believed that the observed hydrocarbon layer attached to the bigger grains and possibly the low temperature reached during the experiment are probably responsible for the lack of consolidation.

4.3 Run No. 1a

Because of the high oil content in the sand after run no.1, we decided to reuse the sample from run no. 1 in run no. 1a. We placed it at the top of the cell and added about two inches of industrial silica sand at the bottom to complete the volume required to fill the Teflon tubing. We start this run injecting distilled water. After experimental conditions were reached, sodium carbonate was injected. Because of the low temperature reached during run no. 1, we decided from now on to isolate the top half of the cell using fiberfax, in order to reduce heat losses.

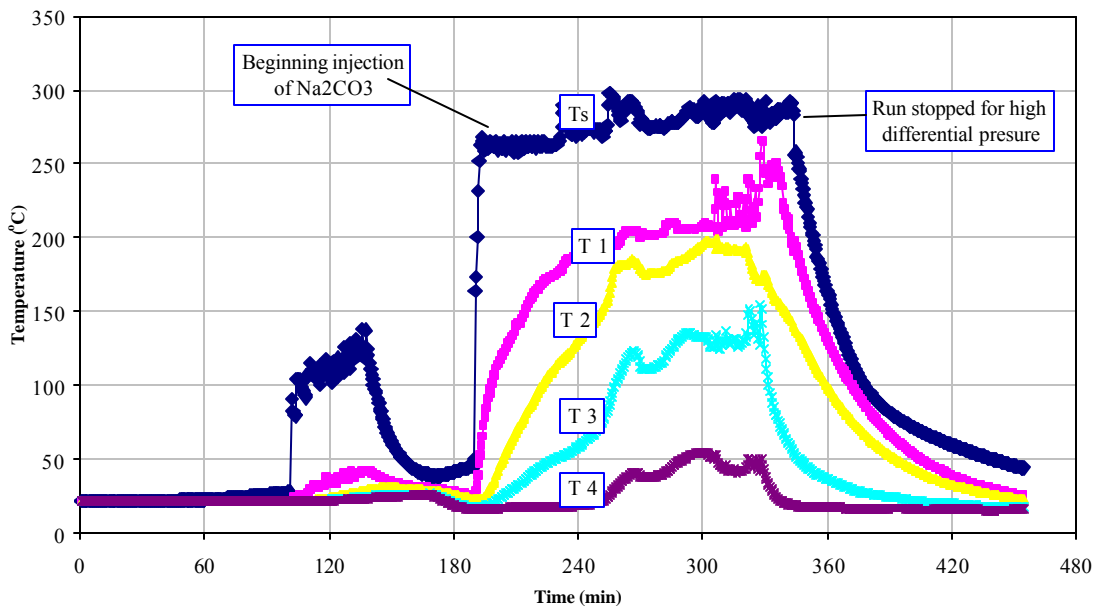


Fig. 4.11-Temperature profiles for run no. 1a.

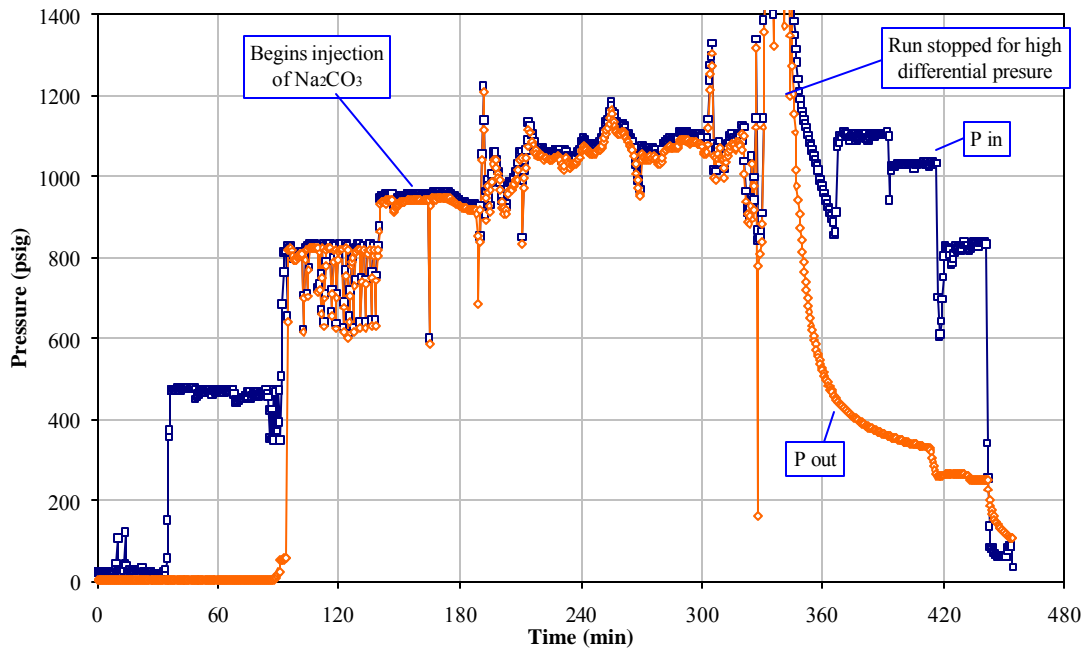


Fig. 4.12-Pressure profiles for run no. 1a.

After 120 min of injection of Na_2CO_3 a very high differential pressure was observed due to plugging so, it was decided to stop the experiment for safety reasons. The temperature and pressure profiles are shown in **Figs. 4.11** and **4.12**.

The temperature of the injected alkaline solution was kept between 260°C and 280°C giving as a result temperatures ranging 180°C to 250°C at the top of the cell. The pressure profiles show that the pressure differential across the cell exceeded 500 psig at the time of the stop of the experiment.

The pH of the effluent liquid was taken every 30 minutes. The average value of the three samples taken was about 10.72, below the original pH of 11.5. This indicated possible solution/sand-pack reaction but very little silica gel was observed in the liquid

samples contradicting the previous statement of reaction. The graph showing the pH during this experiment is shown in **Fig. 4.13**

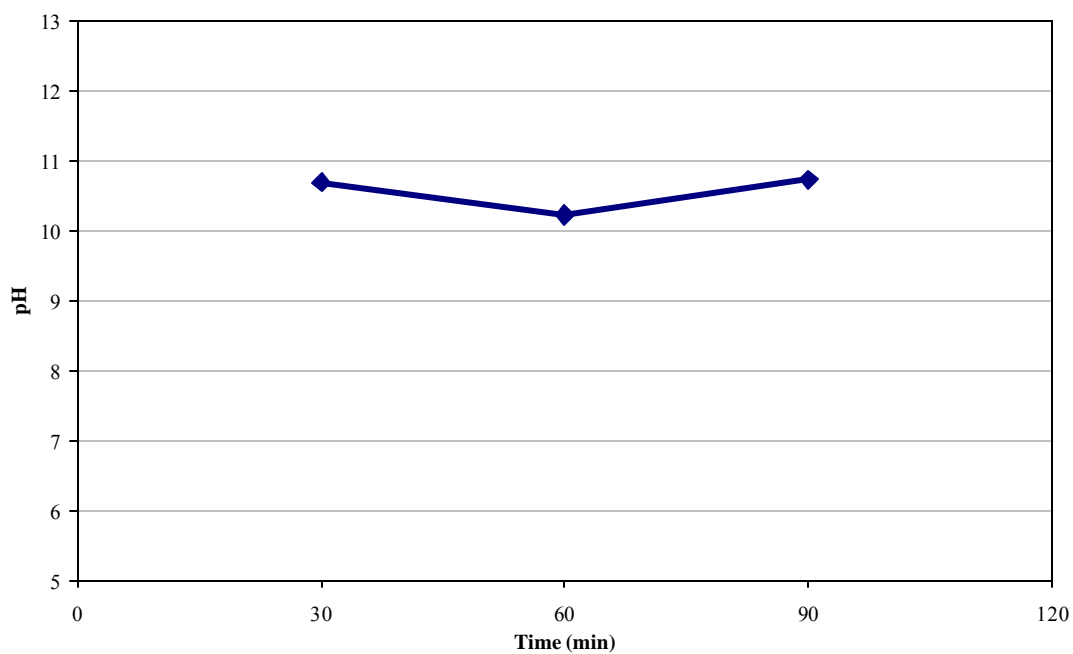


Fig. 4.13-Effluent liquid pH for run no. 1a.

The liquid samples were dark, indicating the presence of oil. A photograph of these samples is shown in **Fig. 4.14**.

After 36 hours, when the sand was removed from the cell we observed some packing but no sign of consolidation and the sample still showed a dark color. Photograph of the sample is shown in **Fig. 4.15**. Sand samples after the experiment were prepared and subjected to electron microprobe analysis. The images of the sand grains after the experiment at the top of the cell are shown in **Fig. 4.16**.

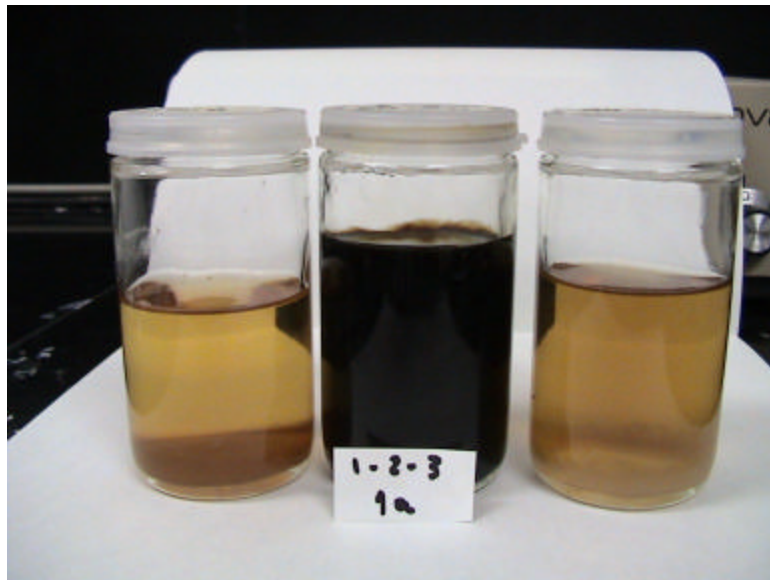


Fig. 4.14-Photograph of the effluent liquid samples after run no. 1a.

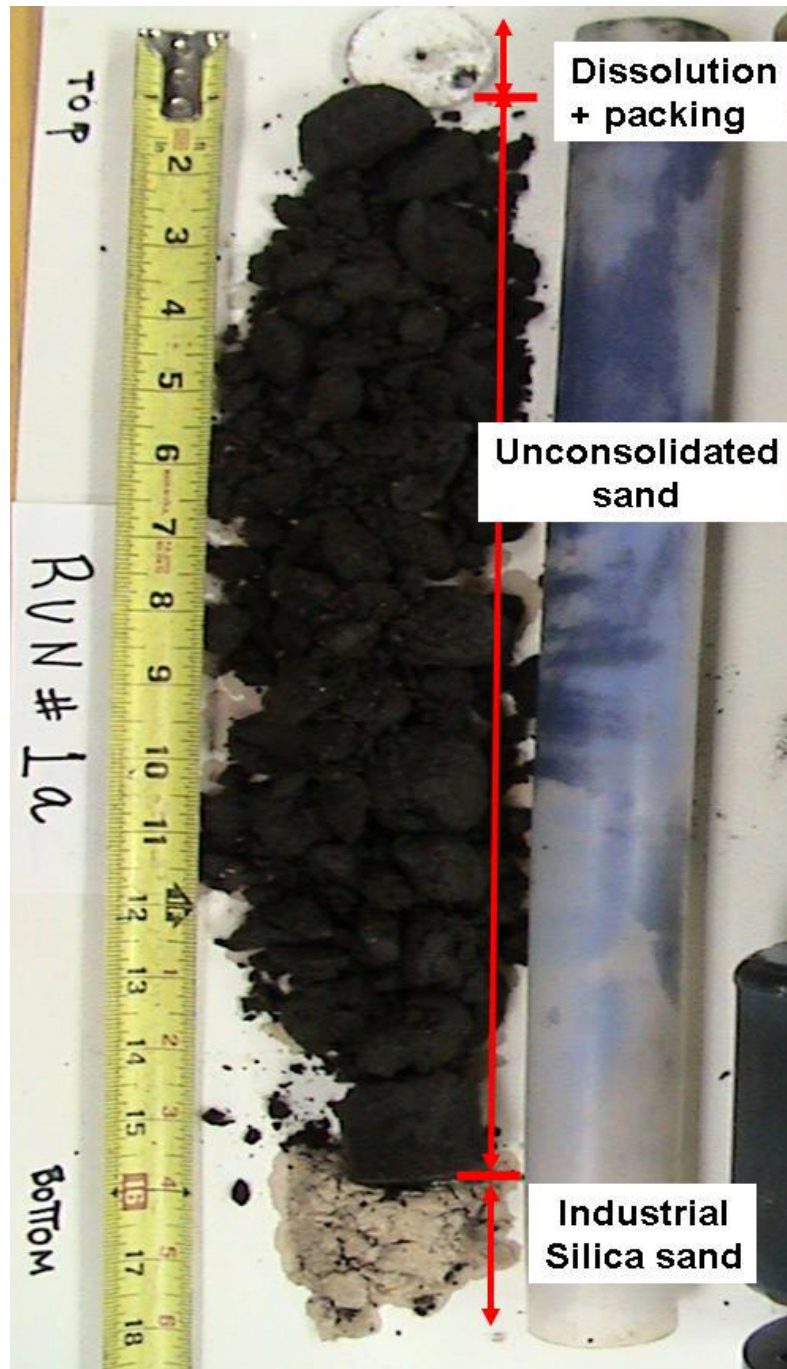


Fig. 4.15-Sand sample after run no. 1a.

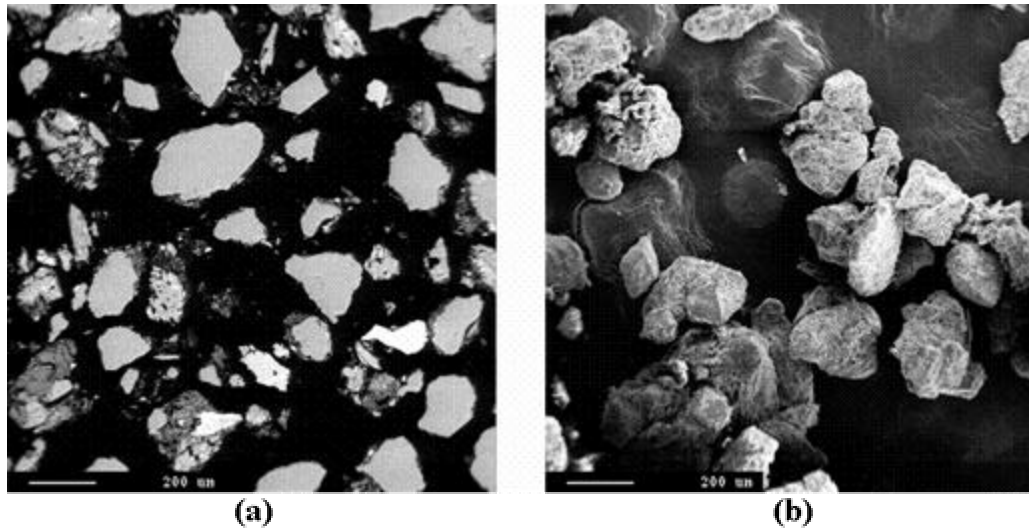


Fig. 4.16-Photomicrographs of the Bachaquero-01 sand after run no.1a, (a) BSE image of the sectioned and polished epoxy-mounted sand grains at 63x, (b) SE image of the loose sand grains at 63x.

There was no evidence of reaction or new minerals being formed. There was nothing really well crystallized. The only noteworthy observation was the original material being covered with hydrocarbon and some sodium carbonate.

It is believed that the observed hydrocarbon layer attached to the bigger grains and the little time of exposure to the alkaline solution during the experiment, are most probably responsible for the lack of consolidation.

4.4 Run No. 1b

This run was made using the sand sample remaining after run no.1a mixed with original sand used in run no.1. We start this run injecting distilled water for about 90 min. until the experimental conditions were reached, and then sodium carbonate was injected. We continue using fiberfax to isolate the top half of the cell.

After 2 hours of injection of Na_2CO_3 a very high differential pressure was observed so, it was decided to stop the experiment. The temperature and pressure profiles are shown in **Figs. 4.17** and **4.18**.

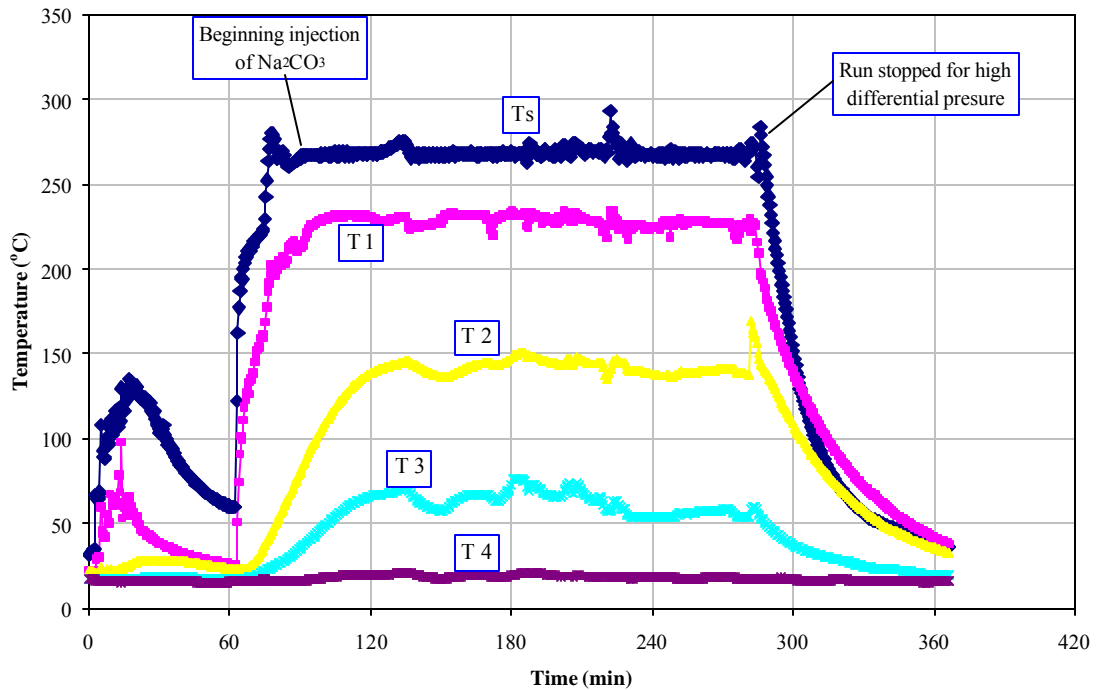


Fig. 4.17-Temperature profiles for run no. 1b.

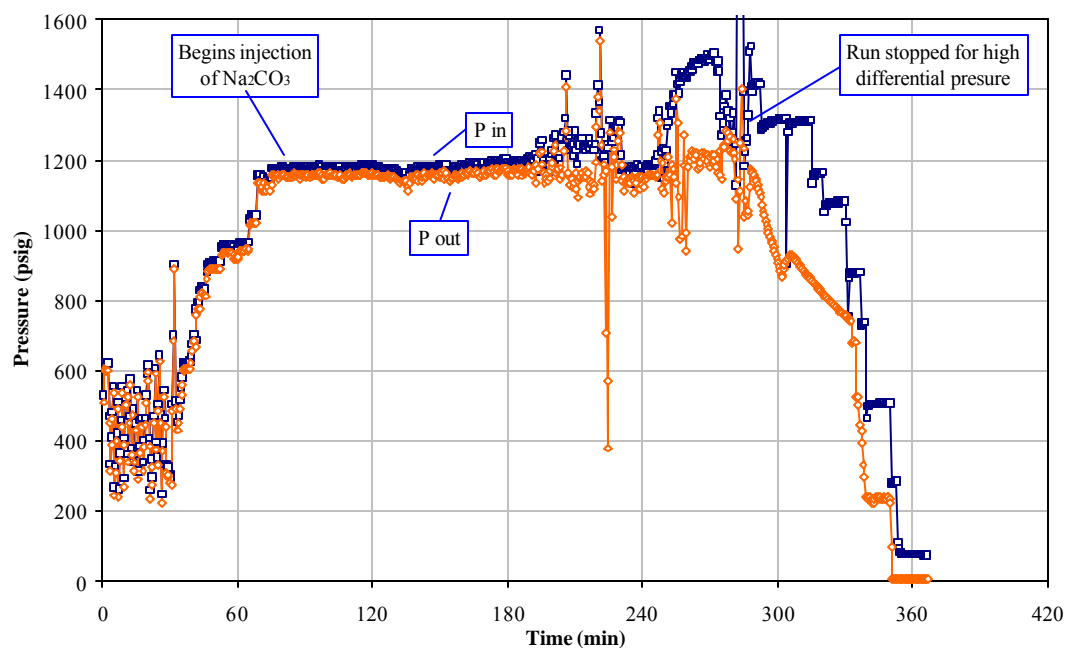


Fig. 4.18-Pressure profiles for run no. 1b.

The temperature of the injected alkaline solution was kept around 270°C giving as a result about 230°C at the top of the cell. The pressure profiles show that the pressure differential across the cell exceeded 500 psig at the time of the stop of the experiment.

The pH of the effluent liquid was taken every 30 minutes. It stabilized around 11.2, almost the same as the original pH of 11.5, indicating little solution/sand-pack reaction. The curve showing the pH during this experiment is shown in **Fig. 4.19**.

The oil content in the liquid samples increased until 90 min (very dark color), then the presence of oil decreased and the last sample showed just a yellowish appearance. The samples after 120 min exhibit also abundant silica gel. A photograph of these samples is shown in **Fig 4.20**.

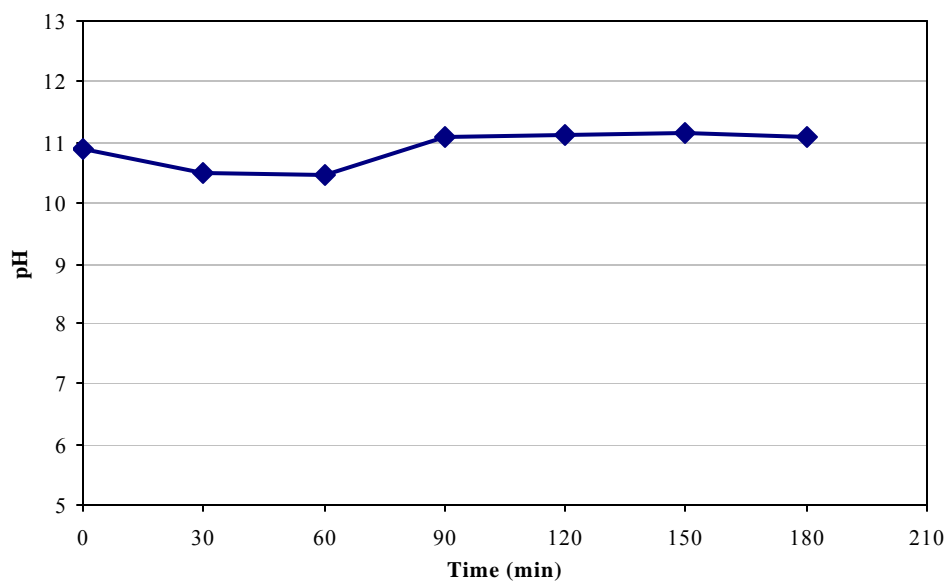


Fig. 4.19-Effluent liquid pH for run no. 1b.

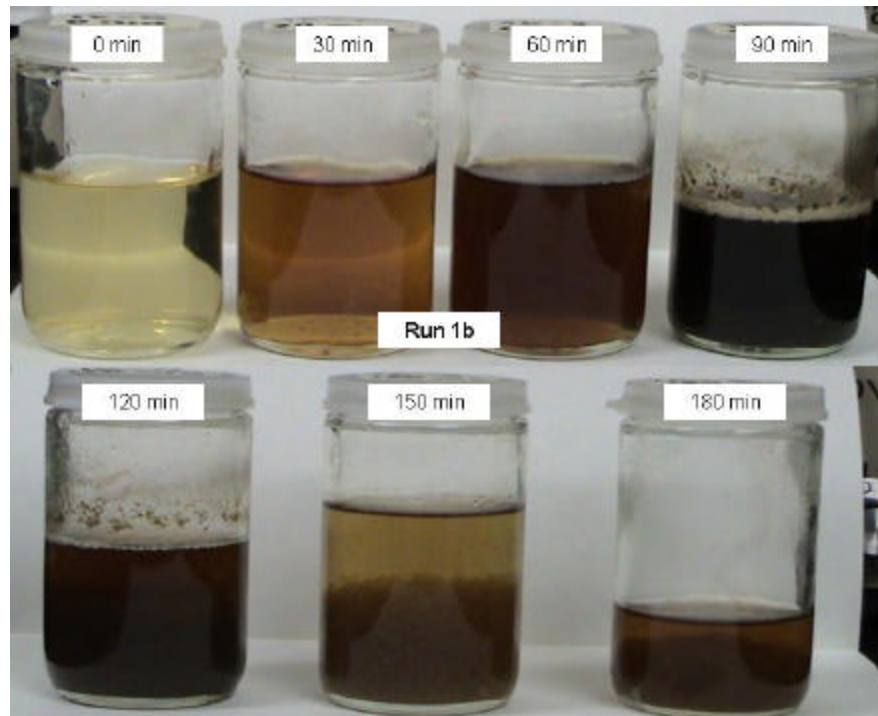


Fig. 4.20-Photograph of the effluent liquid samples after run no. 1b.

After 36 hours, when the sand was extracted from the cell we noticed some packing but no sign of consolidation. The sample still exhibited a dark color indicating oil content. Photograph of the sample is presented in **Fig. 4.21**.

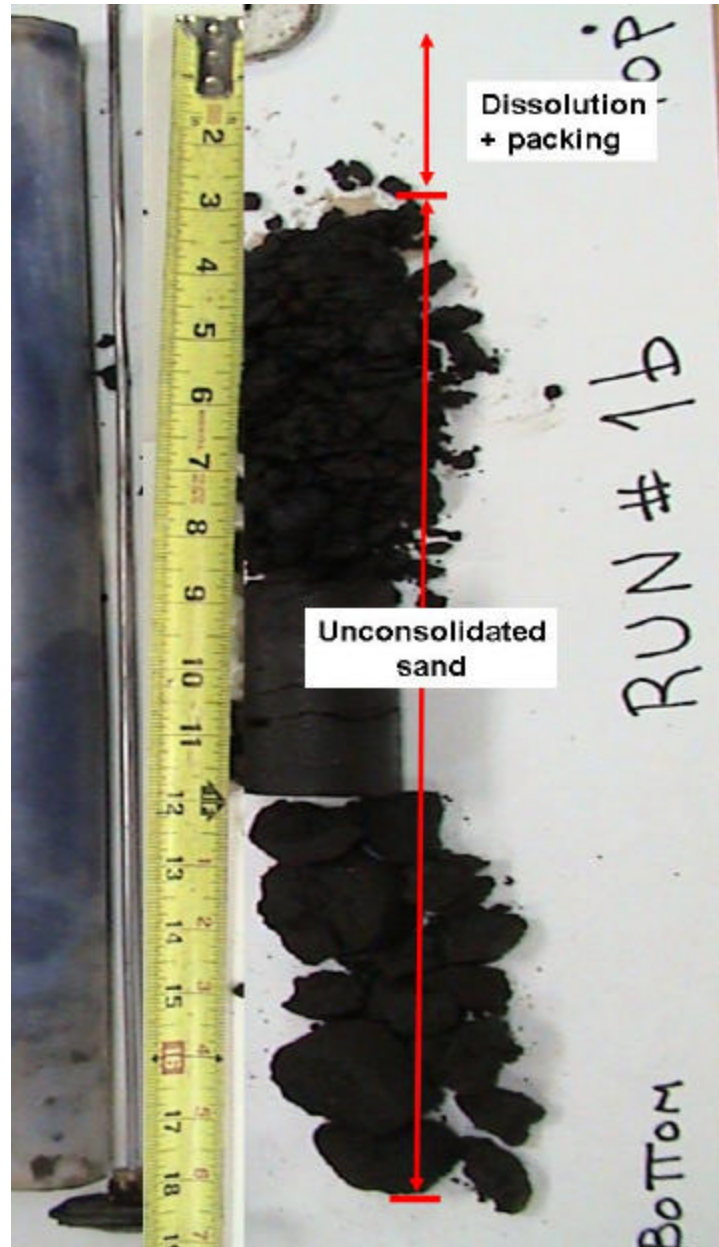


Fig. 4.21-Sand sample after run no. 1b.

Sand samples after the experiment were prepared for analysis with the electron microprobe. The images of the sand grains are presented in **Fig. 4.22**.

The images after the experiment are similar to those in previous runs (no. 1 and no. 1b). No signs of secondary phases are observed.

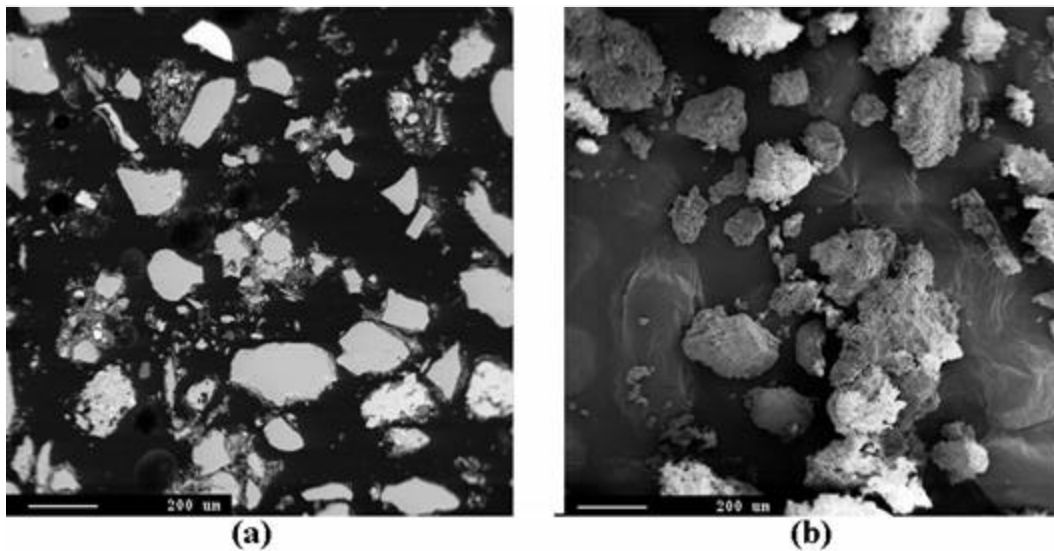


Fig. 4.22-Photomicrographs of the Bachaquero-01 sand after run no.1b, (a) BSE image of sectioned and polished epoxy-mounted sand grains at 63x, (b) SE image of the loose sand grains at 63x.

It is believed that the time of exposure to the sodium carbonate was not enough to clean the sand grains of oil, and therefore this oil coating did not allow the reaction to occur.

4.5 Run No. 2

This run was made with sand sample from the core taken from Bachaquero-01 reservoir, well LL-231 at depth 2586'-2588' (**Fig. 4.1**).

Because of the negative results obtained in the previous runs, possibly caused by the high oil content in the samples, we decided to clean the sample in the cell by injecting toluene and water alternately (about one pore volume each) for about 7 hrs. We applied this process the day before.

We start this run injecting distilled water until experimental conditions were reached, and then injection of sodium carbonate was initiated. After two hours from the beginning of the injection of Na_2CO_3 , the filter was plugged several times caused by the silica gel in the effluent liquid. We decided to bypass the filter and finish the experiment without it. One hour later both the inlet and outlet pressures increased to almost 1600 psig. We immediately stopped injection and waited until the pressures decreased; then we started pumping again. This process was repeated seven times until it was not possible to decrease the pressure. We then decided to stop the run. The differential pressure profile shown in **Fig. 4.23** show how difficult it was to control the pressure during the experiment.

The temperature of the injected alkaline solution was kept around 270°C giving as a result about 235°C at the top of the cell. The temperature and pressure profiles for run no. 2 are presented in **Figs. 4.24** and **4.25**.

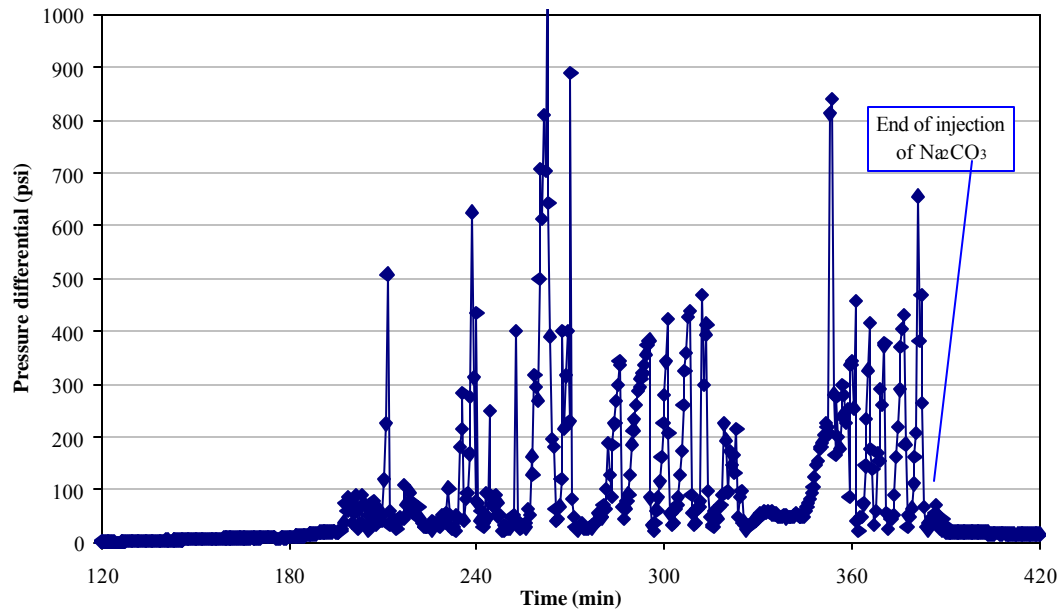


Fig. 4.23-Differential pressure profiles for run no.2.

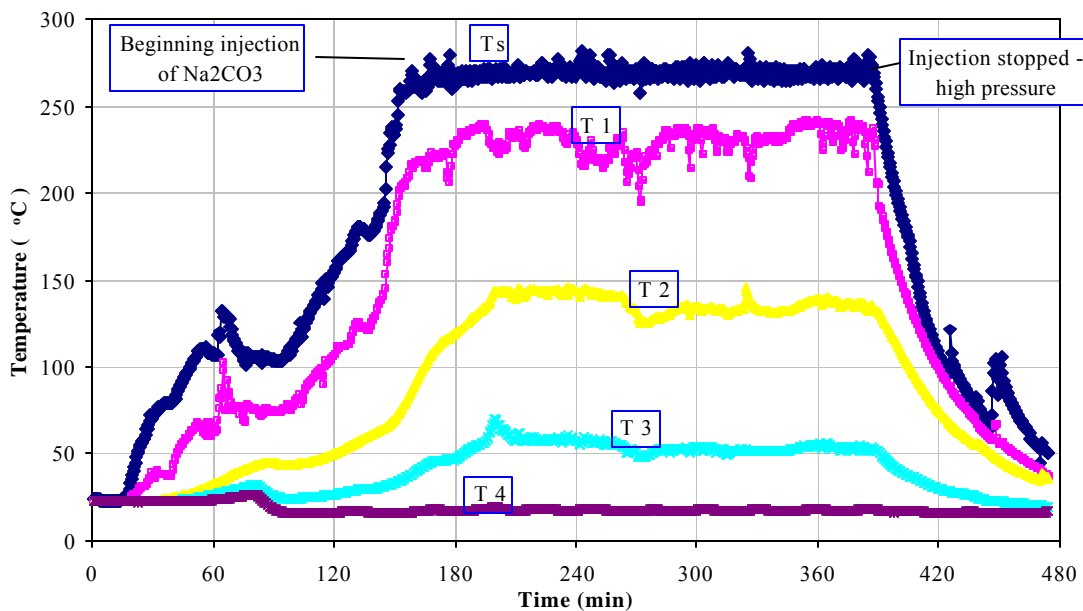


Fig. 4.24-Temperature profiles for run no. 2.

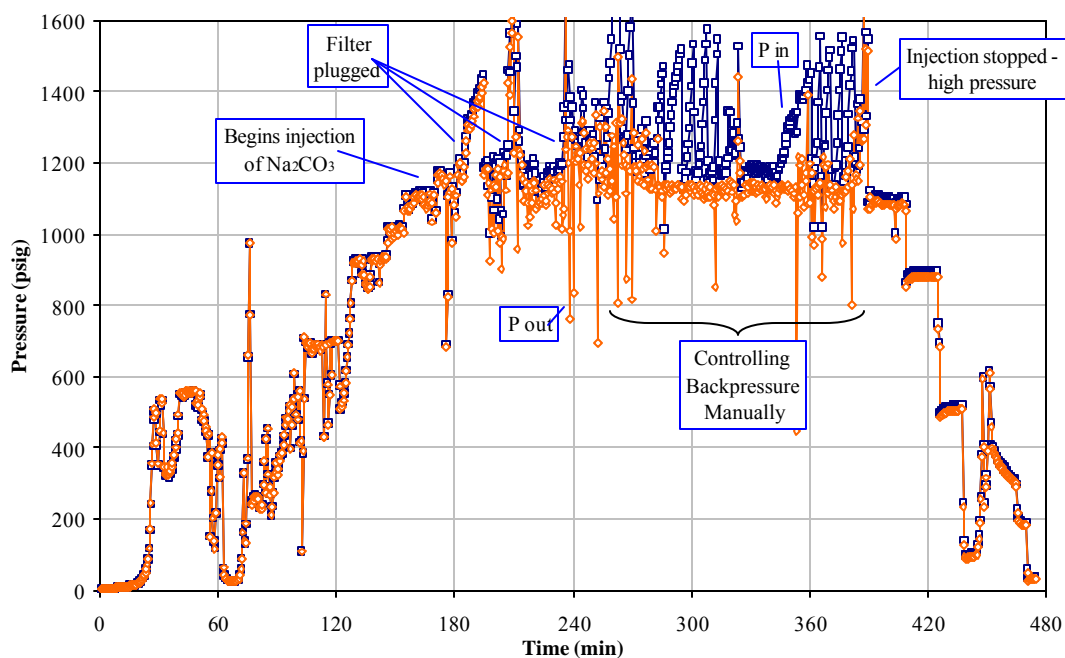


Fig. 4.25-Pressure profiles for run no. 2.

The pH of the effluent liquid was measured every 30 minutes. The graph showing the pH during this experiment is shown in **Fig. 4.26**.

It can be observed that all the bottles of liquid samples contain residue of oil especially those in the first 90 min. Very little silica gel was present in the samples. The samples from 120 to 210 minutes were fairly clear with a small content of oil. A photograph of these samples is shown in **Fig. 4.27**.

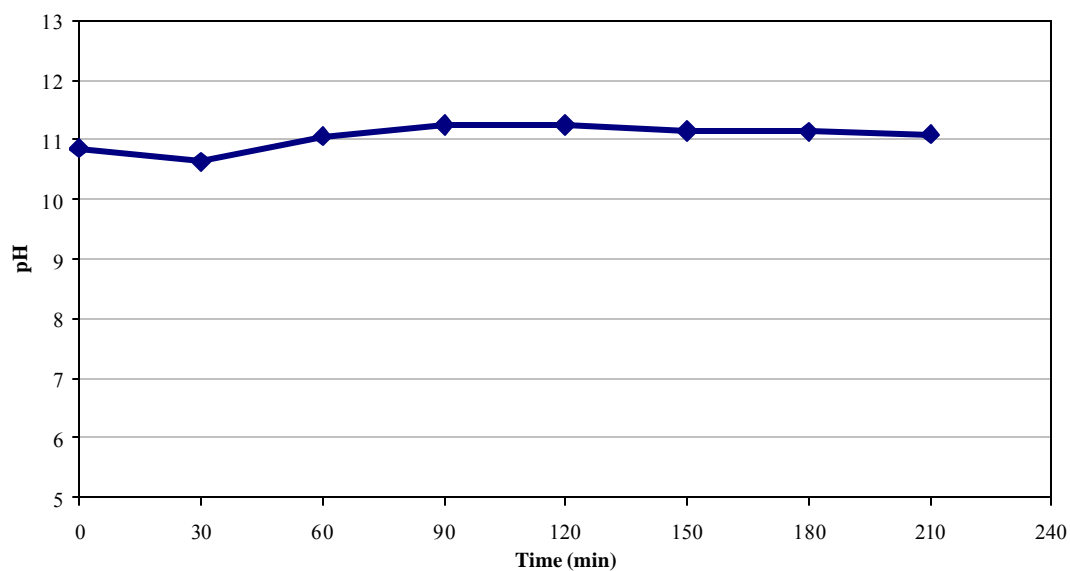


Fig. 4.26-Effluent liquid pH for run no. 2.

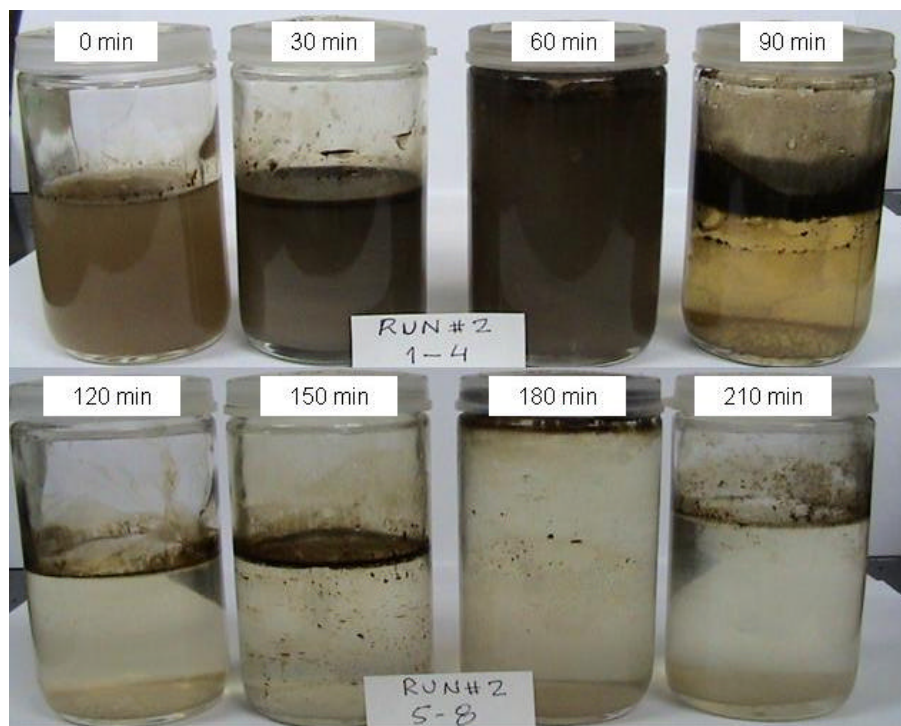


Fig. 4.27-Photograph of the effluent liquid after run no. 2.

After 96 hours, when the sand was taken out of the cell no consolidation was observed. We noticed the sample was dark in color indicating that oil was still present after the experiment. Also we observed liquid at the top of the cell, indicating some kind of plugging in the cell. Photograph of the sample is shown in **Fig. 4.28**.

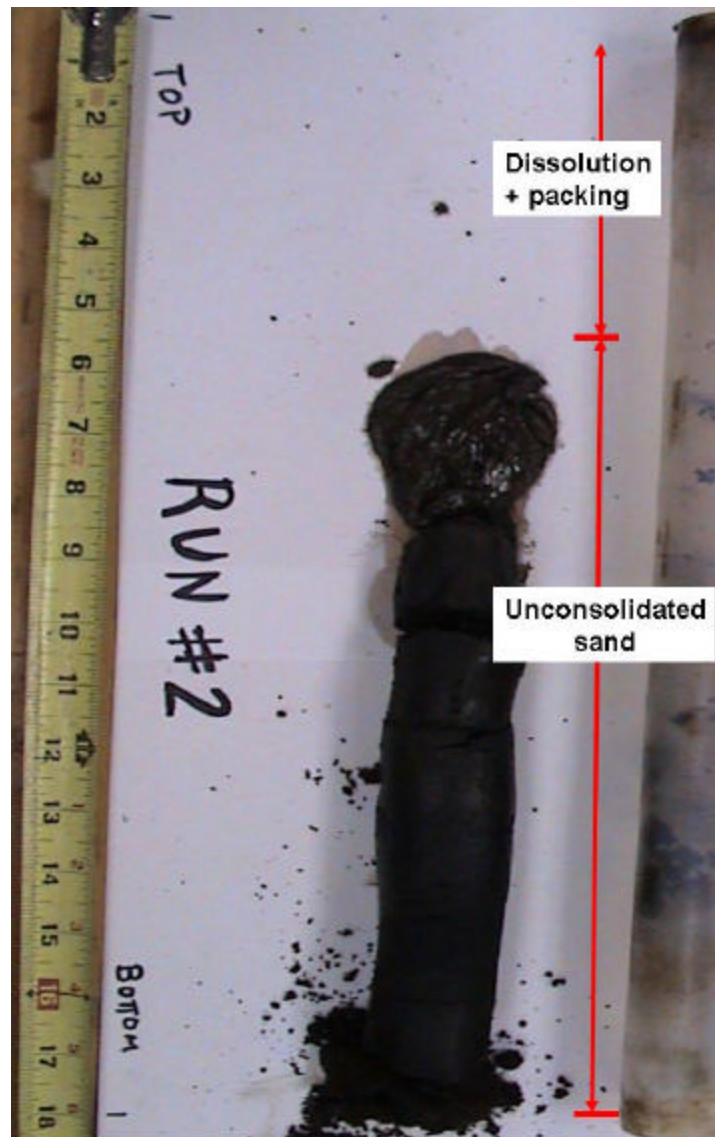


Fig. 4.28-Sand sample after run no. 2.

Electron microprobe images of the sand grains at the top of the cell after the experiment are presented in **Fig. 4.29**.

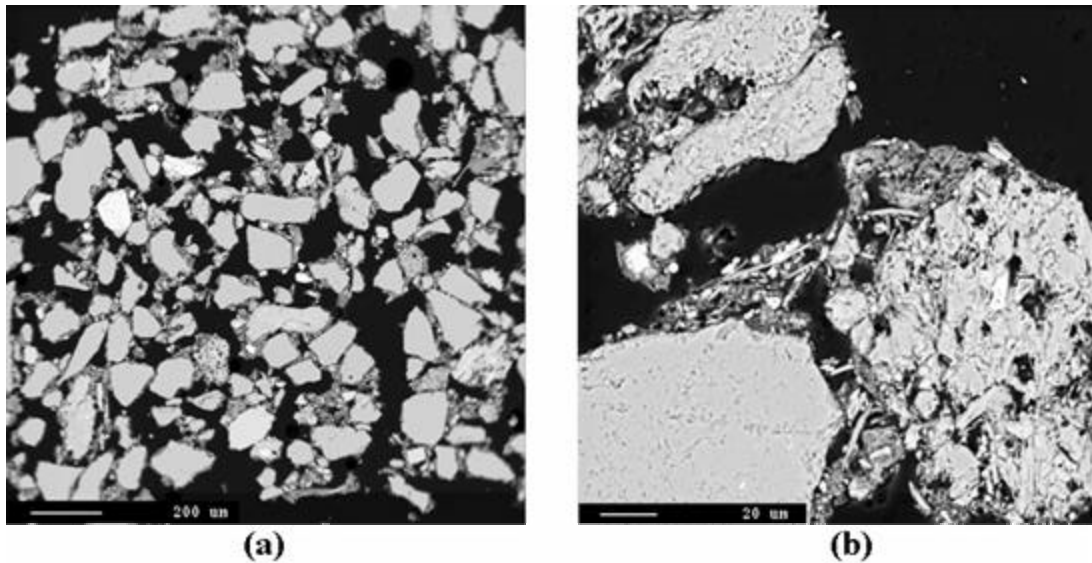


Fig. 4.29-Photomicrographs of the Bachaquero-01 sand after run no.2, (a) BSE image at 63x. (b) BSE image at 500x.

The BSE images do not show the presence of any secondary phase. One could see that a good amount of clays have not reacted with the sodium carbonate. Also a small amount of hydrocarbon is present in the images. In general they show no signs of precipitation or reaction.

4.6 Run No. 2d

For this run we used the same sand that remained after run no. 2. Because of the high oil content observed, we decided to first clean the sample in the cell, in order to reproduce field conditions, by using superheated steam. We injected steam for about 7 hr/day for three days. It is worth mentioning that we called the previous runs with cleanings 2a, 2b and 2c, hence this run is called run 2d. Also because of the high differential pressure obtained in run no. 2, we used just three sieves at the bottom of the cell. Temperature and pressure profiles for run no. 2d are shown in **Figs. 4.30** and **4.31**.

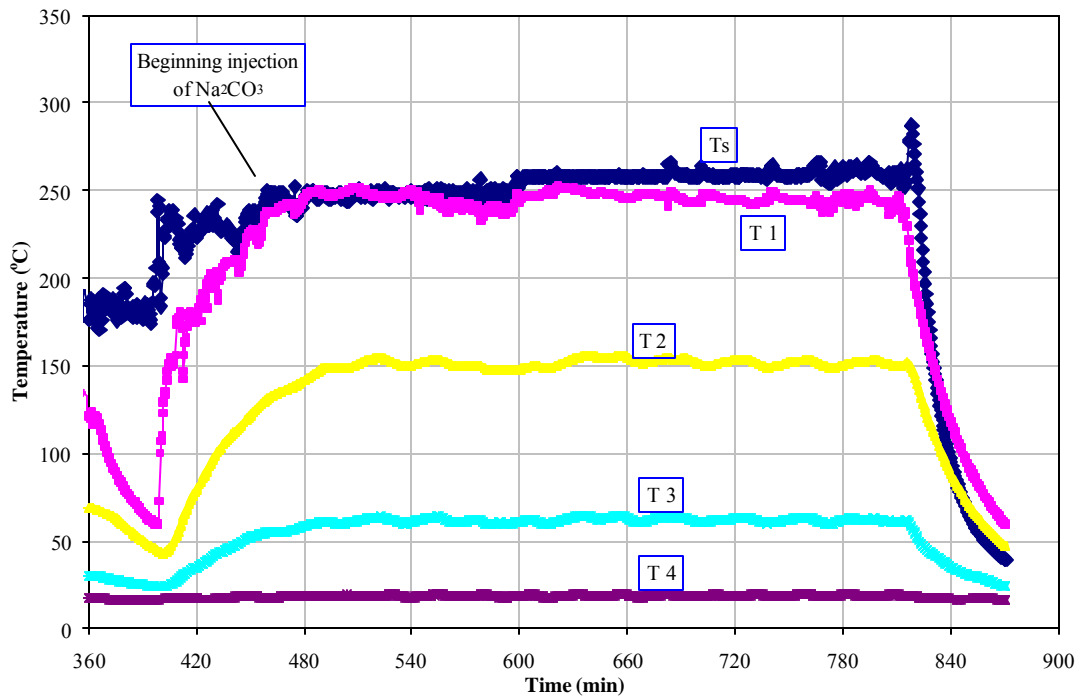


Fig. 4.30-Temperature profiles for run no. 2d.

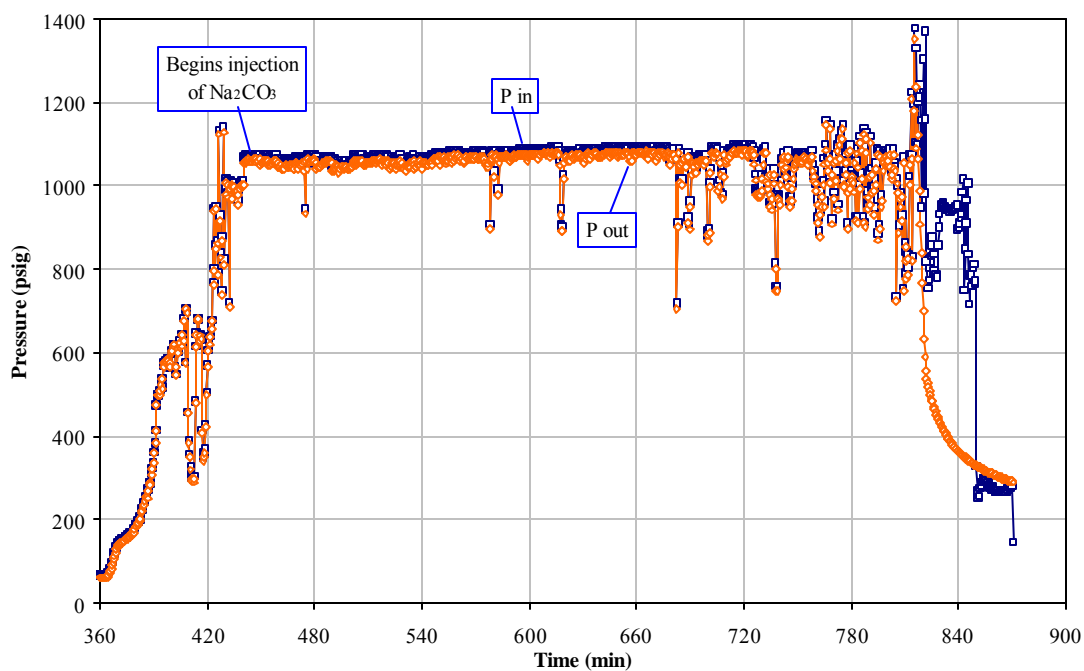


Fig. 4.31-Pressure profiles for run no. 2d.

The temperature of the injected alkaline solution was kept around 265°C giving as a result about 240°C at the top of the cell. The pressure profiles show that the pressure differential across the cell never exceeded 100 psig.

The pH of the effluent liquid was taken every 30 minutes. The curve showing the pH during this experiment is shown in **Fig. 4.32**.

The liquid samples were practically transparent with no residue of silica gel. A photograph of these samples is shown in **Fig. 4.33**.

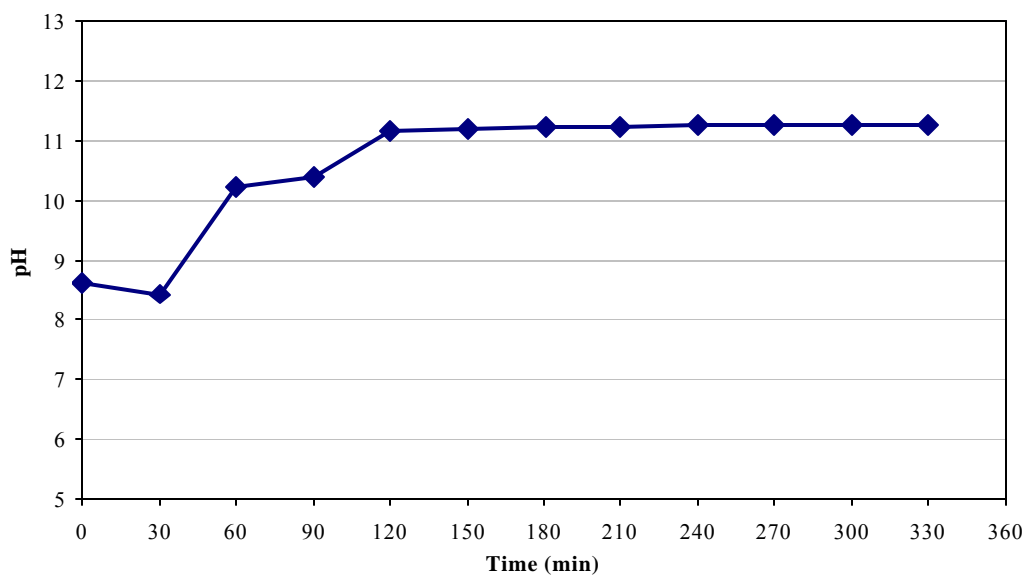


Fig. 4.32-Effluent liquid pH for run no. 2d.

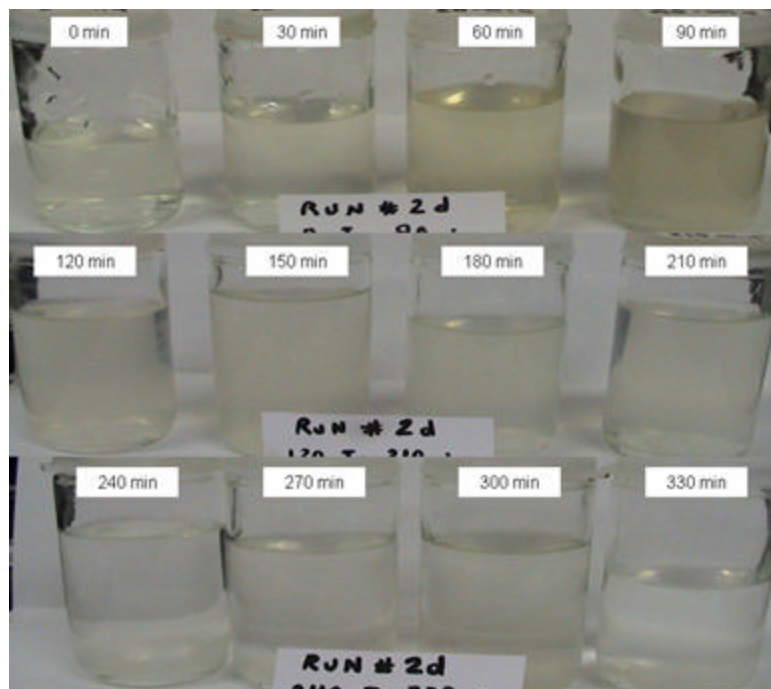


Fig. 4.33-Photograph of the effluent liquid samples for run no. 2d.

After 80 hr the sand was extracted from the cell. No consolidation was observed. We noticed the sample to be dark in color indicating that oil was still present after the experiment. Also we observed liquid on top of the cell, indicating some kind of plugging in the cell. Photograph of the sample is shown in **Fig. 4.34**.

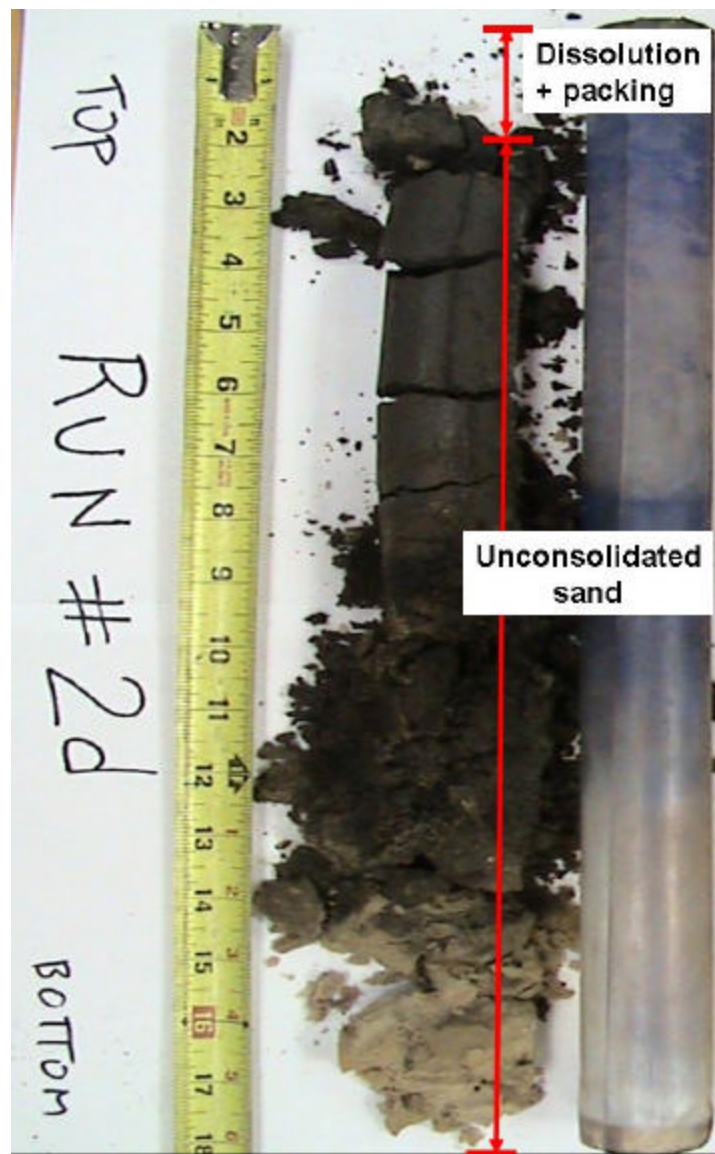


Fig. 4.34-Sand sample after run no. 2d.

The photomicrographs of the sand grains at the top of the cell after the experiment are presented in **Fig. 4.35**.

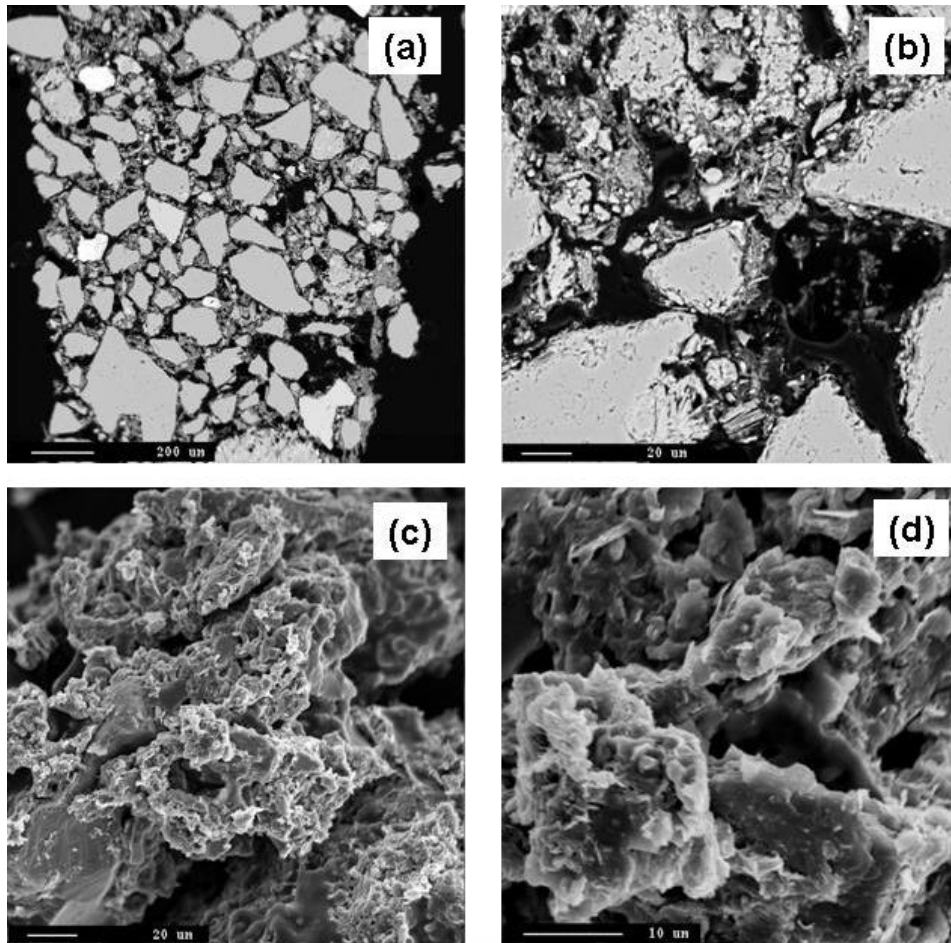


Fig. 4.35-Photomicrographs of the Bachaquero-01 sand after run no.2d, (a) BSE image of the sectioned and polished epoxy-mounted sand grains at 63x, (b) BSE image at 500x, (c) SE image of the loose sand grains at 500x (d) SE image at 2000x.

From the BSE and SE images we can not observe obvious alterations or secondary products. We can see fine grains piled on top of each other, but no signs of any secondary product.

4.7 Run No. 2f

Because there was still oil in the sample and no consolidation was obtained after run no. 2d, we decided to use the same sample for another experiment. We filled the cell up with the remaining sand, from the previous run, on the top half and industrial silica sand in the bottom half of the cell to complete the volume required to fill the cell.

As in the previous run, we decided to first clean the sample into the cell, in order to reproduce field conditions, by using this time xylene and hot water alternately (about one pore volume each slug). We injected 6 hr/day for 2 days before the run.

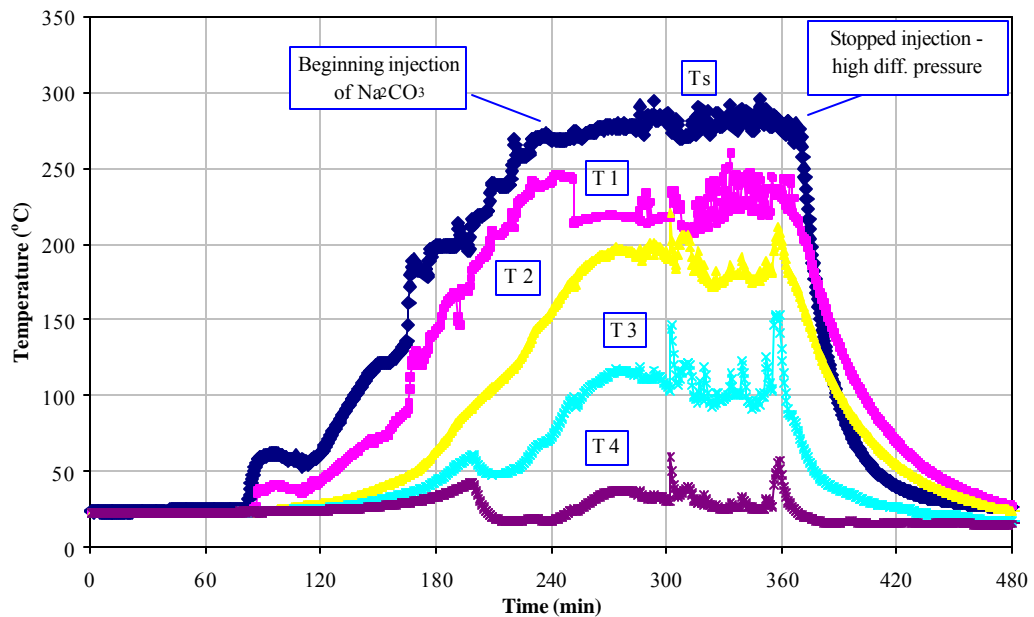


Fig. 4.36-Temperature profiles for run no. 2f.

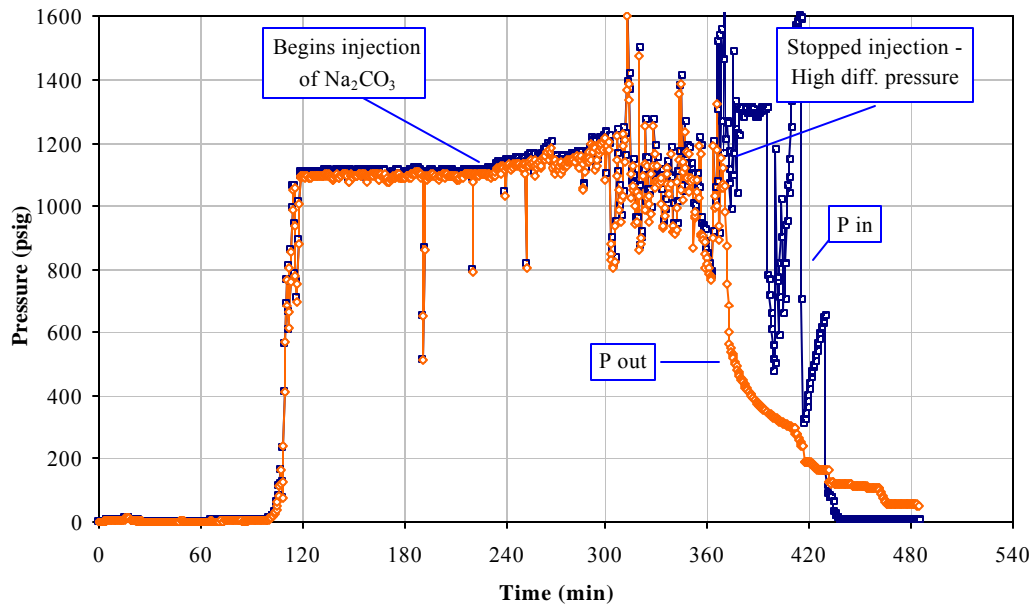


Fig. 4.37-Pressure profiles for run no. 2f.

After 2.5 hours of injection of sodium carbonate the run was aborted because of high differential pressure. Temperature and pressure profiles for run no. 2f are shown in **Figs. 4.36** and **4.37**.

The temperature of the injected alkaline solution was kept around 280°C giving as a result about 235°C at the top of the cell. The pressure profiles show that the pressure differential across the cell exceeded 500 psig at the time the run was aborted. **Fig. 4.38** shows the differential pressure profile during the experiment.

The pH of the effluent liquid was taken every 30 minutes. The graph showing the pH during this experiment is shown in **Fig. 4.39**.

The liquid samples showed some content of silica gel. The samples from 30 to 90 minutes were fairly clear with a small content of oil. A photograph of these samples is shown in **Fig. 4.40**.

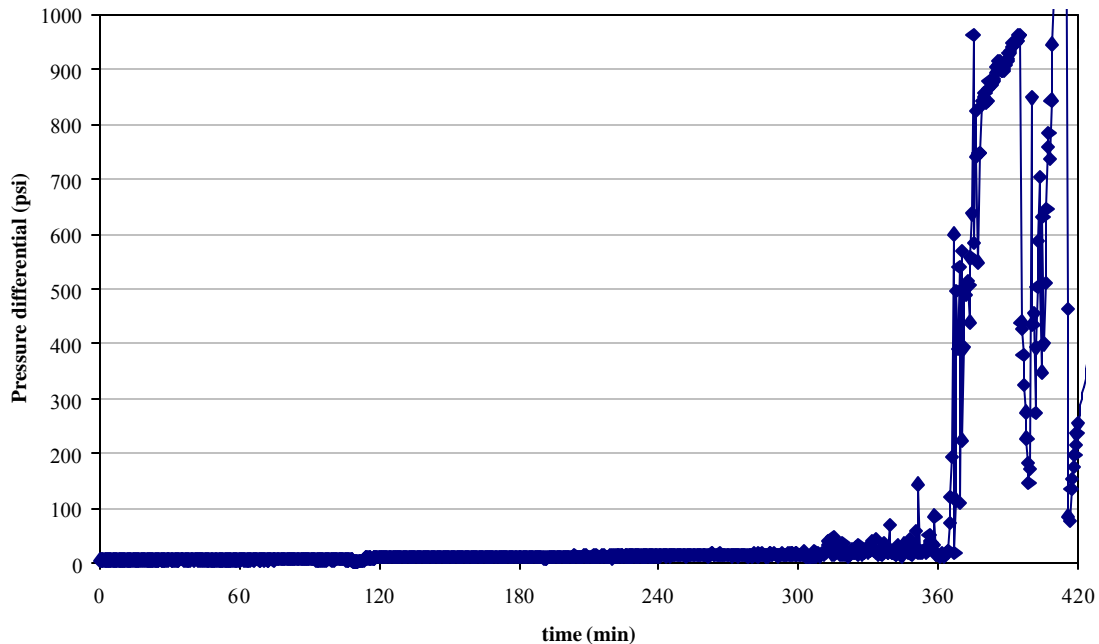


Fig. 4.38-Differential pressure profile for run no. 2f.

After 50 hours, when the sand was extracted from the cell, we noticed some packing but no evidence of consolidation. The sand sample after the experiment still exhibited a dark color indicating some oil content. Photograph of the sample is presented in **Fig. 4.41**.

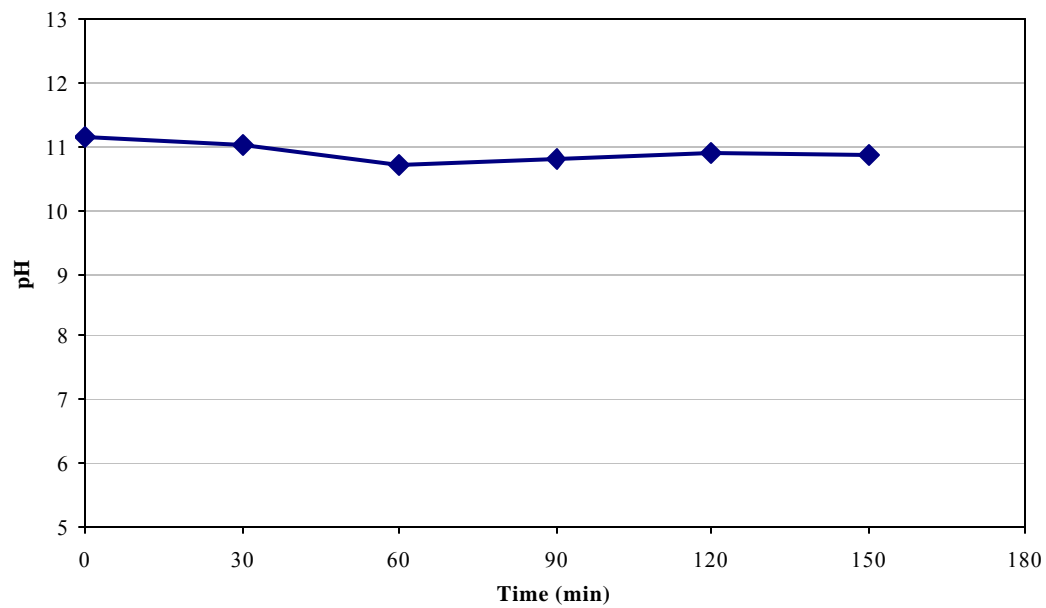


Fig. 4.39-Effluent liquid pH for run no. 2f.

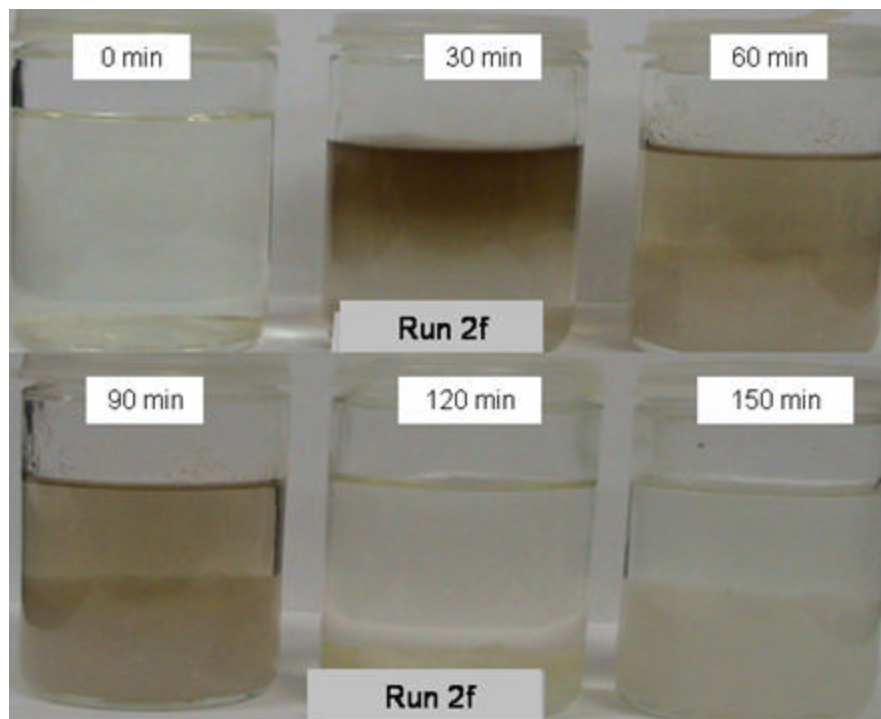


Fig. 4.40-Photograph of the effluent liquid after run no. 2f.

The photomicrographs of the sand grains at the top of the cell after the experiment are presented in **Fig. 4.42**.

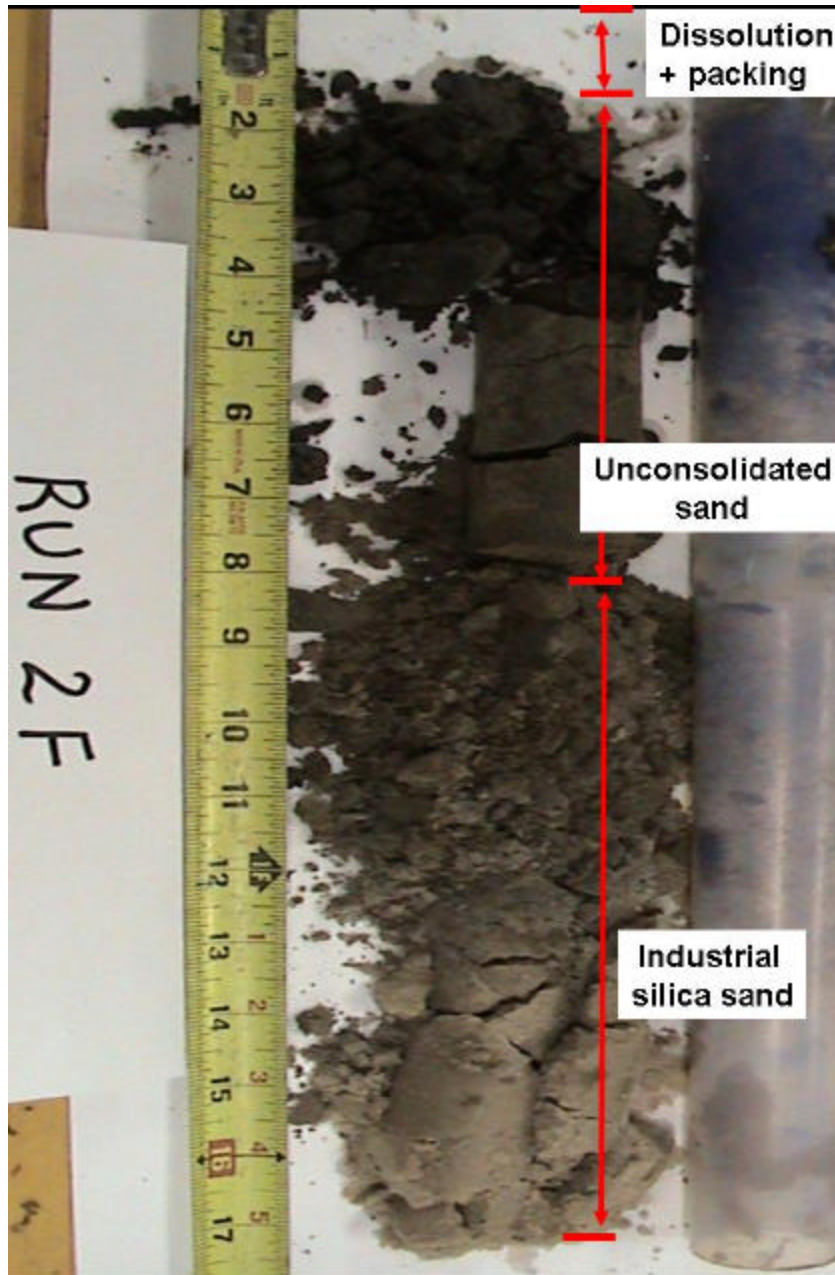


Fig. 4.41-Sand sample after run no. 2f.

The analysis of the photomicrographs shows alteration products but too few and too little to be analyzed in depth. The SE image at 1500x presents some secondary products that seem to be a rosette of zeolite, with a size of 1 to 2 microns which are too small to perform an EDS analysis. In conclusion we obtained what seem to be alteration products but in a quantity not enough to consolidate the grains.

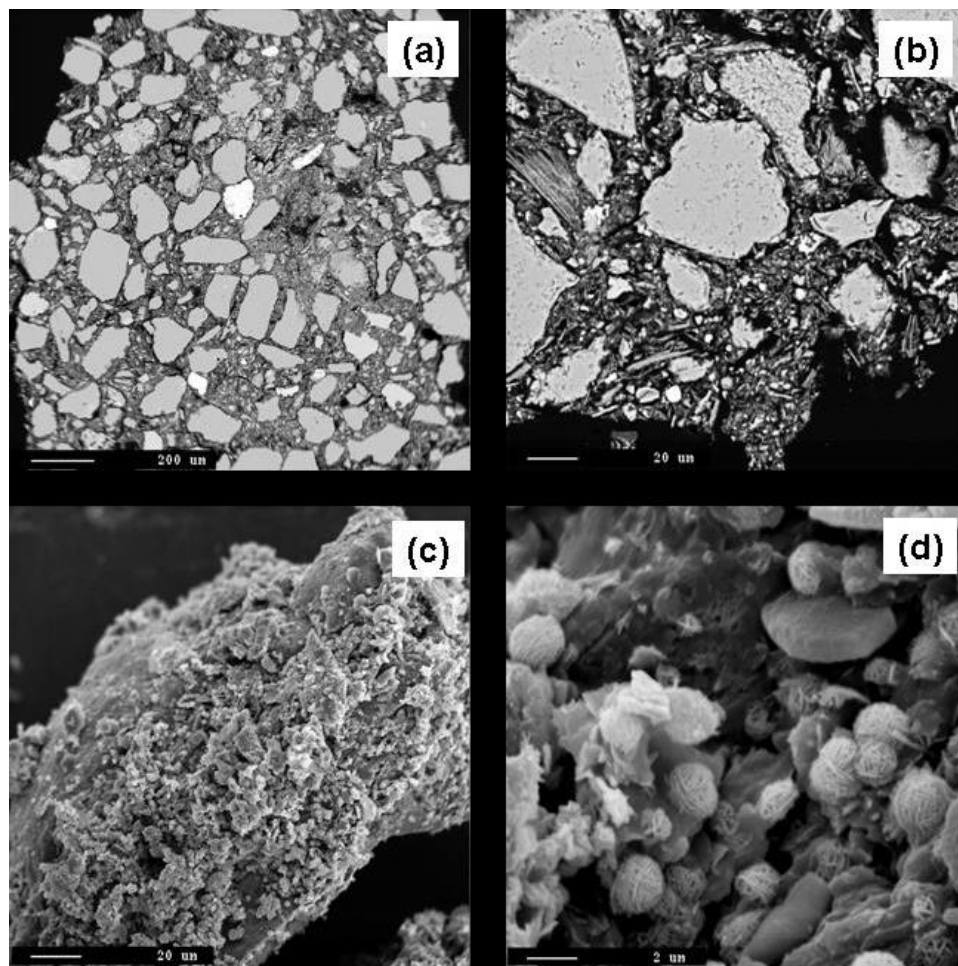


Fig. 4.42-Photomicrographs of the Bachaquero-01 sand after run no.2f, (a) BSE image of the sectioned and polished epoxy-mounted sand grains at 63x, (b) BSE image at 500x, (c) SE image of the loose sand grains at 500x (d) SE image at 1500x.

4.8 Run No. 3

This run was made with original sand from the core taken from Bachaquero-01 reservoir, well LL-231 at depth 2665'-2667' (**Fig. 4.1**).

The sand was cleaned of oil using toluene in a Soxhlet extraction apparatus. After the extraction process the sand was dried in an oven.

We started this run injecting distilled water until the experimental conditions were reached, and then sodium carbonate was injected. After injecting for 2.5 hours the run had to be aborted because of a leak at the top of the cell and high pressure at the inlet. Also the by-pass line showed high pressure, possibly because of sodium carbonate precipitation.

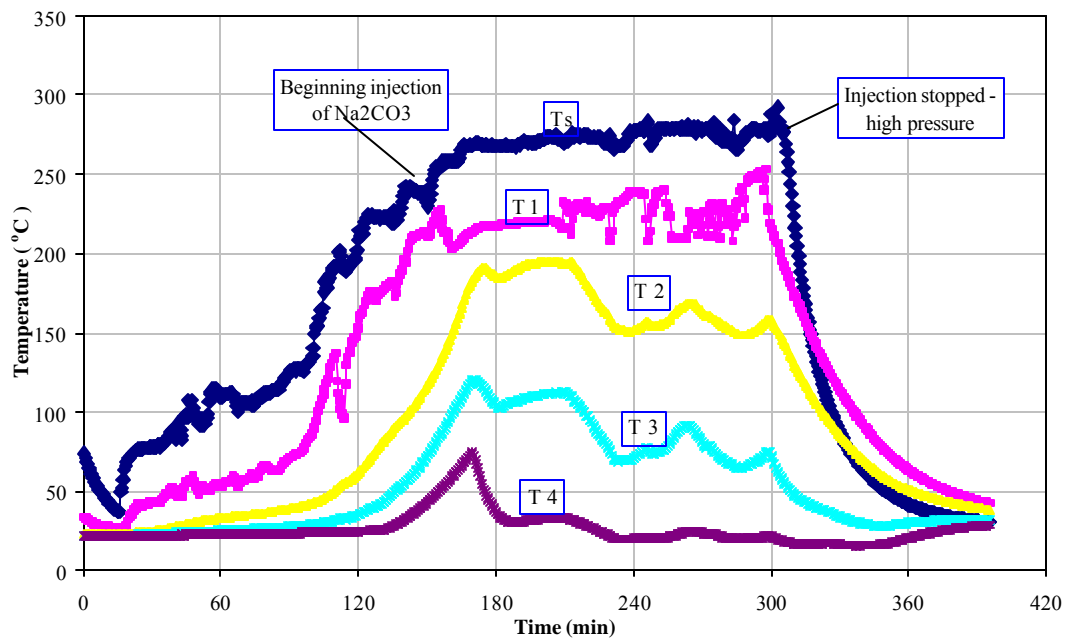


Fig. 4.43-Temperature profiles for run no. 3.

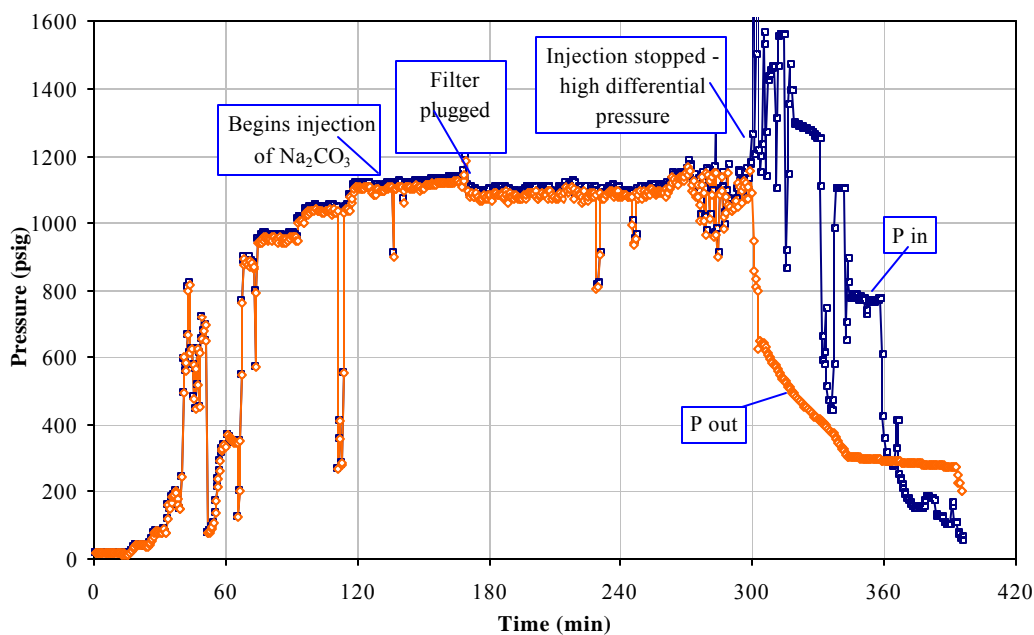


Fig. 4.44-Pressure profiles for run no. 3.

Temperature and pressure profiles for run no. 3 are shown in **Figs. 4.43** and **4.44**. The temperature of the injected alkaline solution was kept around 275°C giving as a result about 230°C to 245°C at the top of the cell. The differential pressure profile show that the pressure differential across the cell exceeded 500 psig by the time we aborted the run.

The pH of the effluent liquid was taken every 30 minutes. The graph showing the pH during this experiment is shown in **Fig. 4.45**.

The liquid samples from 60 to 120 minutes showed high oil content, indicating that the cleaning in the extraction apparatus was not 100% effective. The last three samples also show the presence of some silica gel. A photograph of these samples is shown in **Fig. 4.46**.

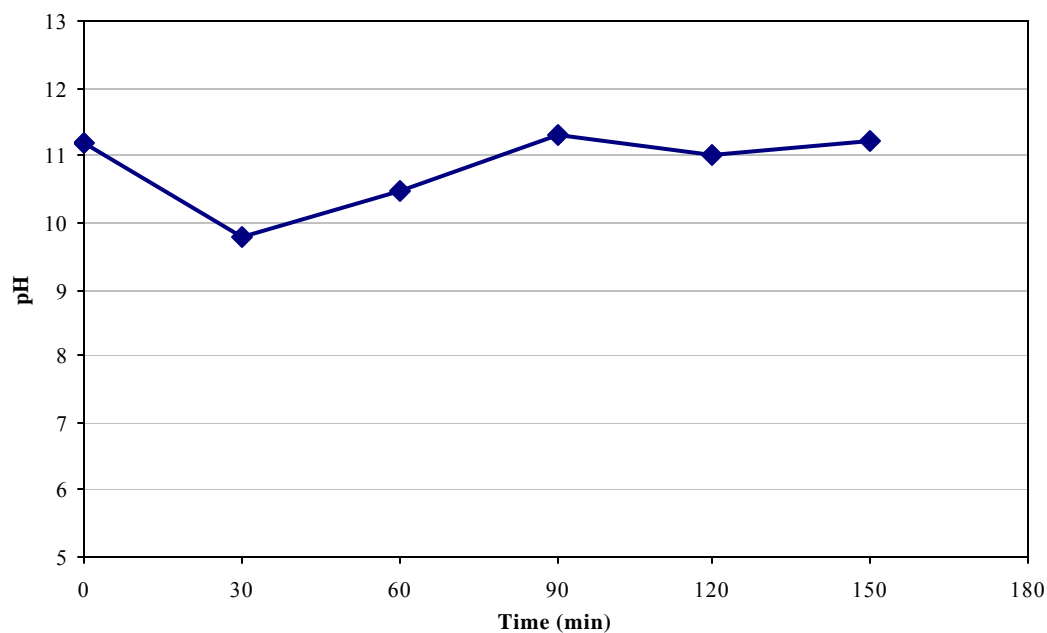


Fig. 4.45-Effluent liquid pH for run no. 3.

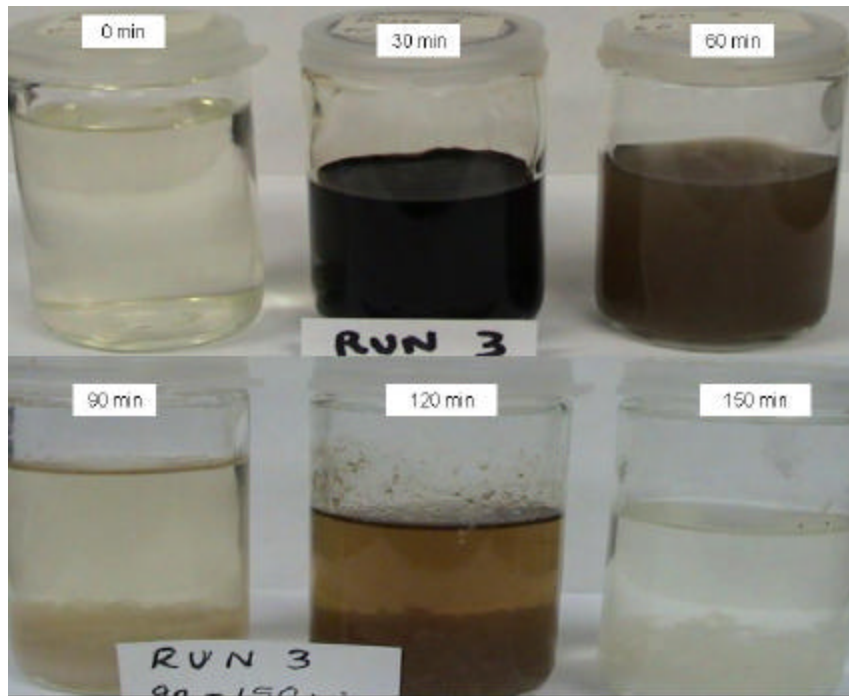


Fig. 4.46-Photograph of the effluent liquid after run no. 3.

After 36 hours, when the sand was extracted from the cell we noticed some packing but no sign of consolidation. Electron microprobe images of the sand grains at the top of the cell after the experiment are presented in **Fig. 4.47**.

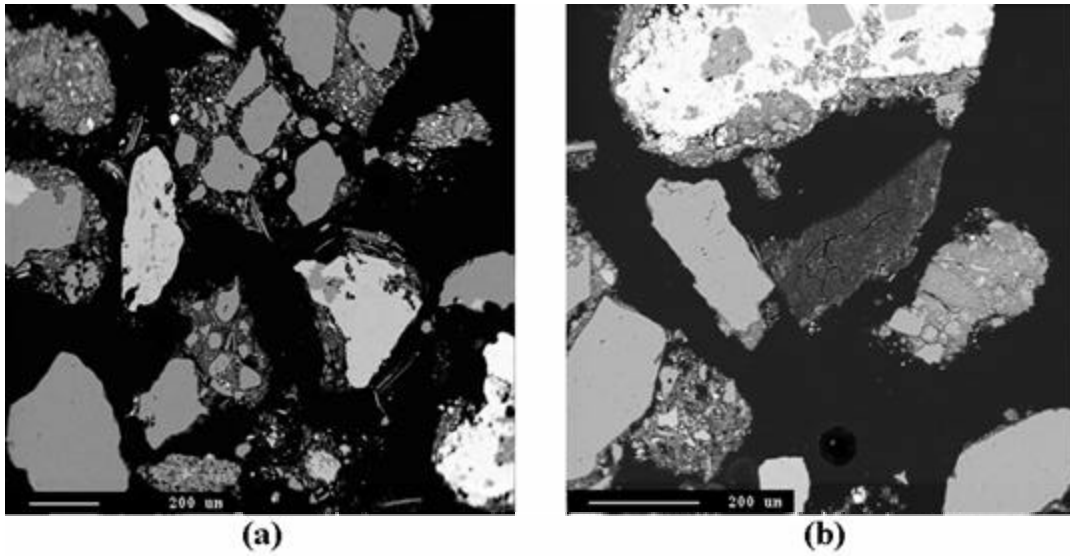


Fig. 4.47-Photomicrographs of the Bachaquero-01 sand after run no.3, (a) BSE image at 63x, (b) BSE image at 100x.

The BSE images did not show obvious alterations or secondary products. We could see fine-grained material surrounded the grains and also some oil was still present in the sample. This oil content indicated that the soxhlet cleaning was not 100% effective.

The presence of oil around the grains, caused by a not effective cleaning in the soxlet and little time of interaction between the alkaline solution and the grains during the experiment, may have interfered with the formation of secondary products.

4.9 Run No. 3a

Because of the oil content observed in the liquid samples after run no.3 and because we had to stop the run after just 2.5 hours, we decided to make another run using the same sand sample. We placed it at the top of the cell and we completed the volume required for filling the Teflon tubing with industrial silica sand. We started this run injecting distilled water until experimental conditions were reached, and then sodium carbonate was injected. After 4.5 hours of injection of sodium carbonate, the run had to be aborted because of a sudden leak at the top of the cell. Temperature and pressure profiles for run no. 3 are shown in **Figs. 4.48** and **4.49**.

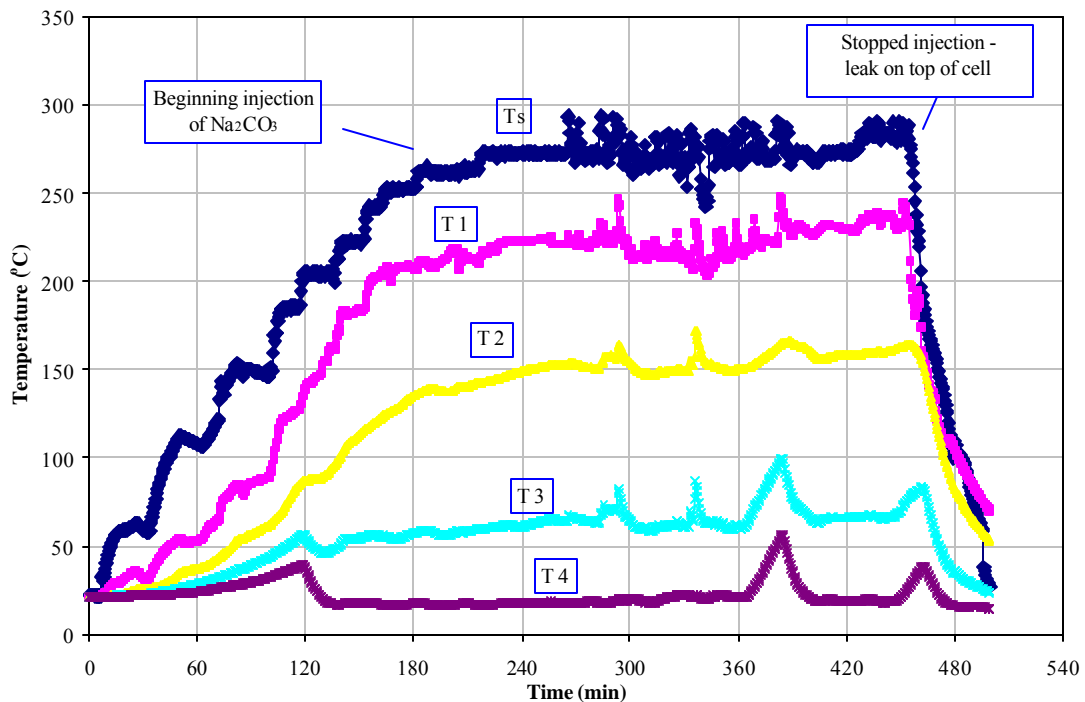


Fig. 4.48-Temperature profiles for run no. 3a.

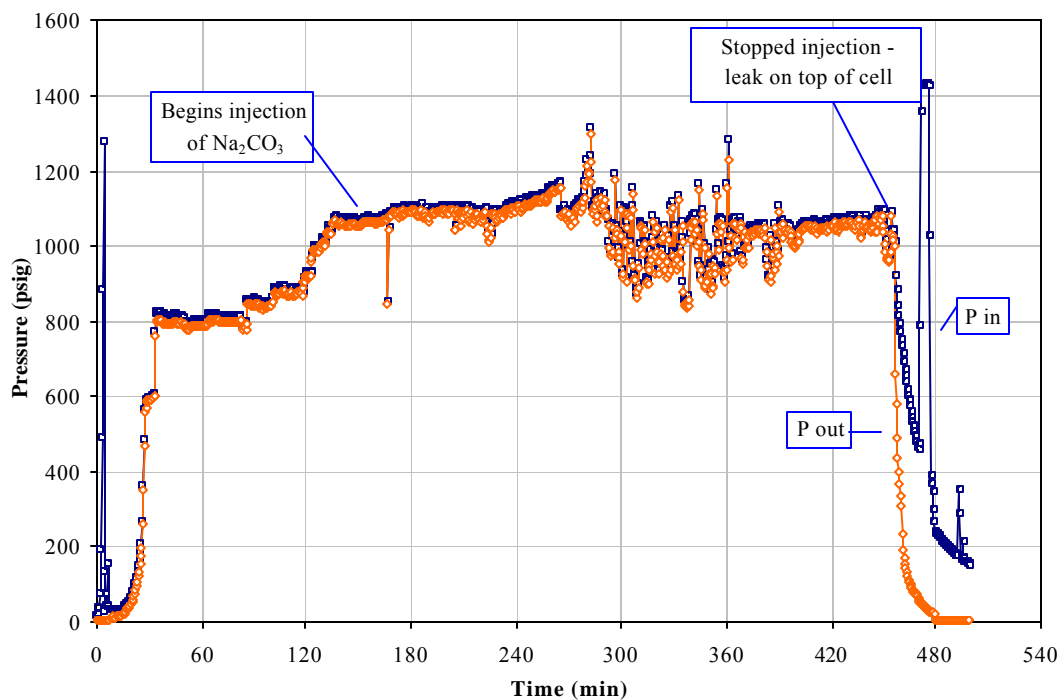


Fig. 4.49-Pressure profiles for run no. 3a.

The temperature of the injected alkaline solution was kept around 270°C giving as a result about 235°C at the top of the cell. The pressure profiles show that the pressure differential across the cell never exceeded 50 psig.

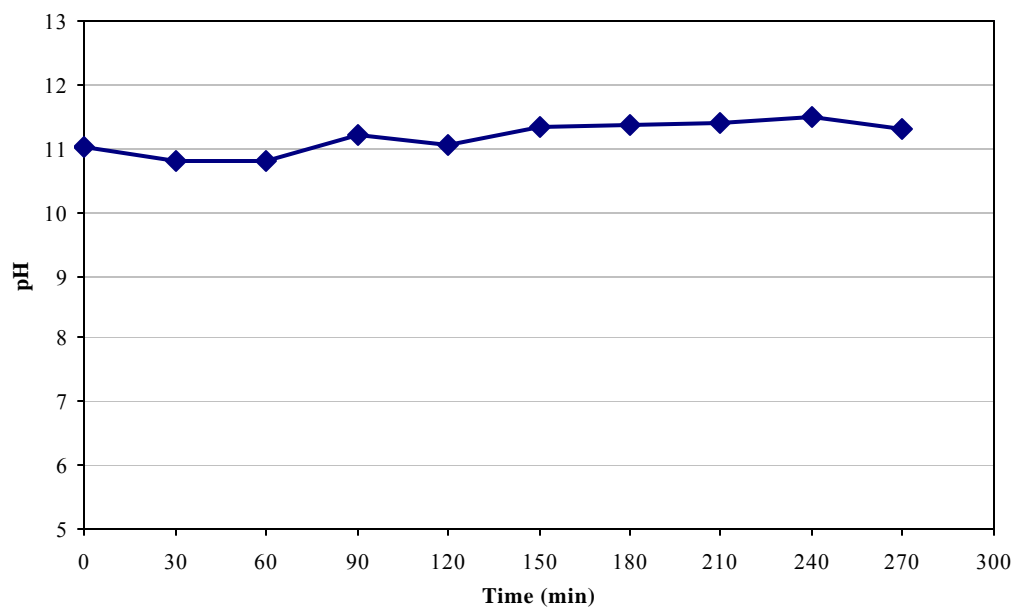


Fig. 4.50-Effluent liquid pH for run no. 3a.

The liquid samples were practically transparent with some residue of silica gel. A photograph of these samples is shown in **Fig. 4.51**.

The pH of the effluent liquid was taken every 30 minutes. The graph showing the pH during this experiment is shown in **Fig. 4.50**.

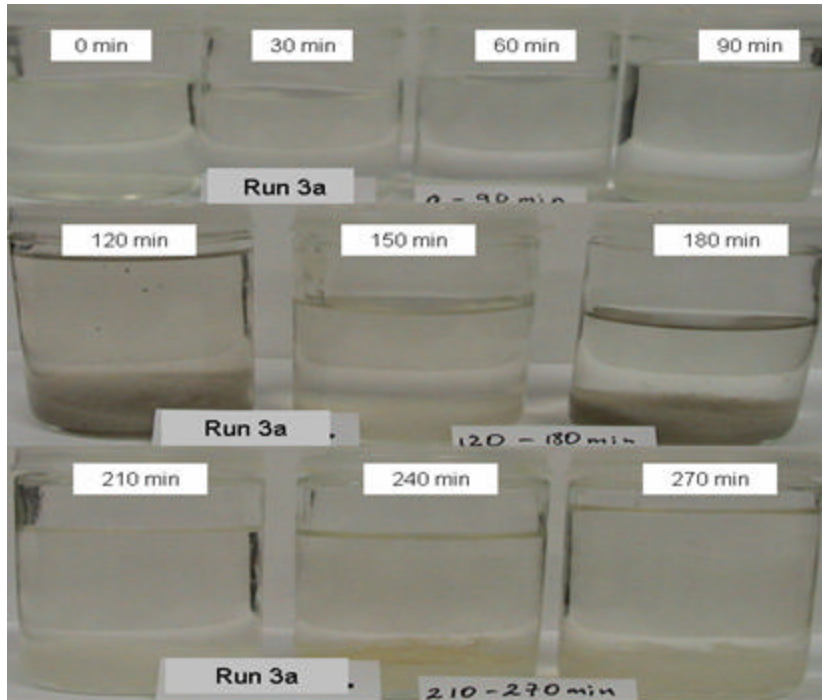


Fig. 4.51-Photograph of the effluent liquid after run no. 3a.

After 36 hours, when the sand was removed from the cell no evident sign of consolidation was observed. Just after we dried the sample in the oven we could see some consolidation, but when we put the sample in water it desegregated rapidly, indicating that the primary cement was the sodium carbonate. Photograph of the sample is shown in **Fig. 4.52**.

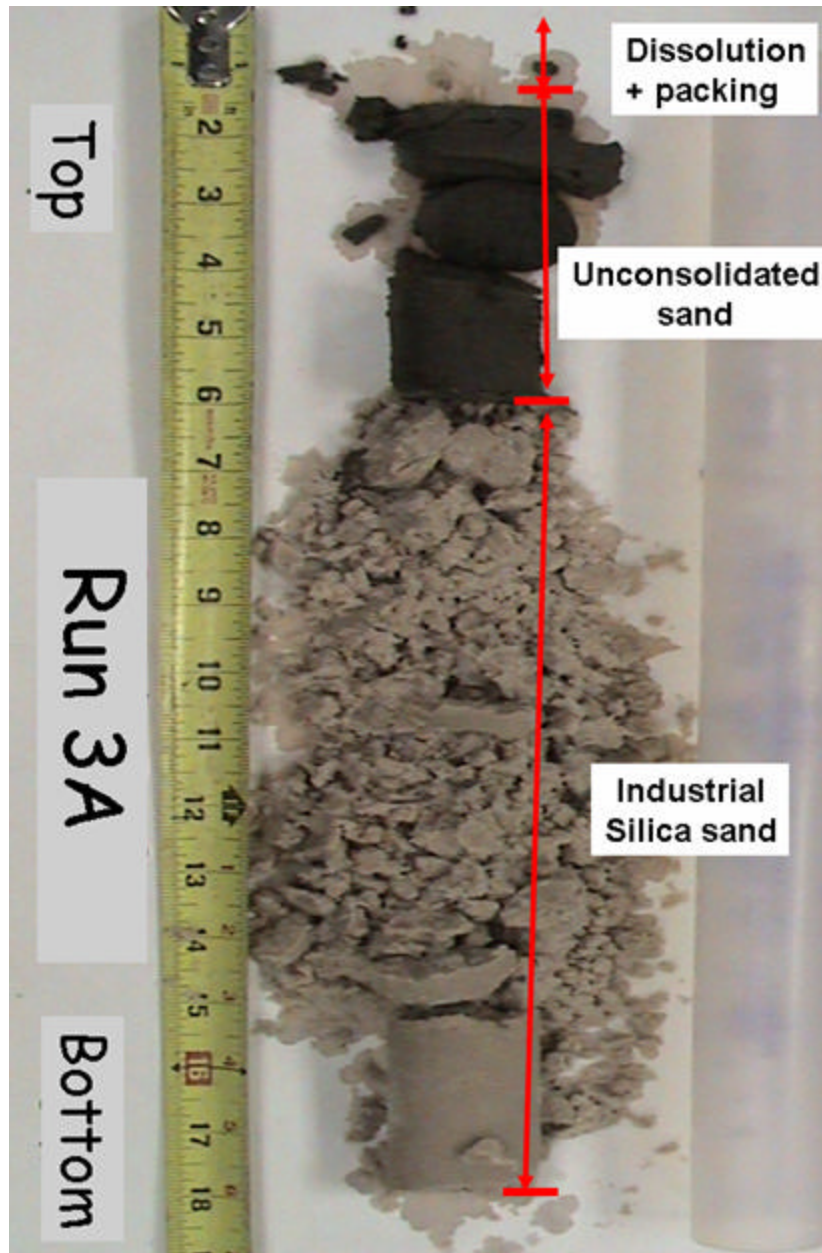


Fig. 4.52-Sand sample after run no. 3a.

The photomicrographs of the sand grains at the top of the cell after the experiment are presented in **Fig. 4.53**.

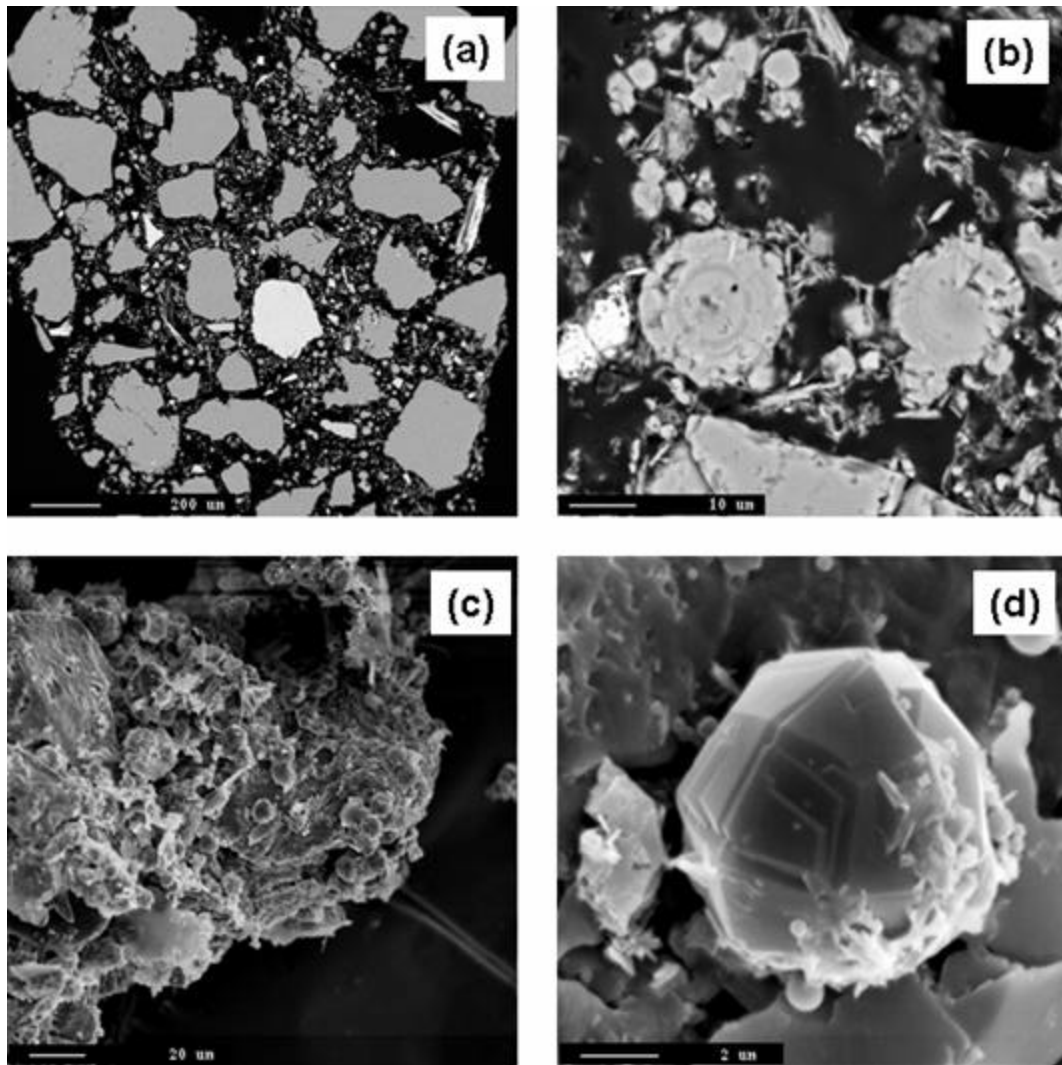


Fig. 4.53-Photomicrographs of the Bachaquero-01 sand after run no.3a, (a) BSE image of the sectioned and polished epoxy-mounted sand grains at 63x, (b) BSE image at 1200x, (c) SE image of the loose sand grains at 500x (d) SE image at 7000x.

The images of this run presented a different panorama. They showed both needle-like and rounded features between the grains, that seemed to be secondary products, but very dispersed across the sample and surrounded by clay-like material. The

surface of the grains showed an etched surface caused by dissolution. Some grains of mica and k-feldspars could also be seen. The fine-grained material appears to be embedded in oil, and therefore may have not been very reactive with the solution

At higher magnifications the images were even more descriptive. One of the secondary phases, the rounded ones corresponded to an analcime-like zeolites and the needle-like crystals seemed to be natrolite-like zeolites. The needle-like crystals could not be analyzed because they were too small for an EDS or WDS analysis. The EDS is a qualitative analysis of materials observed with the scanning electron microscope (SEM) using real-time energy-dispersive X-ray spectrometry. WDS is an automated multi-element quantitative analysis of material in polished section using wavelength-dispersive spectrometry. Also fine-grained material could be seen between grains. The EDS analysis of this fine grained material showed sodium aluminum silicates indicating that they also are secondary products. The calcium observed in the analysis seems to be from what looks like original calcite partially eaten away. **Fig. 4.54** shows the EDS spectra of this fine-grained material.

Although the SE image of the rounded feature showed a analcime-like zeolites, the WDS analysis indicated a chemically different zeolites probably a non-stoichiometric analcime. They presented a high content of iron and silica when compared with an ideal analcime. This difference may be caused by the local chemical environment. **Table 4.1** shows the WDS analysis for these atypical zeolites.

These products of dissolution were between the grains but not in sufficient quantity to bridge the grains and consolidate the sample. It is also believed that the

presence of the “not yet dissolved” clays may be interfering with the bridging process between the secondary phases and the grains.

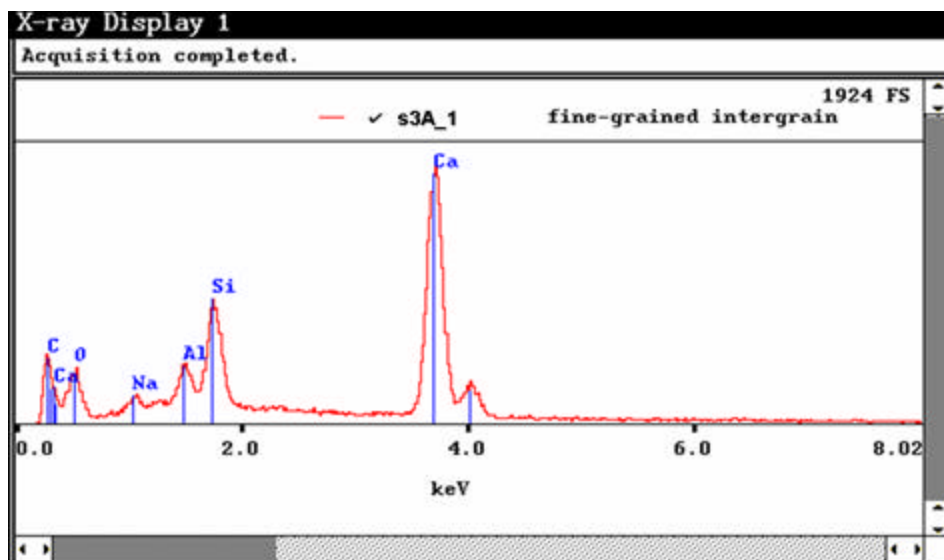


Fig. 4.54-EDS spectra of the fine-grained intergrain material after run no. 3a.

Table 4.1-WDS Analysis of Atypical Zeolites in Run No. 3a.

Analysis	Wt. % oxides							Cations in formula on the basis of 7 oxygens					
	Na ₂ O	Al ₂ O ₃	SiO ₂	K ₂ O	CaO	Fe ₂ O ₃	Total	Na	Al	Si	K	Ca	Fe ³⁺
3a_after round1 cent	9.54	19.01	56.72	0.11	0.10	4.54	89.61	0.81	0.98	2.49	0.01	0.01	0.15
3a_after round2 cent	8.95	19.83	55.74	0.19	0.00	4.85	89.11	0.76	1.03	2.46	0.01	0.00	0.16
3a_after round3 cent	9.06	19.66	57.65	0.16	0.03	3.81	90.03	0.76	1.00	2.49	0.01	0.00	0.13
3a_after round1 edge	3.90	16.91	61.71	0.03	0.01	5.31	87.39	0.33	0.87	2.68	0.00	0.00	0.18
							Analcime (Ideal): Na[AlSi ₂ O ₆]H ₂ O	1.00	1.00	2.00	0.00	0.00	0.00

4.10 Run No. 3b

Based on the results of run no. 3a, where clays seemed to be interfering with the consolidation process, we decided to use the same sample left after run no. 3a but after first treating it with mud acid (3% HF – 12% HCl) to dissolve clay material in the sample. Matrix acid stimulation is a relatively simple technique that is commonly used in the field to enhance well productivity and improve hydrocarbon recovery.

To perform this acid treatment we first soaked the sand in a 5% HCl solution to get rid of the carbonates that could precipitate in contact with hydrofluoric acid (HF). Then we rinsed the sand and let it soak overnight in the mud acid solution. We rinsed the sand using distilled water until a pH about 6 was reached to avoid corrosion of the cell and flow lines during the experiment. The sand sample was placed at the top of the cell and industrial silica sand was used at the bottom to complete the volume required to fill the cell.

We started this run injecting distilled water for about 130 minutes until the experimental conditions were reached, and then sodium carbonate was injected. The experiment ran for 6 hours with some plugging in the filter and backpressure regulator caused by the silica gel produced. Temperature and pressure profiles for run no. 3b are shown in **Figs. 4.55** and **4.56**.

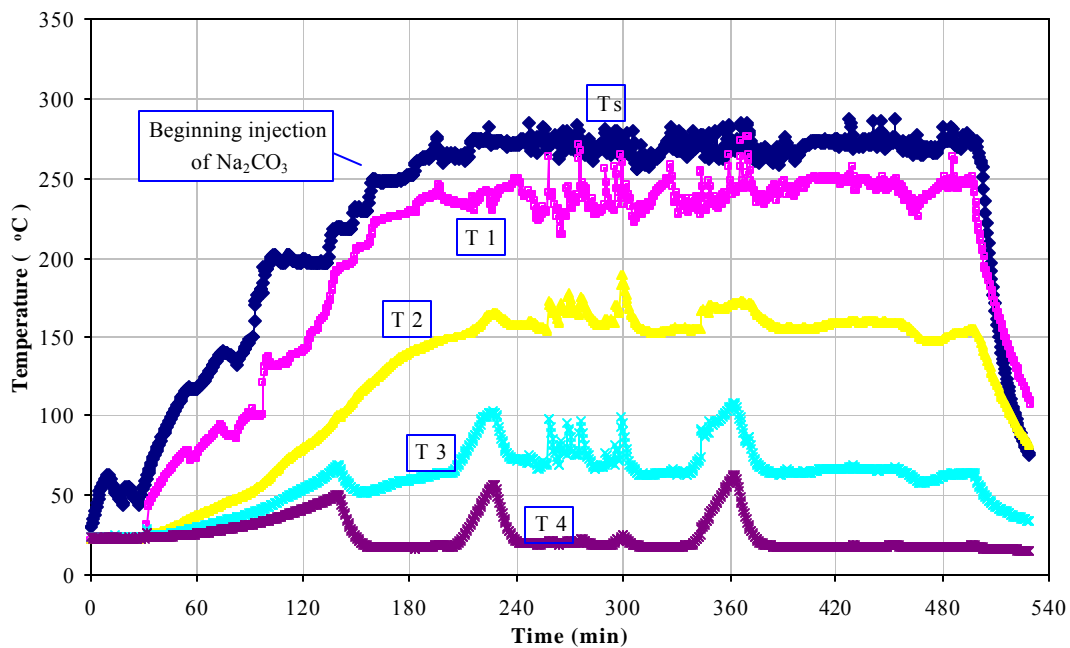


Fig. 4.55-Temperature profiles for run no. 3b.

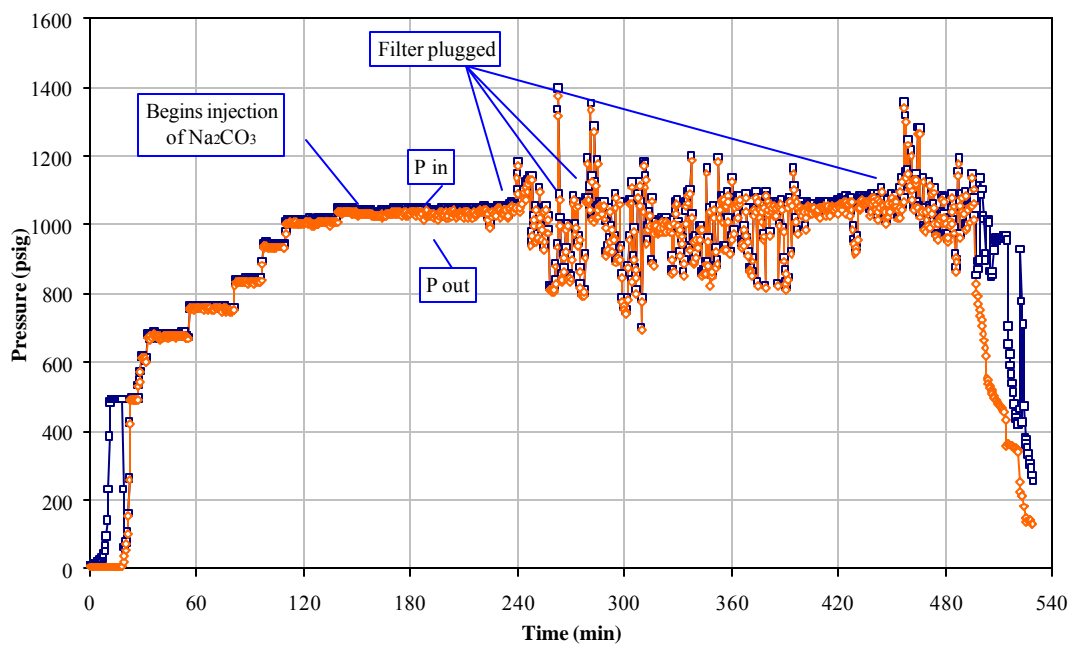


Fig. 4.56-Pressure profiles for run no. 3b.

The temperature of the injected alkaline solution was kept around 275°C giving as a result about 245°C at the top of the cell. The differential pressure profiles showed that the pressure differential across the cell never exceeded 100 psig. The pH of the effluent liquid was taken every 30 minutes. The curve showing the pH during this experiment is shown in **Fig. 4.57**.

The liquid samples from 90 to 150 minutes showed some oil content, indicating that there was still some oil in the sample. The samples from 90 to 240 minutes also showed the presence of some silica gel. A photograph of these samples is shown in **Fig. 4.58**.

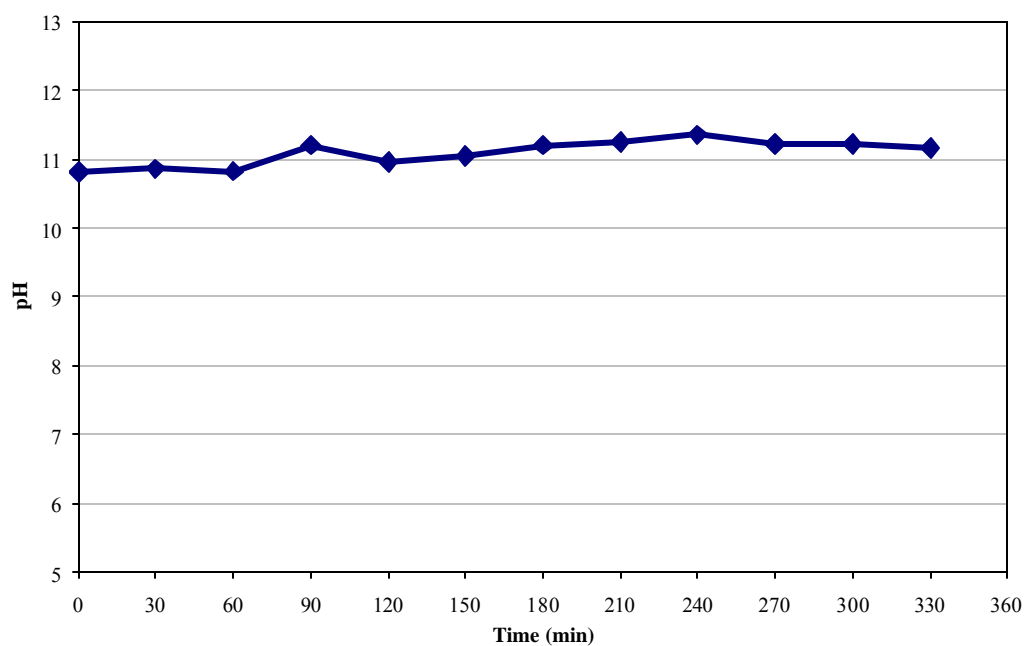


Fig. 4.57-Effluent liquid pH for run no. 3b.

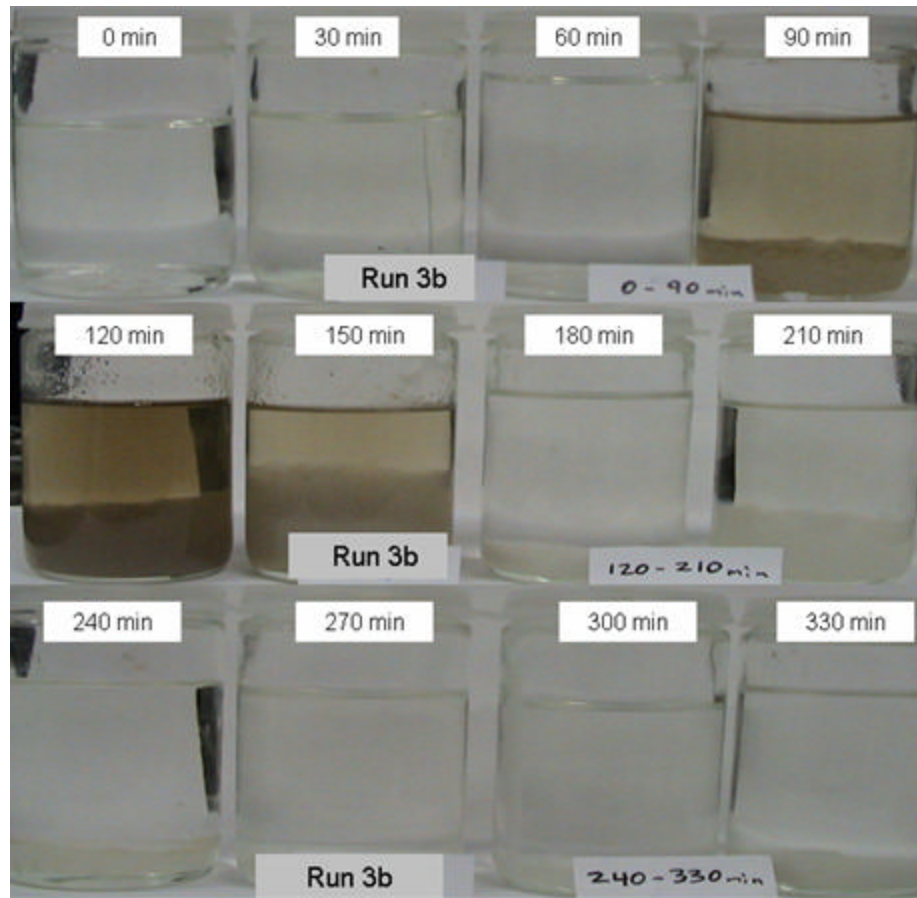


Fig. 4.58-Photograph of the effluent liquid after run no. 3b

After 60 hr the sand was extracted from the cell. No evident consolidation was observed. As we did in run no. 3, we put a piece of sample from the top of the cell to dry overnight and we obtained some consolidation, but when soaked in water, sample disaggregated almost immediately, indicating that the cement was basically sodium carbonate. Photograph of the sample is shown in **Fig. 4.59**.

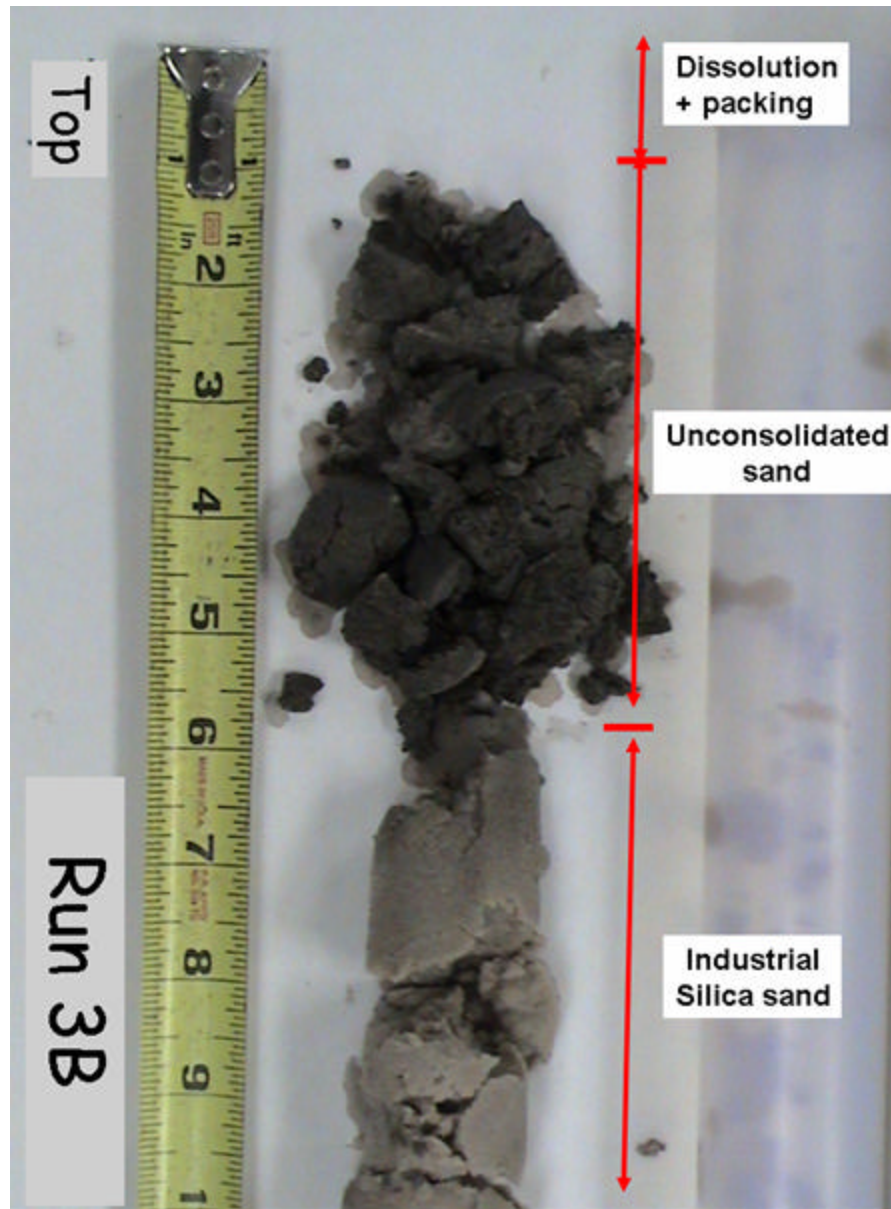


Fig. 4.59-Sand sample after run no. 3b.

The photomicrographs of the sand grains before and at the top of the cell after the experiment are presented in **Figs. 4.60** and **4.61**.

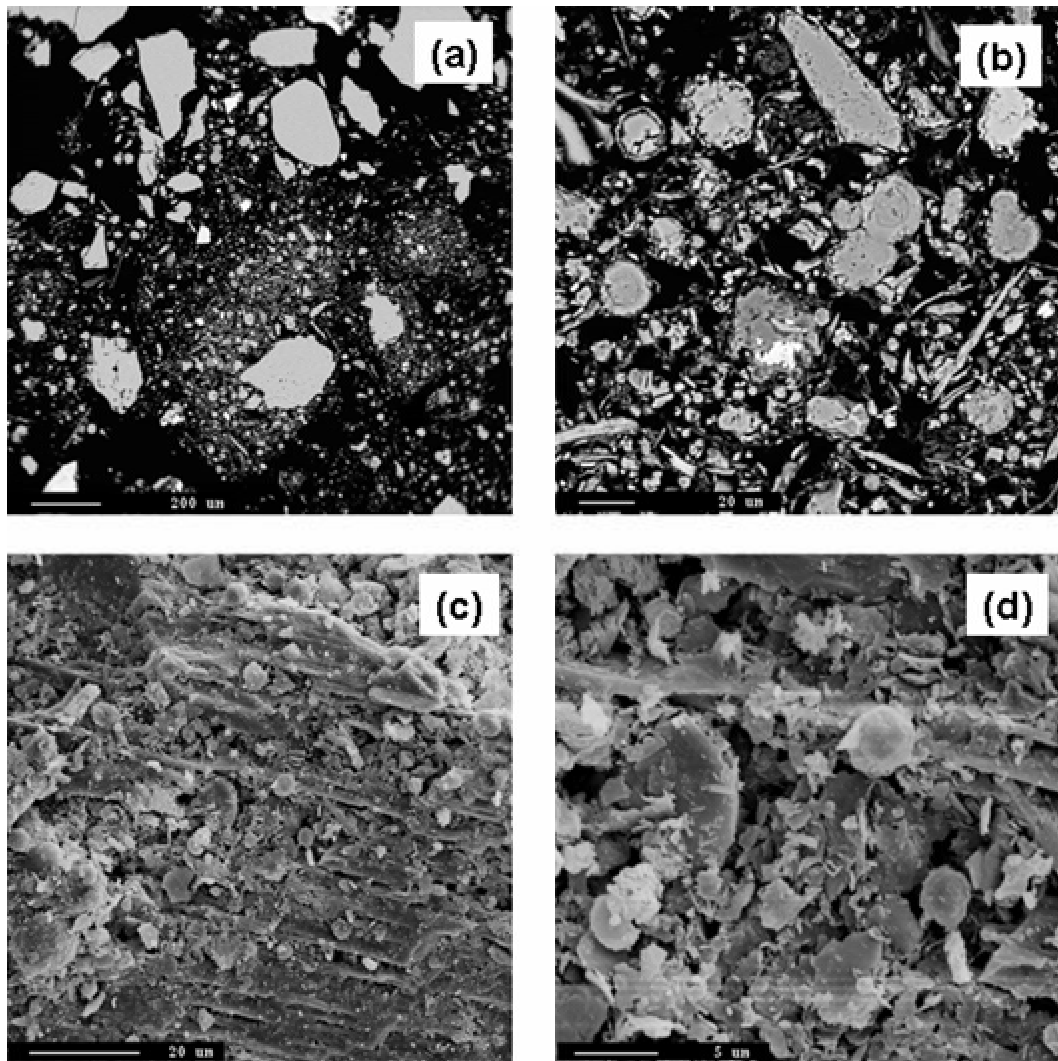


Fig. 4.60-Photomicrographs of the Bachaquero-01 sand before run no.3b, (a) BSE image of the sectioned and polished epoxy-mounted sand grains at 63x, (b) BSE image at 1200x, (c) SE image of the loose sand grains at 500x (d) SE image at 3000x.

The images of the sample before the experiments show that plenty of zeolites survived the mud acid treatment. There is also fine-grained materials present indicating that the mud acid dissolved just part of them.

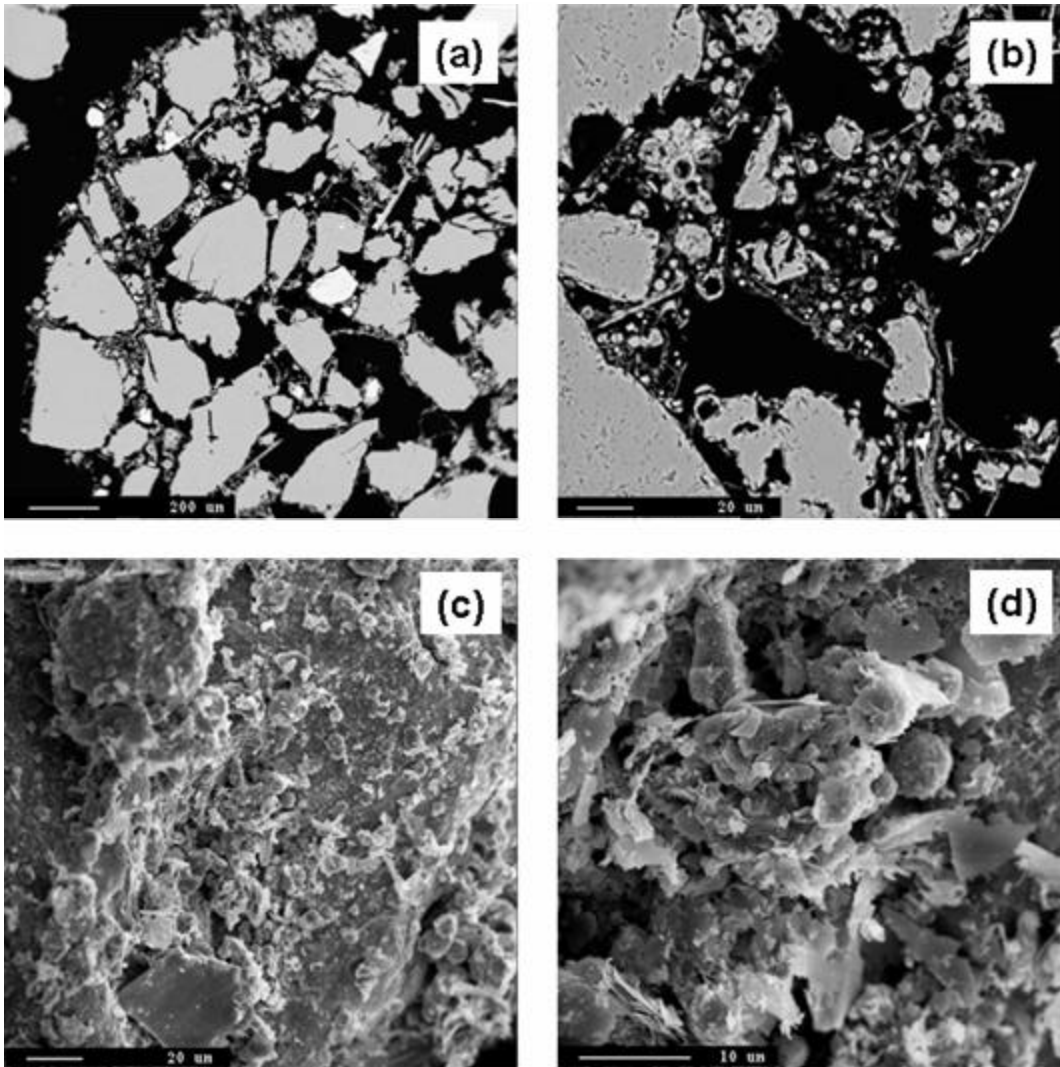


Fig. 4.61-Photomicrographs of the Bachaquero-01 sand after run no.3b, (a) BSE image of the sectioned and polished epoxy-mounted sand grains at 63x, (b) BSE image at 500x, (c) SE image of the loose sand grains at 500x (d) SE image at 2000x.

The images after the run showed some new secondary products but still not enough to bridge the sand grains. Some zeolites had a hole in the center possibly caused by reaction with the sodium carbonate. This dissolved material from the center may have helped form new zeolites.

Some of these zeolites are not well shaped because the structure depends on local chemical environment at the time of formation. They are very small and dispersed and still surrounded by clay-like material. These products of dissolution are not in sufficient quantity to bridge the grains and consolidate the sample. The fine-grained material appears to be embedded in oil, and therefore may not be very reactive with the solution.

As seen in run no. 3a, these zeolites have shape similar to an analcime but the WDS analysis indicates a chemically different zeolite, probably a non-stoichiometric analcime, with a higher content of iron and silica than an ideal analcime. **Table 4.2** shows the WDS analysis for these atypical zeolites.

Table 4.2-WDS Analysis of Atypical Zeolites in Run No. 3b.

Analysis	Wt. % oxides							Cations in formula on the basis of 7 oxygens					
	Na ₂ O	Al ₂ O ₃	SiO ₂	K ₂ O	CaO	Fe ₂ O ₃	Total	Na	Al	Si	K	Ca	Fe ³⁺
3b_after round1 cent	6.61	14.57	68.16	0.21	0.03	1.83	91.24	0.53	0.71	2.81	0.01	0.00	0.06
3b_after round2 cent	5.82	14.66	60.67	0.11	0.04	6.82	87.50	0.50	0.76	2.69	0.01	0.00	0.23
Analcime (Ideal): Na[AlSi ₂ O ₆]·H ₂ O								1.00	1.00	2.00	0.00	0.00	0.00

4.11 Run No. 4

This run was made with original sand from core taken from Bachaquero-01 reservoir, well LL-231 at depth 2705'-2707' (**Fig. 4.1**). The sand was cleaned of oil using toluene in a Soxhlet extraction apparatus. After the extraction process the sand was dried in an oven.

We started this run injecting distilled water for 180 minutes until the experimental conditions were reached, and then sodium carbonate was injected. After injecting for 3.5 hours, the run had to be aborted due to problems controlling the cell pressure with the backpressure regulators. Temperature and pressure profiles are shown in **Figs. 4.62** and **4.63**.

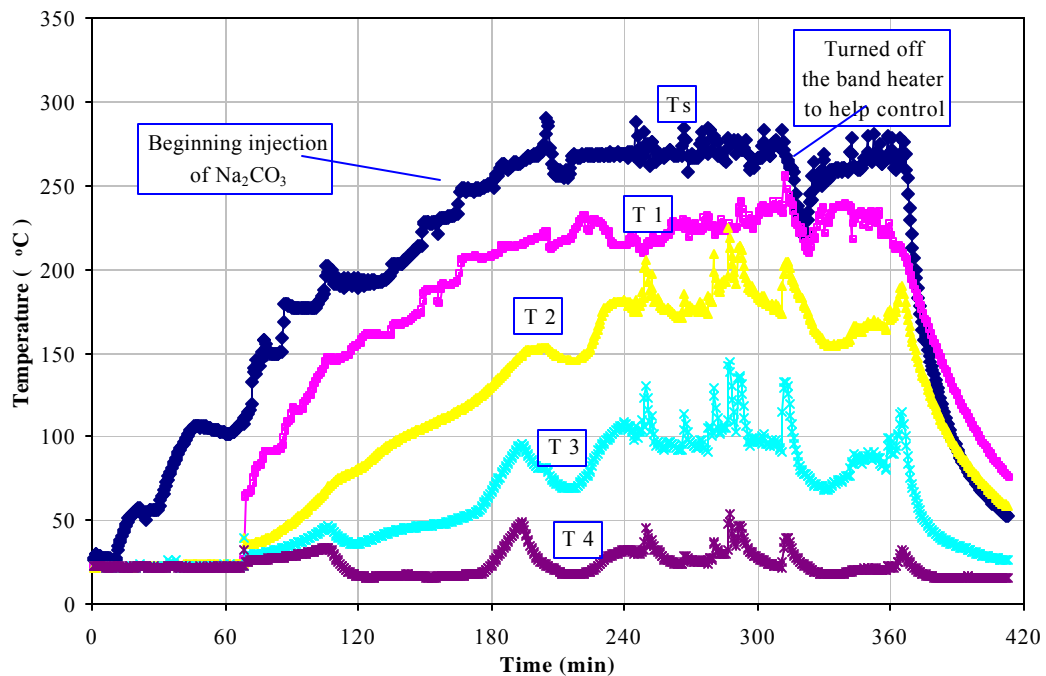


Fig. 4.62-Temperature profiles for run no. 4.

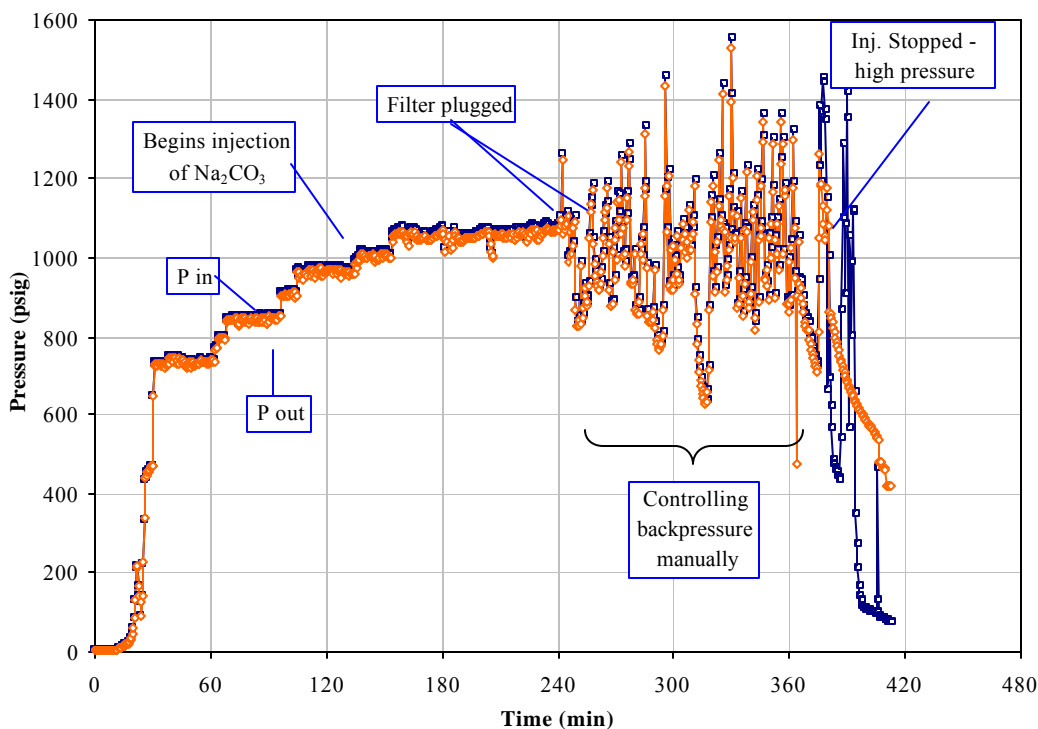


Fig. 4.63-Pressure profiles for run no. 4.

The temperature of the injected alkaline solution was kept around 265°C giving as a result about 235°C at the top of the cell. The pressure profiles show that the pressure differential across the cell exceeded 500 psig by the time we aborted the run.

The pH of the effluent liquid was taken every 30 minutes. The graph showing the pH during this experiment is shown in **Fig. 4.64**.

The liquid samples from 60 to 120 minutes showed high oil content, indicating that the cleaning in the extraction apparatus was not 100% effective. The last three samples also indicated the presence of some silica gel. A photograph of these samples is shown in **Fig. 4.65**.

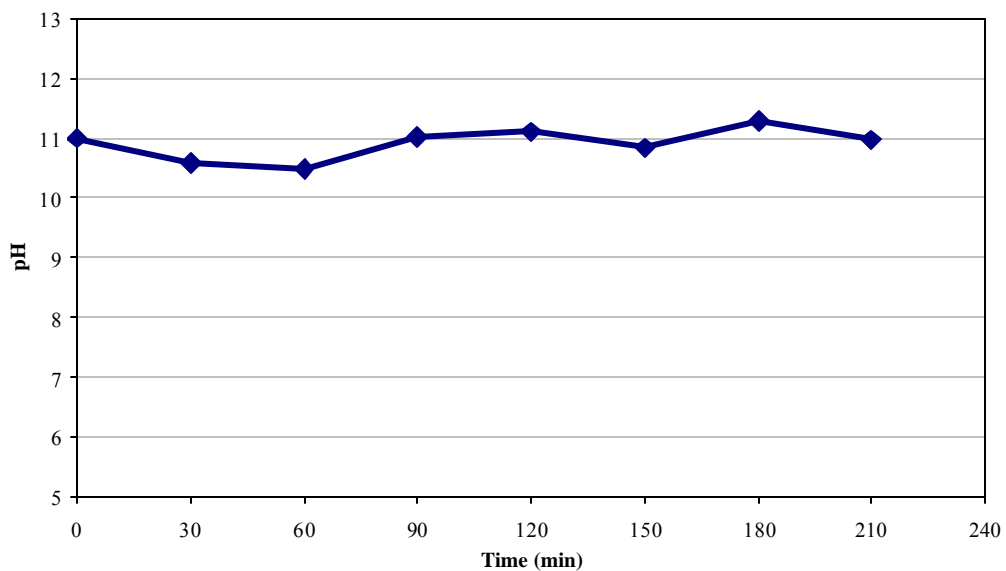


Fig. 4.64-Effluent liquid pH for run no. 4.

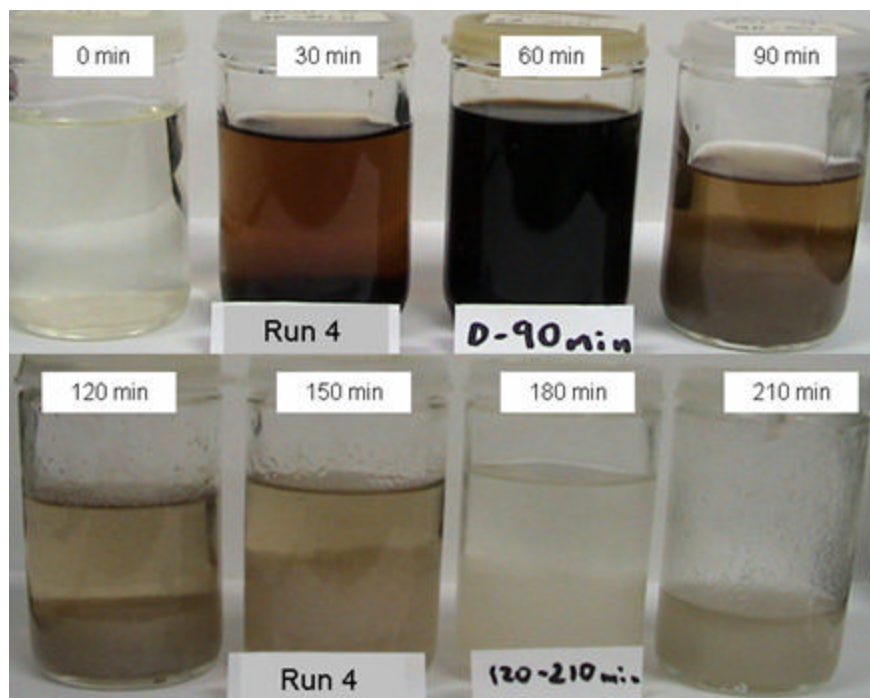


Fig. 4.65-Photograph of the effluent liquid after run no. 4.

After 60 hr the sand was extracted from the cell and no evidence of consolidation was observed. As we did in run no. 3a and 3b, we placed some of the sample from the top of the cell in the oven, to dry overnight. The dried sample showed some consolidation, but when soaked in water, the sample disintegrated almost immediately, indicating that the cement was basically sodium carbonate. Photograph of the sample is shown in **Fig. 4.66**.

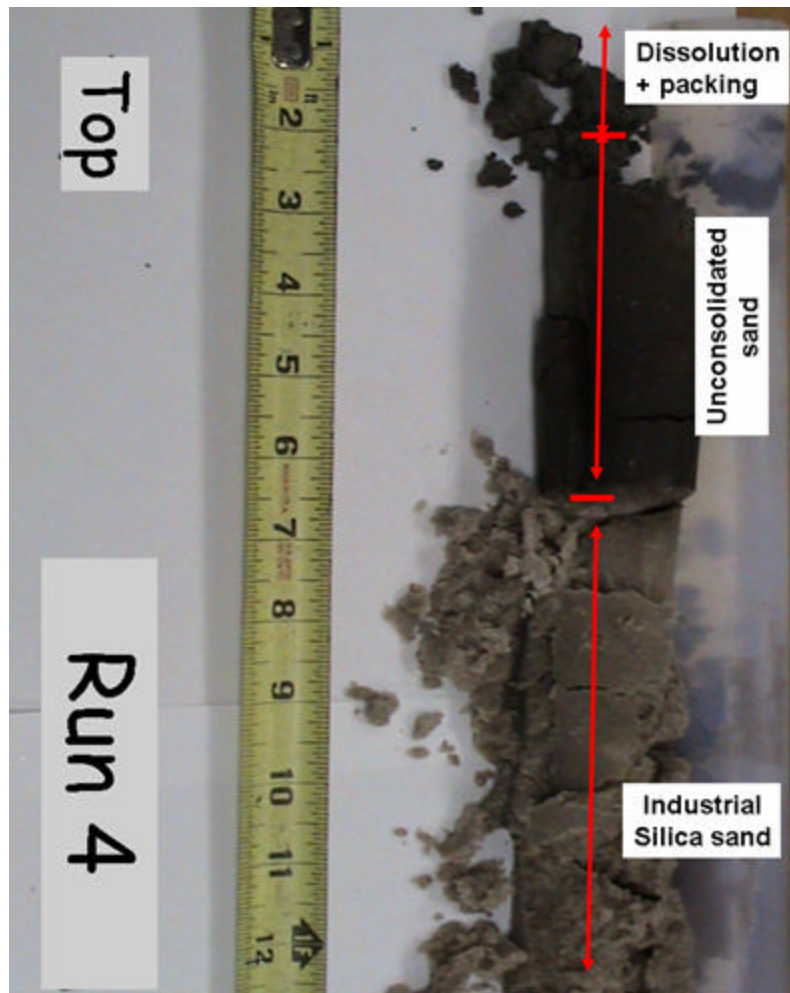


Fig. 4.66-Sand sample after run no. 4.

The photomicrographs of the sand grains before and after the experiment (from top of the cell) are presented in **Figs. 4.67** and **4.68**.

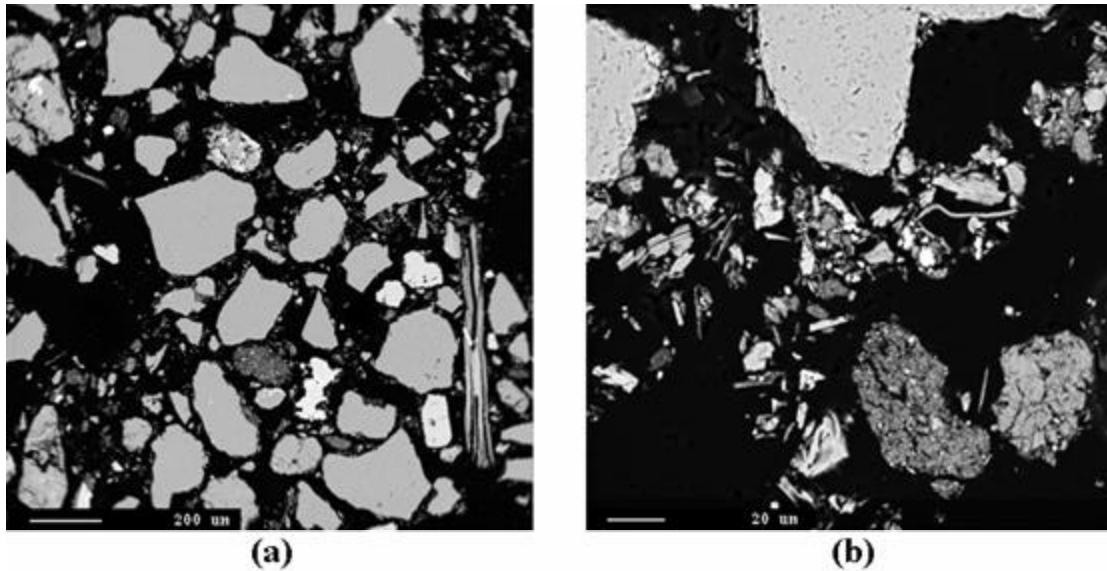


Fig. 4.67-Photomicrographs of the Bachaquero-01 sand before run no. 4, (a) BSE image of the sectioned and polished epoxy-mounted sand grains at 63x, (b) BSE image at 500x.

The images before the experiment show poorly sorted sand at this interval. They show a variety of grain shapes and sizes. While some grains are rounded others show cleavage.

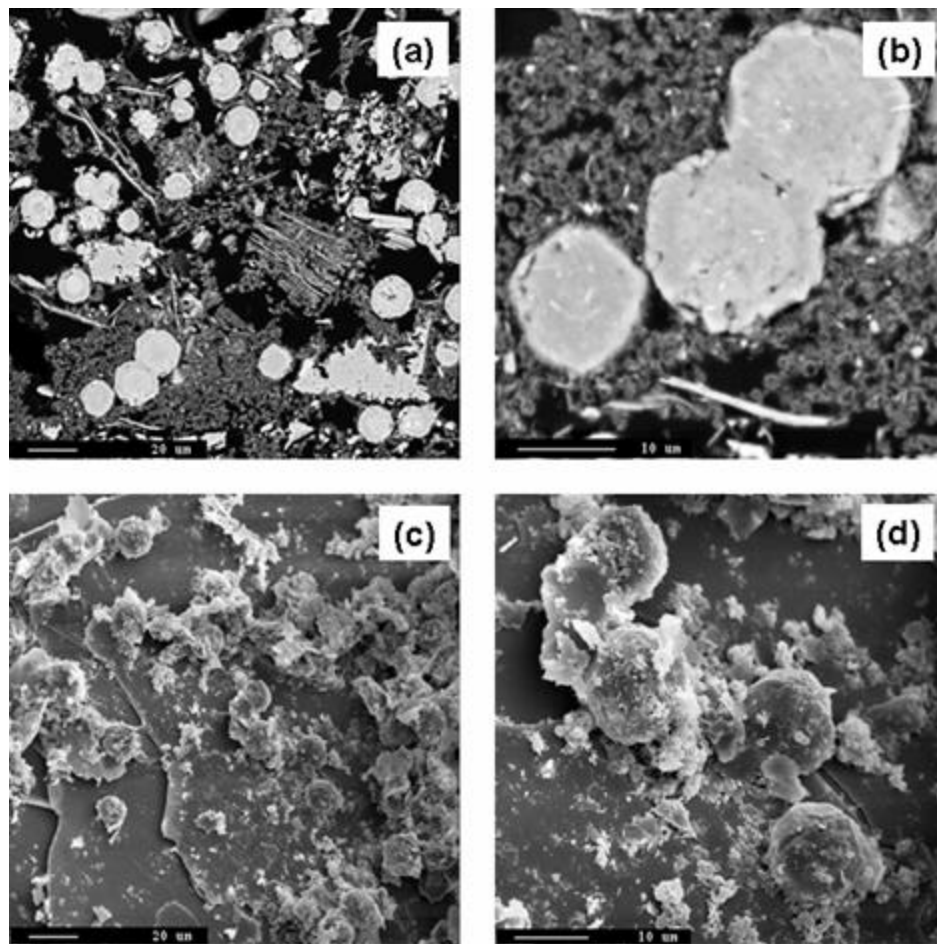


Fig. 4.68-Photomicrographs of the Bachaquero-01 sand after run no.4, (a) BSE image of the sectioned and polished epoxy-mounted sand grains at 500x, (b) BSE image at 2000x, (c) SE image of the loose sand grains at 500x (d) SE image at 2000x.

The images of the sample after the run show significant secondary reaction. We see a lot of fine-grained material impeding the bridging between grains and secondary phases. There are some needle-like materials that according to the EDS analysis are composed mostly of sodium. The rounded features correspond to a secondary mineral with shape similar to an analcime zeolite, but the WDS analysis showed a different chemical composition with more iron and silica than an ideal analcime indicating

probably a non-stoichiometric analcime. **Figs. 4.69** and **4.70** show the EDS spectra of the needle-like material and the rounded feature respectively. **Table 4.3** shows the WDS analysis of the atypical zeolites.

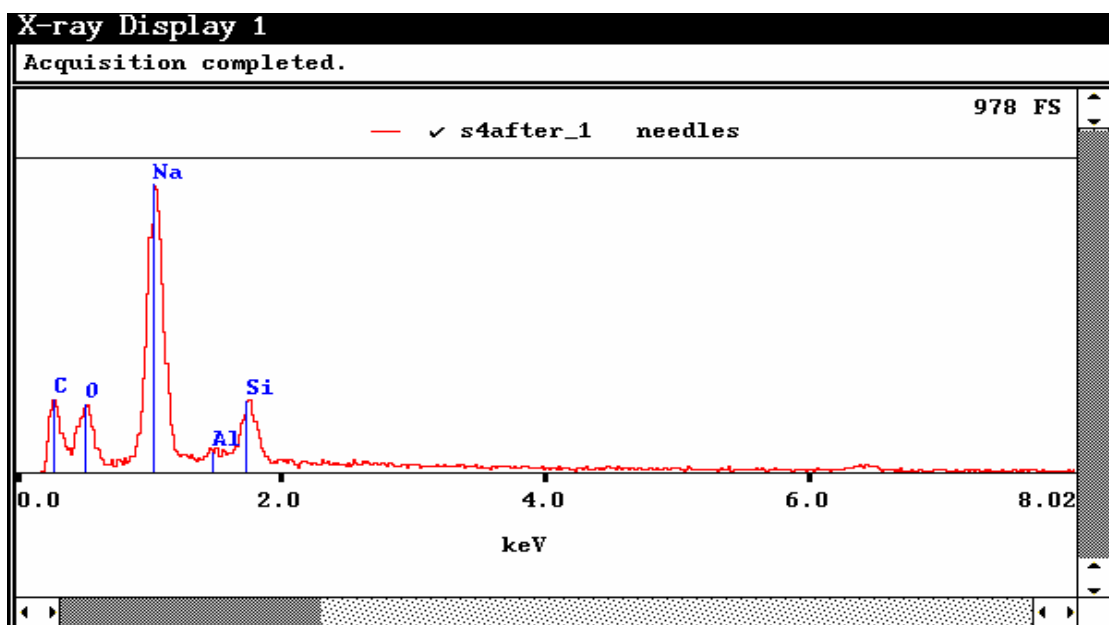


Fig. 4.69-EDS spectra of the needle-like material after run no. 4.

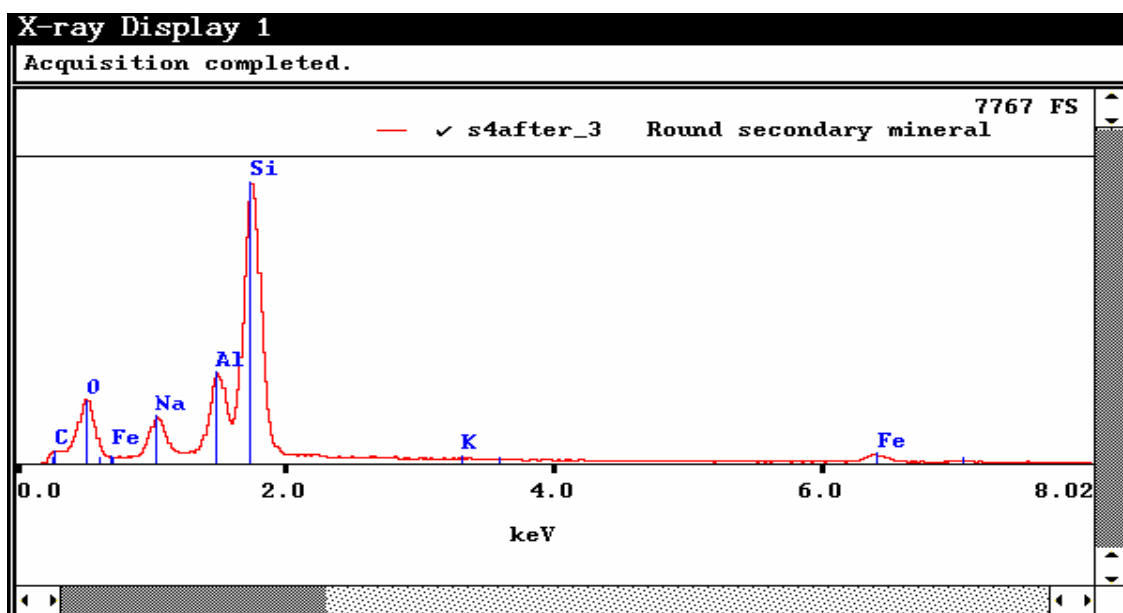


Fig. 4.70-EDS spectra of the round secondary mineral after run no. 4.

Table 4.3-WDS Analysis of Atypical Zeolites in Run No. 4.

Analysis	Wt. % oxides							Cations in formula on the basis of 7 oxygens					
	Na ₂ O	Al ₂ O ₃	SiO ₂	K ₂ O	CaO	Fe ₂ O ₃	Total	Na	Al	Si	K	Ca	Fe ³⁺
4_after round1 cent	7.44	17.45	56.54	0.52	0.07	7.52	88.85	0.64	0.92	2.52	0.03	0.00	0.25
4_after round2 cent	5.94	19.54	57.95	0.66	0.07	4.83	88.55	0.50	1.01	2.53	0.04	0.00	0.16
							Analcime (Ideal): Na[AlSi ₂ O ₆]·H ₂ O	1.00	1.00	2.00	0.00	0.00	0.00

4.12 Discussion of Experimental Results

Ten experiments were performed with just three of them showing some evidence of the formation of secondary phases. Consolidation was not seen in any of the experiments.

All the experiments used sand samples from a core taken in well LL-231 from Bachaquero-01 reservoir. The first three runs (no.1, no. 1a and no. 1b) used sand from the 2528' – 2531' interval. Run no. 1 used the original sand not cleaned of oil, run no. 1a re-used the sand sample from run no. 1, and run no. 1b used a mixture of 50% sand from run no. 1b and 50% original sand not cleaned of oil. Neither of these runs showed consolidation nor secondary phase formation.

Runs no.2, 2d and 2f used sand from the 2586'-2588' interval. Run no.2 used the original sand not cleaned of oil, run no. 2d re-used the sand from run no. 2 treated with 24 hours of steam injection and run no. 2f used sand from run no. 2d treated with 13 alternating xylene and hot water cycles of about one pore volume per cycle. None of these runs resulted in sand consolidation, while run no. 2f showed what seemed to be secondary phases but they were too small to be analyzed.

Runs no.3, 3a and 3b used sand from the 2665'-2667' interval. Run no.3 used the original sand cleaned of oil with toluene in the soxhlet extraction apparatus, run no. 3a re-used sand from run no. 3, and run no.3b re-used sand from run no.3a treated with 5 wt% HCl and mud acid (3 wt% HF and 12 wt% HCl) for 24 hours.

The fines in the samples appeared to be embedded in hydrocarbon, and therefore may not be very reactive with the solution. When we compared Bachaquero-01 and Wilmington reservoirs, we observed differences in oil gravity with Bachaquero-01 oil being heavier than Wilmington. The mineralogical composition indicated that Wilmington contains much more feldspars than Bachaquero-01, and that the feldspars presents in Bachaquero-01 are mostly orthoclase while Wilmington has both plagioclase and orthoclase present.

The WDS analysis of the secondary phases in runs no. 3a, no. 3b and no. 4 indicated what seemed to be analcime-like zeolites in shape but were chemically different. They indicated a high content of iron and silica when compared with an ideal analcime, probably a non-stoichiometric analcime. This difference between the atypical zeolites may be caused by different chemical micro-environments. **Table 4.4** shows the WDS analysis for these runs. **Table 4.5** shows a summary of all the runs.

Table 4.4-WDS Analysis for Secondary Products in Run Nos. 3a, 3b and 4.

Analysis	Wt. % oxides							Cations in formula on the basis of 7 oxygens					
	Na ₂ O	Al ₂ O ₃	SiO ₂	K ₂ O	CaO	Fe ₂ O ₃	Total	Na	Al	Si	K	Ca	Fe3+
3C_after round1_cent	9.54	19.01	56.72	0.11	0.10	4.54	89.61	0.81	0.98	2.49	0.01	0.01	0.15
3C_after round2_cent	8.95	19.83	55.74	0.19	0.00	4.85	89.11	0.76	1.03	2.46	0.01	0.00	0.16
3C_after round3_cent	9.06	19.66	57.65	0.16	0.03	3.81	90.03	0.76	1.00	2.49	0.01	0.00	0.13
3C_after round1_edge	3.90	16.91	61.71	0.03	0.01	5.31	87.39	0.33	0.87	2.68	0.00	0.00	0.18
3D_after round1_cent	6.61	14.57	68.16	0.21	0.03	1.83	91.24	0.53	0.71	2.81	0.01	0.00	0.06
3D_after round2_cent	5.82	14.66	60.67	0.11	0.04	6.82	87.50	0.50	0.76	2.69	0.01	0.00	0.23
4_after round1_cent	7.44	17.45	56.54	0.52	0.07	7.52	88.85	0.64	0.92	2.52	0.03	0.00	0.25
4_after round2_cent	5.94	19.54	57.95	0.66	0.07	4.83	88.55	0.50	1.01	2.53	0.04	0.00	0.16
					Analcime (Ideal): Na[AlSi ₂ O ₆]·H ₂ O			1.00	2.00	2.00	0.00	0.00	0.00

Table 4.5-Summary of Experimental Runs.

Run	Core interval	Starting Material	Ts	T1	P	Efflux pH	Duration	Soak time	Secondary Phases?	Consol?
			°C	°C	Psig		min.	hr.		
1	2528'-31'	Original + Unclean	265	190	900	11.3	360	60	No	No
1a	2528'-31'	From run 1	285	220	1100	10.7	120	36	No	No
1b	2528'-31'	50% run 1a +50% original	270	230	1200	11.1	180	36	No	No
2	2586'-88'	Original Unclean	270	240	1200	11.1	210	96	No	No
2d	2586'-88'	From run 2, treated w/steam 24hr	265	245	1100	11	330	96	No	No
2f	2586'-88'	13 cycles of xylene and water (1PV ea.)	280	240	1150	10.9	150	50	Very small	No
3	2665'-67'	Orig. cleaned w/toluene in soxhlet	275	235	1100	11.2	210	36	No	No
3a	2665'-67'	From run 3	270	230	1050	11.2	270	36	Dispersed	No
3b	2665'-67'	From run 3 and soaked 24hr in mud acid	275	245	1050	11.3	330	60	Dispersed	No
4	2705'-07'	Orig. cleaned w/toluene in soxhlet	275	240	1100	11.2	210	60	Dispersed	No

Ts: Steam generator temperature

T1: Temperature at top of cell

P: Pressure at top of cell

Duration: Duration of run

Consol.?: Consolidation seen?

CHAPTER V

SUMMARY, CONCLUSIONS AND RECOMMENDATIONS

This research is part of a continuing effort to better understand the process of sand consolidation and thus develop efficient field application procedures. The research was first proposed to look for an alternative to reduce the costs of completion for new and workover wells in the Bachaquero-01 reservoir.

5.1 Summary

The main objectives of this research were to verify experimentally whether sand consolidation by high-temperature alkaline treatment was possible for the heavy oil Bachaquero-01 reservoir and, if consolidation occurred, to determine the main parameters that controlled consolidation such as temperature, soak period and injection rate.

Ten experiments were performed with just three of them showing some evidence of secondary phase formation. No run resulted in consolidation of the sample. In all the experiments, the alkaline solution consisted of 100 g/l of sodium carbonate that was injected at 20 cc/min at temperatures ranging from 190 °C to 245°C. The cell pressure was kept at 900 – 1100 psig. to ensure that the injected solution was in liquid phase.

All the experiments used sand samples from a core taken from well LL-231 from Bachaquero-01 reservoir. The first three runs (no.1, no. 1a and no. 1b) used sand from the 2528' – 2531' interval. Run no. 1 used the original sand not cleaned of oil, run no. 1a

re-used the sand sample from run no. 1, and run no. 1b used a mixture of 50 wt% sand from run no. 1b and 50 wt% original sand not cleaned of oil. None of these runs resulted in consolidation of the samples nor secondary phase formation.

Runs no.2, 2d and 2f used sand from the 2586'-2588' interval. Run no.2 used the original sand not cleaned of oil, run no. 2d re-used the sand from run no. 2 treated with 24 hours of steam injection and run no. 2f used sand from run no. 2d treated with 13 alternating xylene and hot water cycles of about one pore volume for each cycle. None of these runs yielded consolidation of the samples, and run no. 2f showed what appeared to be the formation secondary phases but they were too small to be analyzed.

Runs no.3, 3a and 3b used sand from the 2665'-2667' interval. Run no.3 used the original sand cleaned of oil with toluene in the soxhlet extraction apparatus, run no. 3a re-used sand from run no. 3, and run no.3b re-used sand from run no.3a treated with 5 wt%HCl and mud acid (3 wt% HF and 12 wt% HCl) for 24 hours.

It was observed that the fines in the samples appeared to be embedded in hydrocarbon, and therefore may not be very reactive with the solution. The WDS analysis of the secondary phases in runs no. 3a, no. 3b and no. 4 indicated what seemed to be analcime-like zeolites in shape but were chemically different. They indicated a high content of iron and silica when compared with an ideal analcime. This difference between the atypical zeolites may have been caused by different local chemical conditions of formation.

5.2 Conclusions

The main conclusions of this study may be summarized as follows.

- (i) Sand consolidation of the Bachaquero-01 core samples using hot alkaline solution under the experimental conditions used in this research is not possible.
- (ii) The results indicated that the presence of oil covering the sand grains before and after the treatment most likely prevents reaction between the alkaline solution and the silicate grain surface and also prevents direct contact between sand grains and thus “cementation” of the grains.
- (iii) Electron microprobe analysis indicates that the fine-grained material present in the Bachaquero-01 sand samples is important for the production of secondary materials, but it may also interfere with the bridging of the grains if excess amounts are left or not dissolved during the treatment.
- (iv) Crystals with a framework of sodium-aluminum-silicate called zeolites are expected to be very important secondary phases in the cementation of Bachaquero-01 sand when adequate conditions are reached.
- (v) Temperature in excess of 250°C is expected to play an important role in consolidation of Bachaquero-01 sand. A higher temperature will improve the cleaning of hydrocarbons from grain surfaces and accelerate the dissolution of the sand grains.

- (vi) Difference in soaking period seems not to be an important parameter for the growth of secondary crystals. However, further research is required to confirm this tentative conclusion.

5.3 Recommendations

Based on the results of this research the following recommendations are made.

- (i) Field application of the hot alkaline injection for the Bachaquero-01 sand is not recommended.
- (ii) The cleaning of the samples before experiments should be done by using a more aggressive solvent, e.g. xylene.
- (iii) Conduct experiments at temperatures higher than 250°C to improve the removal of residual oil and to increase the process reactions for sand consolidation.
- (iv) More research is required to evaluate the effect of soaking period on the consolidation process.
- (v) The effect of the injection rate should also be evaluated in further research.

NOMENCLATURE

ac-ft	acre feet
Al	aluminum
API	API gravity, °API
bbbl	barrels
BPD	barrels per day
BSTB	billion of stock tank barrels (10 ⁹ STB)
BSE	back-scattered electron
°C	degrees Celsius
Ca	calcium
cc	cubic centimeter
cm	centimeter
CO ₂	carbon dioxide
cP	centipoises
CWEB	cold water equivalent barrels
D	darcy
EDS	energy dispersive X-ray spectrometry
EOR	enhanced oil recovery
Fe	iron
ft	feet
°F	degrees Fahrenheit

g	grams
gal	gallons
GOR	gas-oil ratio
H	hydrogen
HCl	hydrochloric acid
HCO ₃ ⁻	bicarbonate ion
HPLC	high-performance liquid chromatograph
hr	hours
lb	pounds
I.D.	inner diameter
in.	inches
K	potassium
K ₂ CO ₃	potassium carbonate
Kg	kilograms
L	length
l	liter
m	meters
m ³	cubic meters
mg	milligram
Mg	magnesium
mD	milli-Darcy
min.	minutes

ml	milliliter
mm	millimeter
MSTB/D	thousands of stock tank barrels per day (10^3 STB/D)
Na	sodium
Na ₂ CO ₃	sodium carbonate
NaOH	sodium hydroxide
O	oxygen
O.D.	outer diameter
OH ⁻	hydroxide
OOIP	original oil-in-place
P Top	inlet pressure
P Bottom	outlet pressure
psi	pounds per square inch
psia	pounds per square inch absolute
psig	pounds per square inch gauge
PT	pressure transducer
SCF	standard cubic feet
Si	silicon
Sec	second
SiO ₂	quartz or amorphous silica
T 1	inlet temperature, °C
T 2	temperature 6 inches down in the cell, °C

T 3	temperature 12 inches down in the cell, °C
T 4	outlet temperature, °C
WDS	wavelength dispersive X-ray spectrometry
WT	wall thickness
XRD	X-ray diffraction
µm	micro meter, 10 ⁻⁶ m

REFERENCES

1. Boberg, T. C.: "B-1 Reservoir Engineering Study", Research application report, Exxon Production Research Company, December 1981.
2. Davies, D.K., Mondragon, J.J., and Hara, P.S.: "A Novel, Low Cost Well Completion Technique Using Steam for Formations with Unconsolidated Sands, Wilmington Field, California," paper SPE 38793 presented at the 1993 SPE Annual Technical Conference and Exhibition, San Antonio, Texas, 5-8 October.
3. Hara, P.S., Mondragon, J.J. and Davies, D.K.: "A Well Completion Technique for Controlling Unconsolidated Sands Formations by Using Steam" Class III Mid-Term Project – Cooperative Agreement No. DE-FC22-95BC14939, paper presented at the 1999 U.S. Department of Energy Oil and Gas Conference, Dallas, 28-30 June.
4. Nilsen, K.A.: "Investigation of Sand Consolidation Using Steam for the Tar Zone, Wilmington Field, California," M.S. Thesis, Texas A&M University, College Station, (1999).
5. Moreno, F.E.: "Experimental Investigation of Sand Consolidation Using High-Temperature Alkaline Solution," M.S. Thesis, Texas A&M University, College Station, (2001).
6. Moreno, F.E, Mamora, D.D, Nilsen, K.A., and Guillemette, R.: "Sand Consolidation Using High-Temperature Alkaline Solution," paper SPE 62943 presented at the 2000 SPE Annual Technical Conference and Exhibition, Dallas, 5-8 October.
7. Moreno, F.E, and Mamora, D.D.: "Sand Consolidation Using High-Temperature Alkaline Solution – Analysis of Reaction Parameters," paper SPE 68847 presented at the 2001 SPE Western Regional Meeting, Bakersfield, California, 26-30 March.

8. Moreno, F.E, and Mamora, D.D.: "Sand Consolidation Using High-Temperature Alkaline Solution," *JPT* (May 2001) 55.
9. Penberthy, W.L. Jr and Shaughnessy, C.M: *Sand Control*, SPE Series on Special Topics, SPE, Richardson, Texas (1992) **1**.
10. Butler, R.M.: *Thermal Recovery of Oil and Bitumen*, Prentice-Hall, Englewood Cliffs, NJ, (1991) **1**.
11. Mathews, C.S.: "Steamflooding," *JPT* (March 1983) 465.
12. Reed, M.G.: "Gravel Pack and Formation Sandstone Dissolution During Steam Injection," *JPT* (June 1980) 941.
13. Okoye, C.U., Onuba, N.L., Ghalambor, A., and Hayatdavoudi, A.: "Formation Damage in Heavy Oil Formation During Steam Flooding," paper SPE 22980 presented at the 1991 SPE Asia-Pacific Conference, Perth, Australia, 4-7 November.
14. Heald, M.T., and Renton, J.J.: "Experimental Study of Sandstone Cementation," *J. of Sedimentary Petr.*(1966) **36**, No.4, 977
15. Hajdo, L.E., and Clayton, C.A.: "Formation Damage of a Unconsolidated Reservoir During Steamflooding," paper SPE 27385 presented at the 1994 SPE International Symposium on Formation Damage Control, Lafayette, Louisiana, 7-10 February.
16. McCorrison, L.L., Demby, R.A., and Pease, E.C.: "Study of Reservoir Damage Produced in Heavy Oil Formations Due to Steam Injection," paper SPE 10077 presented at the 1981 SPE Annual Technical Conference and Exhibition, San Antonio, Texas, 5-7 October.
17. Shotts, N.J., Surles, B.W., and Fader, P.D.: "Case Histories of Low-Cost Sand Consolidation in Thermal Wells," paper SPE 24840 presented at the 1992 SPE Annual Technical Conference and Exhibition, Washington, DC, 4-7 October.

18. Poston, S.W., Turner, S.E., Tobola, D.P., and Barger, B.R.: "Development of a Two-Stage Sand Consolidation Technique," paper SPE 14814 presented at the Seventh SPE Symposium of Formation Damage Control, Lafayette, Louisiana, 26-27 February, 1986.
19. Friedman, R.H., Surles, B.W., and Kieke, D.E.: "High Temperature Sand Consolidation," paper SPE 14093 presented at the 1986 SPE International Meeting on Petroleum Engineering, Beijing, China, 17-20 March.
20. Burger, J.G., Gadelle, C.P. and Marrast, J.R.: "Development of a Chemical Process for Sand Control," paper SPE 15410 presented at the 1986 SPE Annual Technical Conference and Exhibition, New Orleans, Louisiana, 5-8 October.
21. Aggour, M.A., and Osman, E.A.: "Development of a New Sand Control Technique – Phase I: Laboratory Development," paper SPE 63237 presented at the 2000 SPE Annual Technical Conference and Exhibition, Dallas, Texas, 1-4 October.
22. El-Sayed, A.H., and Al-Homadhi, E.: "Two New Chemical Components for Sand Consolidation Techniques," paper SPE 68225 presented at the 2001 SPE Middle East Oil Show, Bahrain, 17-20 March.
23. Keith, D.C., Harrison, W.J., and Wendlandt, R.F.: "Mineralogical Responses of Siliciclastic Carbonate Cemented Reservoirs to Steamflood Enhanced Oil Recovery," *Applied Geochemistry* (1998) **13**, 491.
24. Rodriguez, J. R.: "Degradacion de gravas por Inyeccion de Vapor," Informe Final, INTEVEP, Caracas, 1983.
25. Burroughs, M. H.: "Core Analysis Report B-1 Reservoir, Well LL-2318," Research Application Report, Exxon production research company, October 1982.
26. Prats, M.: *Thermal Recovery*, Monograph Volume 7, Henry L. Doherty series, Second print, New York, (1986) 1.

27. Green, W., and Willhite, P.: *Enhanced Oil Recovery*, Textbook Series Volume 6, SPE, Dallas, (1998) 310.
28. Huang, W., and Longo, J. M.: “Experimental Studies of Silicate-Carbonate Reactions – I. Applications to Diagenesis,” *Applied Geochemistry* (1994) **9**, 501.

VITA

Name : César Amabilis Valera Villarroel

Born: January 10, 1968
Cabimas, Estado Zulia - Venezuela

Permanent Address: Urbanización Los Laureles, calle Falcón
Casa 173, Cabimas, Estado Zulia – Venezuela
Phone number : (58) 264-2316931

Education: B.S. Civil Engineering (December 1988)
Universidad Nacional Experimental de las Fuerzas
Armadas, Maracay, Estado Aragua - Venezuela
M.S. Petroleum Engineering (December 2003)
Texas A&M University, College Station

Professional Affiliations : Colegio de Ingenieros de Venezuela
Society of Petroleum Engineers
Venezuelan Student Association – TAMU

Professional Experience: Petróleos de Venezuela S.A., Reservoir Engineer (1991-
2001)